crystals

MDPI

Review

Magnesium Oxide (MgO) Nanoparticles: Synthetic Strategies and Biomedical Applications

Maria-Anna Gatou [1], Eirini Skylla [1,†], Panagiota Dourou [1,†], Natassa Pippa [2], Maria Gazouli [3,4], Nefeli Lagopati [3,5,*] and Evangelia A. Pavlatou [1,*]

[1] Laboratory of General Chemistry, School of Chemical Engineering, National Technical University of Athens, Zografou Campus, 15772 Athens, Greece
[2] Section of Pharmaceutical Technology, Department of Pharmacy, School of Health Sciences, National and Kapodistrian University of Athens, 15771 Athens, Greece
[3] Laboratory of Biology, Department of Basic Medical Sciences, Medical School, National and Kapodistrian University of Athens, 11527 Athens, Greece
[4] School of Science and Technology, Hellenic Open University, 26335 Patra, Greece
[5] Biomedical Research Foundation, Academy of Athens, 11527 Athens, Greece
* Correspondence: nlagopati@med.uoa.gr (N.L.); pavlatou@chemeng.ntua.gr (E.A.P.); Tel.: +30-210-7462362 (N.L.); +30-210-7723110 (E.A.P.)
† These authors contributed equally to this work.

Abstract: In recent times, there has been considerable interest among researchers in magnesium oxide (MgO) nanoparticles, due to their excellent biocompatibility, stability, and diverse biomedical uses, such as antimicrobial, antioxidant, anticancer, and antidiabetic properties, as well as tissue engineering, bioimaging, and drug delivery applications. Consequently, the escalating utilization of magnesium oxide nanoparticles in medical contexts necessitates the in-depth exploration of these nanoparticles. Notably, existing literature lacks a comprehensive review of magnesium oxide nanoparticles' synthesis methods, detailed biomedical applications with mechanisms, and toxicity assessments. Thus, this review aims to bridge this gap by furnishing a comprehensive insight into various synthetic approaches for the development of MgO nanoparticles. Additionally, it elucidates their noteworthy biomedical applications as well as their potential mechanisms of action, alongside summarizing their toxicity profiles. This article also highlights challenges and future prospects for further exploring MgO nanoparticles in the biomedical field. Existing literature indicates that synthesized magnesium oxide nanoparticles demonstrate substantial biocompatibility and display significant antibacterial, antifungal, anticancer, and antioxidant properties. Consequently, this review intends to enhance readers' comprehension regarding recent advancements in synthesizing MgO nanoparticles through diverse approaches and their promising applications in biomedicine.

Keywords: magnesium oxide nanoparticles; synthesis; biomedical applications; antibacterial activity; antifungal activity; anticancer activity; tissue engineering; drug delivery; bioimaging; biosensors

Citation: Gatou, M.-A.; Skylla, E.; Dourou, P.; Pippa, N.; Gazouli, M.; Lagopati, N.; Pavlatou, E.A. Magnesium Oxide (MgO) Nanoparticles: Synthetic Strategies and Biomedical Applications. *Crystals* **2024**, *14*, 215. https://doi.org/10.3390/cryst14030215

Academic Editors: Giancarlo Salviati and Michele Iafisco

Received: 19 December 2023
Revised: 9 February 2024
Accepted: 20 February 2024
Published: 23 February 2024

1. Introduction

In recent times, nanotechnology has become a focal point in research owing to its diverse applications across scientific and technological domains. This field focuses on crafting nanoparticles (NPs) and harnessing their potential in areas like biomedicine, sensing, and catalysis [1]. The significance of NPs stems from their unique properties, such as small size, adaptable shapes, substantial surface area compared to volume, and outstanding magnetic, electronic, optical, and mechanical traits [2–5]. Yet, the distinctiveness of each nanoparticle primarily relies on the utilized synthesis method [6]. In general, nanoparticles have been synthesized using a variety physical, chemical, and green approaches [7–12].

Metal oxide nanoparticles represent a crucial category of nanomaterials extensively utilized today due to their distinct physical and chemical properties, finding applications across diverse fields like biosensing technology, tissue engineering, catalysis, food

packaging, biomedicine, and environmental sciences [13]. The key members within the category of metal oxide nanoparticles include silicon dioxide (SiO_2), ferric oxide (Fe_2O_3), copper oxide (CuO), zinc oxide (ZnO), titanium dioxide (TiO_2), and magnesium oxide (MgO) [14]. Among these metal oxide nanoparticles, magnesium oxide (MgO) nanoparticles have gained considerable attention because of their exceptional biocompatibility, non-toxic nature, robust stability in abrupt conditions, and extensive applications, especially in biomedicine [15]. Furthermore, the United States Food and Drug Administration regards magnesium oxide as a safe material for human consumption [16]. MgO nanoparticles possess several advantageous physicochemical characteristics, such as enhanced ionic character, substantial specific surface area, distinctive crystal structures, as well as oxygen vacancies, enabling seamless interaction with various biological systems [17,18]. These nanoparticles have found widespread utility in diverse areas, including toxic waste remediation, paints, antiseptics, catalysis, superconductors, catalytic devices, semiconductors, additives in heavy fuel oils, refractory materials, adsorbents, reflective coatings, lithium-ion batteries, and more [19–21]. In the realm of biomedicine, magnesium oxide nanoparticles have been employed for stomach relief, heartburn alleviation, and bone regeneration [21,22], as well as for therapeutic applications, such as coated capsules, biological labeling, band-aids, blood collecting vessels, etc. [19]. Additionally, MgO nanoparticles have exhibited potential as antibacterial [21–23], fungicidal [24], anticancer [25,26], antioxidant [27], and antidiabetic [27] agents, as well as in applications such as tissue engineering [28,29], bioimaging [30], and drug delivery [31]. Hence, the pursuit of novel synthetic methods for producing magnesium oxide nanoparticles becomes imperative owing to their escalating usage in biomedicine.

Therefore, the present review article centers on the creation of biocompatible magnesium oxide nanoparticles through diverse synthesis methods, aiming for their potential use in combating bacteria, fungi, cancer, and oxidative stress, as well as ailments such as diabetes. Upon reviewing available literature, it became apparent that no comprehensive review on magnesium oxide nanoparticles exists, encompassing detailed insights into their synthesis, biomedical applications, and toxicity mechanisms. Hence, this present review extensively covers various synthesis methods commonly employed in magnesium oxide nanoparticles' preparation. Furthermore, emphasis is placed on the potential biomedical roles of these synthesized magnesium oxide nanoparticles, particularly their effectiveness against bacteria, fungi, cancer, and oxidative stress, elucidating plausible mechanisms. Additionally, a summary of the toxicity effects of synthesized magnesium oxide nanoparticles, limitations in prior studies, and proposed future research directions are provided. This comprehensive review offers an extensive understanding of diverse synthesis methods for generating MgO nanoparticles, showcasing their potential in biomedical applications, while minimizing toxicity. The findings of this study aim to assist scientists and researchers in further exploring the versatility of this nanomaterial for various biomedical uses.

2. Distinct Attributes of Nanostructured Magnesium Oxide

Over the past twenty years, magnesium oxide has gained attention among non-magnetic oxides due to the presence of several noteworthy phenomena within its nanostructures.

MgO stands out among different non-magnetic oxide systems as a crucial material in technology. This is primarily attributed to its uncomplicated crystal structure and the absence of d orbital electrons. These characteristics greatly contribute to comprehending various physical [32–34] and chemical behaviors [35–38].

While the conventional MgO in bulk form presents itself as a highly insulating substance with an optical bandgap of around 7.6 eV [39], its nanostructured variations display altered optical bandgap properties. For instance, MgO nanoparticles sized at 7 nm exhibit an optical bandgap of 2.8 eV [39], while 1D magnesium oxide nanostructures present an optical bandgap equal to 3.2 eV [40]. Similarly, MgO nanocubes demonstrate a comparable optical bandgap (3.2 eV) [41].

Despite the dielectric constant of bulk MgO and thin films being around 10 [42–44], the material showcases significantly enhanced dielectric constants based on the specific morphology of its nanostructures [45–47].

Spin-dependent electron reflection has been documented in MgO thin films grown on Fe substrate. The electron reflectivity displays quantum interference, leading to the determination of two MgO energy bands with Δ1 symmetry in the conducted research [48,49].

Additionally, MgO-based structures exhibit resistive switching [50,51]. Notably, reports indicate the presence of ferromagnetism in combination with multi-level switching characteristics in magnesium oxide capacitors [52,53]. At ambient temperatures, broad-spectrum laser emissions ranging from near ultraviolet to blue-green have been observed in MgO microcrystals formed via a solid-phase reaction between SiO and Mg at 450 °C in an Ar atmosphere [54,55]. Luminescence represents another observed phenomenon in MgO nanocrystals [56,57]. Various forms of luminescence, including photoluminescence [58,59], electroluminescence [60], radioluminescence [61], and thermoluminescence [62], have also been reported in magnesium oxide nanostructures.

These phenomena are observed not only in reduced dimensions but also manifest when defects accumulate within this material. For instance, magnetism is observed in thin films and nanoparticles of magnesium oxide, which is attributed to surface and extended defects [63]. Furthermore, the luminescent properties of nanostructured MgO can be customized by regulating the defect states within the material [64,65].

Cataluminescence represents another significant phenomenon exhibited in MgO-based nanostructures and serves as a pathway for potential utilization as a gas sensor [66,67].

3. Synthetic Approaches for the Production of MgO Nanoparticles

Various methods exist for producing nanostructured magnesium oxide. This review focuses on insights derived from commonly employed chemical and biological synthesis techniques, known as the bottom-up approach [68]. The aforementioned techniques encompass sol-gel [69], solvothermal/hydrothermal [70], combustion [71], and co-precipitation [72], as well as environmentally friendly green synthesis [73]. Among these chemical methods, the sol-gel technique stands out as a commonly employed method for fabricating MgO nanostructures, due to its ability to generate a higher product yield, its straightforward procedure, and its minimal temperature requirements [74]. The preference for the bottom-up approach lies in its superior control over the size and shape of nanostructures [75] (Figure 1). Crucial to this approach are nucleation, as well as crystal growth, through LaMer burst nucleation. Mechanisms such as Ostwald ripening [76] or coalescence [77] elucidate subsequent particle enlargement [78].

However, MgO can be also synthesized through several physical techniques (top-down approach), such as the vapor deposition method [79], plasma irradiation [80], and ultrasonic irradiation [81]. Typically, these methods necessitate high energy input and robust equipment to achieve the production of magnesium oxide nanoparticles.

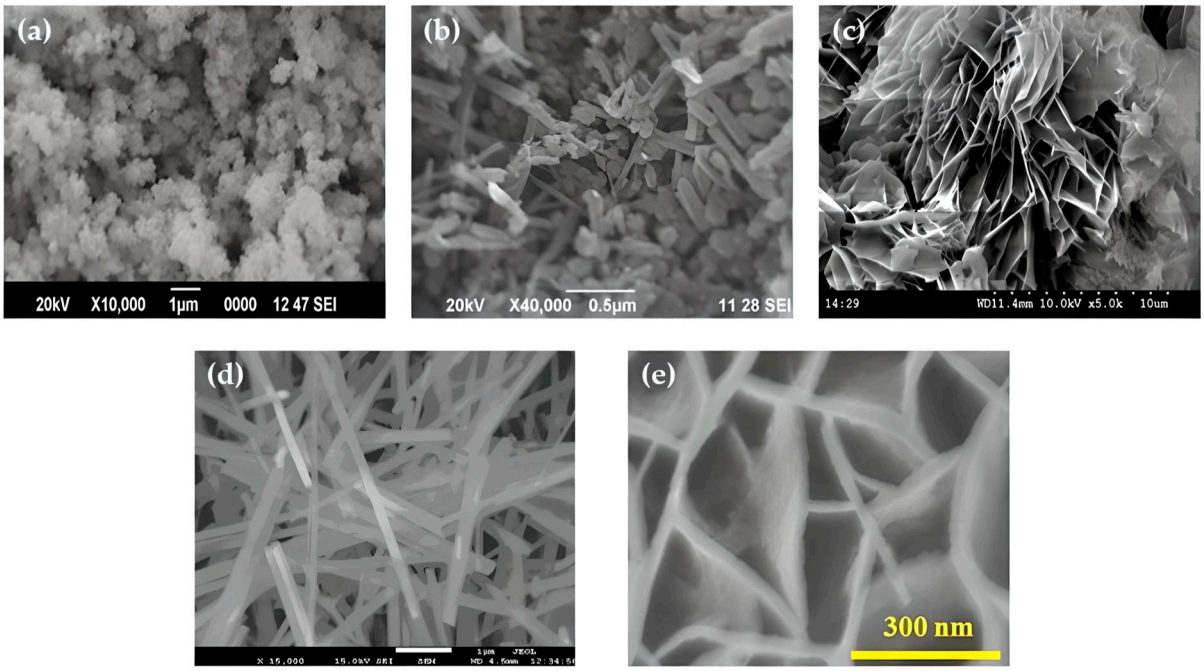

Figure 1. Different morphologies of nano-MgO structures: (**a**) nanoparticles; Reprinted from [82] with permission from Elsevier Copyright 2019, (**b**) nanorods; Reprinted from [82] with permission from Elsevier Copyright 2019, (**c**) nanoflakes; Reprinted from [83] with permission from Elsevier Copyright 2022, (**d**) nanowires; Reprinted from [84] with permission from Elsevier Copyright 2012, and (**e**) nanosheets; Reprinted from [85] with permission from Elsevier Copyright 2022.

3.1. Co-Precipitation Synthetic Approach

This synthetic approach finds widespread application in synthesizing nanoparticles (Figure 2). It relies on precipitation as its fundamental principle and is predominantly associated with liquid-phase synthesis [86], occasionally involving vapor-phase synthesis [87]. NaOH serves as a typical precipitating agent in this approach [88,89]. The underlying concept involves the harmonization of a precipitation reaction entailing two primary processes: (a) nucleation and (b) the growth of nuclei [90]. Typically, three fundamental principles are judged: (i) achieving single nucleation and homogeneous growth through diffusion; (ii) nucleation, growth, and aggregation of smaller subunits; and (iii) multiple nucleations and subsequent Ostwald ripening growth [91]. The precise concentration of the critical solute initiating this process significantly influences the typical procedure, where surficial solute diffusion prompts growth. Moreover, it is essential to distinctly separate these two procedures. The derived precipitate is subsequently subjected to washing as well as drying processes.

In their study, Kumar and his team [92] employed the co-precipitation approach, employing magnesium nitrate [$Mg(NO_3)_2$] as the precursor and NH_4OH solution as the precipitating agent, yielding particles averaging about 11 nm in size.

Moreover, Karthikeyan and his team [93] conducted research exploring the impact of polyethylene glycol concentration on the characteristics of magnesium oxide nanoparticles synthesized via the co-precipitation approach. $Mg(NO_3)_2$ served as the precursor and NaOH as the precipitating agent. XRD analysis revealed that the utilization of PEG (polyethylene glycol) nearly doubled the crystallite size in comparison to pure magnesium oxide nanoparticles (8.62 nm compared to 14.76–15.78 nm). Additionally, noticeable variations in morphology were attributed to the presence of PEG. Also, pure magnesium oxide nanoparticles exhibited a sphere-like structure, while polyethylene glycol-modified magnesium oxide nanoparticles presented a flake-like structure.

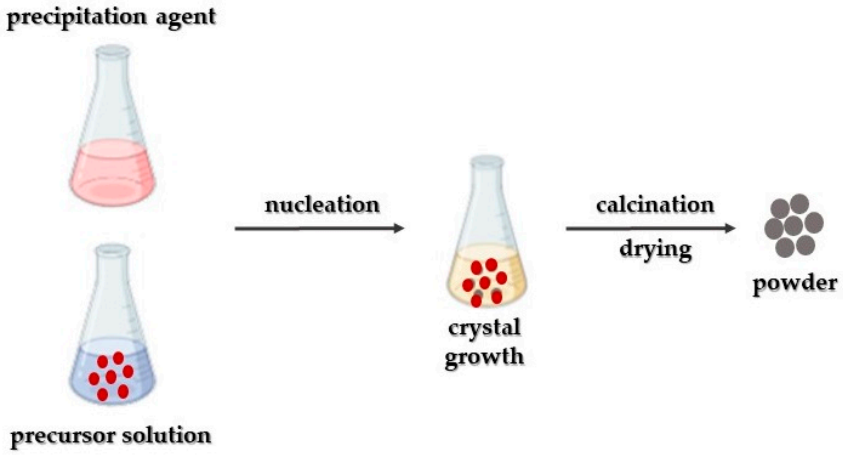

Figure 2. Schematic representation of MgO nanoparticles' synthesis utilizing the co-precipitation approach.

Furthermore, Tandon and Chauhan [94] synthesized magnesium oxide nanotubes utilizing $Mg(CH_3COO)_2$ and NaOH, determining an average crystalline size equal to 34.04 nm. FESEM observations showcased a tubular morphology, characterized by an outer diameter of roughly 78 nm and an inner diameter of 31 nm. Furthermore, they reported a bandgap of 5.73 eV.

Finally, Yadav and co-researchers [95] synthesized magnesium oxide nanoparticles through a feasible and low-cost chemical co-precipitation approach, followed by annealing at several temperatures (350 °C, 450 °C, and 550 °C). XRD analysis data demonstrated that the prepared samples exhibited sizes smaller than 20 nm and maintained a pure phase. An intriguing transition from hexagonal $Mg(OH)_2$ nanoparticles to discretely cubic structured magnesium oxide nanoparticles was observed as the annealing temperatures were progressively increased.

3.2. Sol-Gel Synthetic Approach

The sol-gel approach stands as a fundamental synthetic method directed towards generating novel structures, predominantly focusing on metal oxides and similar inorganic materials by employing an inorganic precursor and an organic solvent [96]. By combining metal alkoxides with appropriate solvents and reactants, uniform solutions are formed, subsequently developing into colloidal suspensions (sol) and progressing into integrated networks through poly-condensation (gel) [97]. These networks are subsequently converted into xerogels or aerogels, relying on the specific drying process employed (Figure 3).

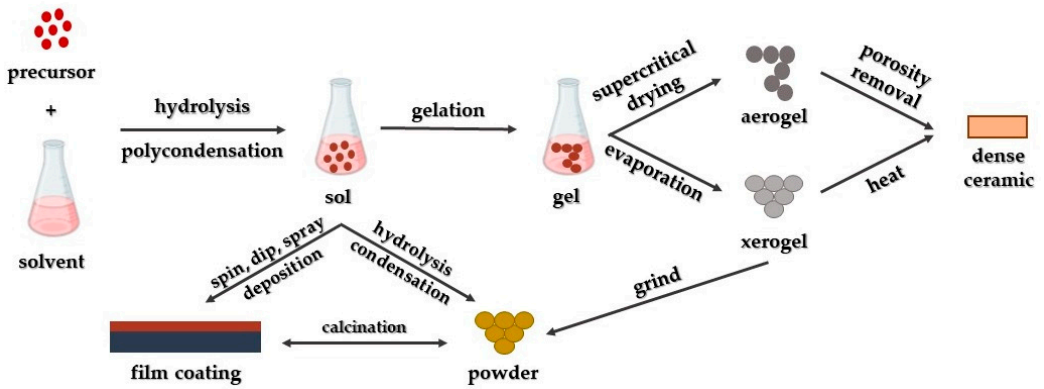

Figure 3. Schematic representation of MgO nanoparticles' synthesis through the sol-gel approach.

Sutapa and co-researchers [98] utilized the same precursor and complexing agent to synthesize magnesium oxide nanoparticles. Their study delved into stress, strain, and crystal energy, achieving the development of cubic-shaped crystals. These findings were confirmed through SEM analysis, where they documented the highest texture coefficient value of 0.98 in the crystal plane (222).

Furthermore, Wahab and his team [99] engaged in synthesizing magnesium oxide nanoparticles using the sol-gel approach, through the utilization of $Mg(NO_3)_2$ and NaOH as precursor and precipitating agent, respectively. The methods outlined in their study resulted in the production of cubic-shaped magnesium oxide nanoparticles measuring between 50 and 60 nm in size.

On the contrary, Boddu and co-researchers [100] outlined an approach for developing magnesium oxide nanoparticles characterized by a coralline structure, utilizing Mg ribbons as a precursor. The aforementioned process commenced with the formation of a magnesium methoxide solution, subsequent to hydrolysis, supercritical drying, and then thermal activation. As a result, particles with the as-described structure were produced, characterized by sizes ranging between 200 and 300 nm.

Moreover, Dercz and his team [101] conducted an analysis of nanopowder derived from magnesium oxide xerogel, which was synthesized via magnesium methoxide as a precursor, followed by methanol and toluene. Following the methodology detailed in their research, they attained an average crystallite size of 7.5 nm and a specific surface area equal to 138 m^2/g.

Nanostructured magnesium oxide was also synthesized by Nassar and his team [102], employing a combined sol-gel/combustion approach. Using magnesium nitrate along with several fuels (urea, oxalic acid, and citric acid), they observed that the fuel's choice significantly impacted both crystallite size as well as morphology. Specifically, the use of citric acid resulted in the smallest crystallite size of ≈12 nm.

3.3. Solvothermal/Hydrothermal Synthetic Approach

The solvothermal method comprises one of the extensively utilized approaches for the controlled crystal growth of several materials [103]. This technique involves placing a precursor and an appropriate solvent within an autoclave under elevated temperature and pressure conditions, having as a result the synthesis of the preferred products [104]. These specific reaction conditions, notably temperature and pressure, facilitate the production of materials with enhanced crystallinity as compared to the co-precipitation synthetic approach [89]. In the context of defining the "solvothermal" approach that involves utilizing a solvent apart from water, such as alcohols or various organic and inorganic solvents. Alternatively, when water serves as the solvent, the approach is defined as "hydrothermal" (Figure 4).

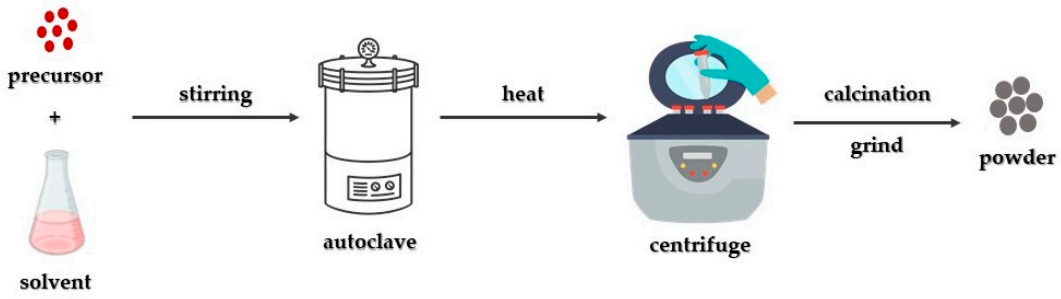

Figure 4. Schematic representation of MgO nanoparticles' synthesis via the hydrothermal approach.

Devaraja and his team [57] detailed the production of nanocrystalline magnesium oxide nanopowder prepared from $Mg(NO_3)_2 \cdot 6H_2O$ and NaOH. The as-mentioned procedure yielded porous magnesium oxide nanoparticles characterized by an average crystallite size

of 25 nm. Among the properties observed for the fabricated nanoparticles was a bandgap value equal to 5.5 eV.

Then, Al-Hazmi and co-researchers [84] conducted the synthesis of nanofibers through a direct reaction, involving $Mg(CH_3COO)_2$ and urea. The as-prepared nanofibers exhibited an average diameter of 6 nm, with a length measured through TEM analysis at ≈10 nm.

In another study, Ding and his research team [105] detailed the production of both rod-like and tube-like magnesium hydroxide, followed by the production of magnesium oxide nanoparticles through thermal decomposition. The team demonstrated that the hydrothermal approach favored the relatively facile control over crystallite size, shape, and structure. Employing magnesium powder, magnesium sulfate, or magnesium nitrate hexahydrate as base materials in the synthesis process, diverse morphologies were achieved (including rod-like, lamellar, and needle-like), due to variations in experimental conditions. The obtained particles exhibited dimensions ranging from 20 to 600 nm, presenting an exceptionally enhanced specific surface area (>100 m^2/g).

Additionally, Rukh and co-workers [106] employed magnesium powder as the precursor material in their study, while using hydrogen peroxide and distilled water as the reaction medium. Through this approach, they achieved the development of magnesium oxide nanoparticles possessing an average crystallite size of 18 nm.

3.4. Combustion Synthetic Approach

The combustion method (Figure 5) constitutes a widely utilized approach for synthesizing metal oxide nanoparticles, given its effectiveness and cost-efficiency [107]. This method encompasses two primary approaches: self-propagating synthesis and volume combustion synthesis [108]. Self-propagating synthesis involves spontaneous redox reactions ignited by an external source between the precursor (oxidizer) and reductant (fuel), mixed at the molecular level in a solution. Solid product formation occurs without additional energy input [109]. On the other hand, in volume combustion synthesis, the entire sample is heated until the reaction initiates throughout its volume. This preparation approach is more challenging to control and is particularly suitable for weak exothermic reactions that necessitate preheating before ignition [110].

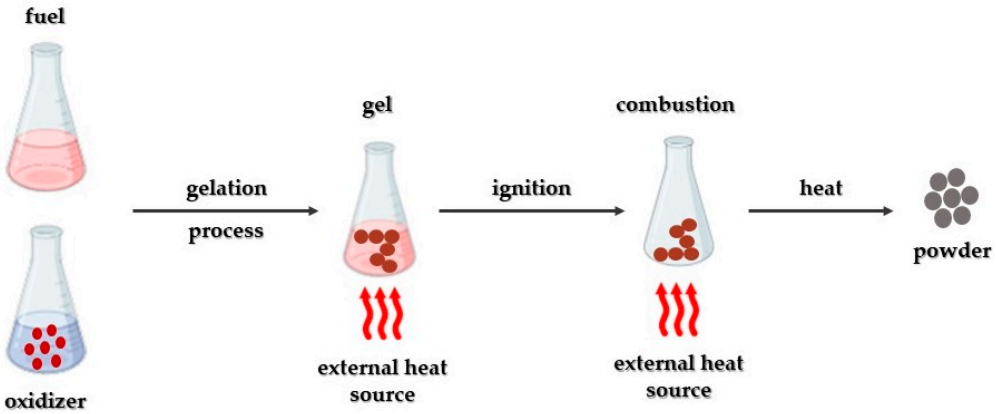

Figure 5. Schematic representation of MgO nanoparticles' synthesis using the combustion synthetic approach.

Balakrishnan and his team [111] utilized the solution combustion approach to synthesize magnesium oxide nanoparticles, employing $Mg(NO_3)_2$ as an oxidizer and urea as a fuel. This method yielded magnesium oxide nanoparticles exhibiting a cubic structure with a crystallite size of ≈22 nm, as observed through XRD analysis. SEM analysis indicated spherical nanoparticles with uniform size distribution. Notably, the synthesized nanoparticles exhibited a bandgap equal to 2.9 eV, differing from other studies.

Rao and co-researchers [112] used the same starting materials for magnesium oxide nanoparticles synthesis, aiming to explore the impact of the fuel–oxidizer ratio. The

obtained results demonstrated that a higher fuel ratio led to larger crystallite sizes (ranging from 18 to 53 nm), except in the case of a 0.75 ratio, possibly ascribed to variations in ignition temperature, burn rate, or enthalpy.

Furthermore, Therami and his team [113] utilized citric acid as a fuel and examined its impact on various parameters. Considerable alterations were observed: an increase in bandgap (from 4.72 to 5.35 eV) with higher ratios, a reduction in particle size (from 35 to 20 nm) with increased ratios, and diversity in morphology (flake-like, vacuolar, and flower-like structures).

Additionally, Kumar and co-researchers [114] synthesized magnesium oxide nanoparticles using $Mg(NO_3)_2$ solution and extracts from parthenium plants. Their study focused on analyzing the influence of fuel quantity on bandgap width (5.3–5.45 eV) and crystallite size (27–35 nm); however, the observed alterations were less pronounced compared to the previous case.

3.5. Biosynthesis or Green Synthetic Approach

The approach known as green synthesis or biosynthesis represents a novel approach in producing nanoparticles, characterized by minimal or no prerequisites for specific reaction conditions, such as enhanced pressure, temperature, or excessive energy usage, while avoiding the use of toxic chemicals [115,116]. The primary objective is to reduce waste generation and foster sustainable development within this realm [117]. This approach employs non-toxic reagents, which encompass a diverse array of substances ranging from plant substrates—namely leaves, stems, fruits, flowers, roots, bark, etc. [118–122]—to microorganisms such as bacteria, fungi, and algae [123,124] or biomolecules involving DNA, protein, and enzymes, as well as vitamins [125]. Typically, double-distilled water serves as the primary extraction medium in this synthetic procedure. In essence, this approach involves three essential stages: (i) activation, (ii) growth, and (iii) process completion (Figure 6). The biosynthesis of nanoparticles relies on several reaction parameters, including the concentration of biological substrates, as well as the metal precursor, reaction duration, temperature, and pH level. Modifying the aforementioned factors leads to the creation of nanoparticles varying in size and structure, significantly impacting their physical and chemical properties and their biological functionalities [8,126]. Nonetheless, despite its benefits, the green synthesis approach also exhibits certain drawbacks.

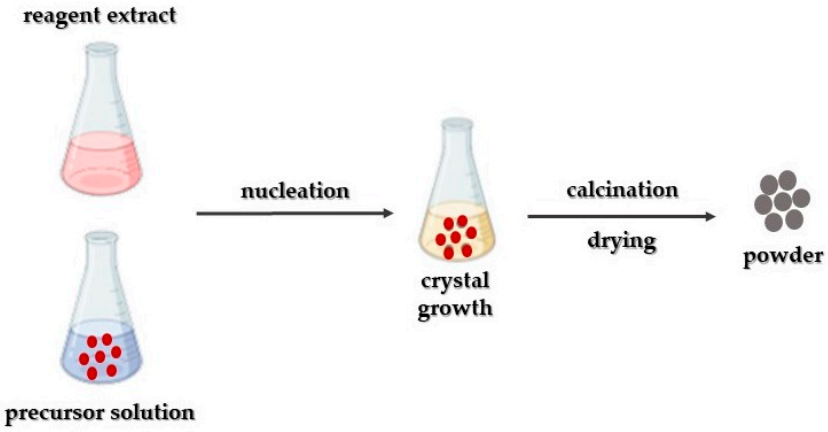

Figure 6. Schematic representation of MgO nanoparticles' synthesis utilizing the green synthesis approach.

Plants are the most frequently employed biological sources for the environmentally friendly synthesis of nanoparticles, due to their easy accessibility and compatibility with biological systems. The process of nanoparticle biosynthesis using plants involves various methods, such as utilizing living plants (intracellular), plant extracts (extracellular), and phytochemicals. Among these approaches, synthesis through plant extracts stands as

the most commonly adopted method by numerous researchers [127–129]. Plant extracts encompass a diverse array of phytochemicals and biomolecules, including flavonoids, terpenoids, phenolic acids, saponins, methylxanthines, proteins, enzymes, alkaloids, and polysaccharides. These components serve multifunctional roles as reducing, stabilizing, capping, and chelating agents during nanoparticle synthesis [8,130]. While a precise mechanism that could describe the development of metal oxide nanoparticles utilizing plant extracts remains unclear, the literature suggests two potential mechanisms. Based on the first potential mechanism, phytochemicals within the plant extract initially reduce metal salts into metal ions. Subsequently, these metal ions react with oxygen, sourced either from degraded phytochemicals or from the atmosphere, leading to the production of metal oxide ions [131]. The produced ions then pass through a growth phase, forming metal oxide nanoparticles that are further stabilized by the phytochemicals, preventing their agglomeration [131]. An alternative mechanism proposes that the phytochemicals bind to the metal ions, creating metal coordination complexes. The obtained complexes are subsequently subjected to thermal degradation or calcination, resulting in the formation of metal oxide nanoparticles [8,132].

In their study, Suresh and his team [133] employed an extract from *Nephelium lappaceum* L. combined with double-distilled water for eco-friendly synthesis, utilizing magnesium nitrate as the precursor. Their investigations confirmed magnesium oxide's cubic structure, with an average crystallite size equal to 55 nm, aligning closely with SEM analysis indicating a grain size range between 60 and 70 nm.

In their research, Younis and co-researchers [134] utilized *Rosa floribunda* powder dispersed in double-distilled water, employing $Mg(NO_3)_2$ as the precursor, resulting in high-purity cubic structured nanoparticles with an approximate size of 10 nm as determined through high-resolution TEM analysis.

Furthermore, Abdallah and his team [135] investigated the production of *Rosmarinus officinalis* L. with bulk magnesium oxide, yielding nanoparticles characterized by a minimum number of impurities, as well as a hexagonal crystalline structure, while the average crystallite size was found to be equal to 8.8 nm.

Sharma and colleagues [136] employed phyto-assisted synthesis with *Swertia chirayaita* as the reactant and $Mg(NO_3)_2$ as the precursor, achieving the formation of magnesium oxide nanoparticles sized below 20 nm. Their SEM findings depicted these nanoparticles as predominantly spherical with slight variations in shape.

Additionally, Fatiquin and co-researchers [137] aimed to produce magnesium oxide nanoparticles using $MgCl_2$ as the precursor and *Moringa oleifera* as the reagent, yielding nanoparticles possessing crystallite size of ≈21 nm. TEM analysis confirmed a cubic structure with particle sizes ranging from 2 to 50 nm.

Moreover, Singh and his research team [138] synthesized nano-MgO particles utilizing *R. arboreum* leaves' extract. Based on the study's results, the as-prepared MgO nanoparticles presented enhanced bactericidal efficiency towards *E. coli*, *S. mutans*, and *P. vulgaris*.

Researchers have utilized various microorganisms, alongside plants, to produce magnesium oxide nanoparticles. Numerous investigations highlight the capability of certain bacterial species to generate metal or metal oxide nanoparticles. The process of synthesizing these nanoparticles primarily occurs through intracellular or extracellular mechanisms (Figure 7). Intracellularly, metal ions are assimilated into cells, undergoing reduction facilitated by diverse enzymes and proteins within the cell, resulting in nanoparticle formation. Conversely, in the extracellular mechanism, bacterial-secreted enzymes and proteins catalyze the reduction of metal ions for the production of nanoparticles. Additionally, bacterial enzymes and proteins play a role in stabilizing these nanoparticles [8]. Nevertheless, some researchers have proposed a non-enzymatic mechanism for metal ion reduction, in order to produce nanoparticles [139–141]. The aforementioned alternative synthetic process relies on the interaction between metal ions and specific functional groups that are present on the bacterial cell walls, leading to the metal ions' reduction into nanoparticles. Furthermore,

this mechanism is influenced by environmental factors such as temperature, pH, and other associated conditions [126].

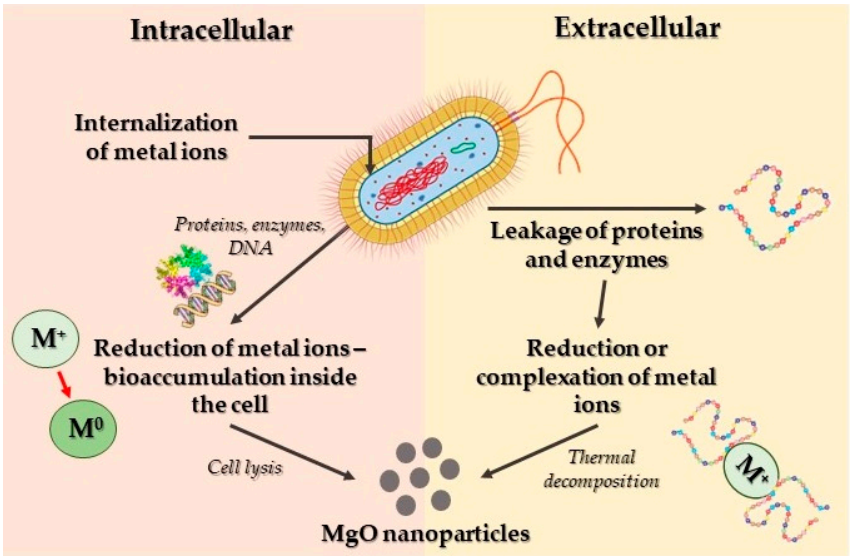

Figure 7. The process of MgO nanoparticles' synthesis by bacteria involves two mechanisms: extracellular and intracellular. Extracellular synthesis transpires as precursor salts are captured by external proteins, followed by their reduction. On the other hand, intracellular synthesis happens as these precursor materials migrate into the cell membrane and undergo reduction catalyzed by intracellular enzymes.

Apart from bacteria, fungi are recognized as a highly effective biological resource for producing metal and metal oxide nanoparticles, primarily owing to the array of intracellular enzymes they possess. The utilization of fungal strains for the eco-friendly synthesis of these nanoparticles demonstrates comparable mechanistic pathways, both intracellular and extracellular, as mentioned in the nanoparticles' biosynthesis facilitated by bacteria (Figure 8). Additionally, fungi have the capacity to yield larger quantities of nanoparticles compared to bacteria due to their ability to excrete an enhanced concentration of bioactive metabolites, including enzymes and proteins, into the culture media [8].

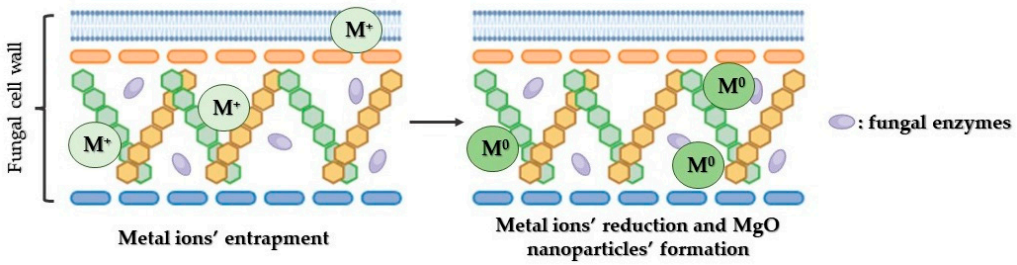

Figure 8. Suggested process outlining the production of MgO nanoparticles utilizing fungal extract.

Algae, being aquatic microorganisms, harbor diverse phytochemicals like flavonoids and polyphenols, akin to those found in plant extracts. Consequently, the process of biogenic synthesis of magnesium oxide nanoparticles employing algae as a bio-source shares similarities with the mechanism mentioned in plant-mediated synthesis of magnesium oxide nanoparticles. Within the as-described synthetic route mechanism, phytochemicals function as agents for reduction, stabilization, and chelation, playing pivotal roles in the biosynthesis of metal oxide nanoparticles. Table 1 presents selected synthetic bottom-up approaches for the fabrication of nano-MgO particles.

Table 1. Nano-MgO structures synthesized through distinct bottom-up approaches.

Synthetic Approach	Utilized Precursor	Size (nm)	Studied Activity	Reference
Co-precipitation	$Mg(NO_3)_2$	11	Antibacterial	[92]
Co-precipitation	$Mg(NO_3)_2$	14–16	Antibacterial	[93]
Co-precipitation	$Mg(NO_3)_2$	78	Antibacterial	[94]
Sol-gel	$Mg(OCH_3)_2$	200–300	-	[100]
Sol-gel	$Mg(OCH_3)_2$	≈8	-	[101]
Solvothermal	$Mg(CH_3COO)_2$	6	Antibacterial	[84]
Solvothermal	Mg	18	Antibacterial	[106]
Combustion	$Mg(NO_3)_2$	20–35	Antibacterial	[113]
Green (plant-mediated)	$Mg(NO_3)_2$	10	Antibacterial	[134]
Green (plant-mediated)	Bulk MgO	≈9	Antibacterial	[135]
Green (plant-mediated)	$Mg(NO_3)_2$	<20	Antibacterial	[136]
Green (plant-mediated)	$MgCl_2$	≈21	Antibacterial	[137]
Green (plant-mediated)	-	-	Antibacterial	[138]
Green (plant-mediated)	$Mg(NO_3)_2$	30 and 42	Antioxidant and antibacterial	[142]
Green (plant-mediated)	$Mg(NO_3)_2$	18.2 and 16.5	Antibacterial	[143]
Green (algae-mediated)	$Mg(NO_3)_2{\cdot}6H_2O$	68.6	Antimicrobial	[144]
Green (bacteria-mediated)	$Mg(NO_3)_2$	30	Anticancer	[145]
Green (fungi-mediated)	$MgCl_2$	43–91	Antibacterial	[146]

4. Biomedical Applications of MgO Nanoparticles

4.1. Antibacterial Activity

In recent times, the rise of bacterial resistance to commonly used antibiotics has significantly impacted the effective treatment of bacterial infections. The United Nations General Assembly has highlighted antibiotic resistance as a critical global peril that humanity confronts [147]. Consequently, exploring alternative strategies to combat bacterial growth has become imperative, with nanoparticles emerging as a promising solution, due to their strong antibacterial properties. Among these nanoparticles, MgO nanoparticles have garnered attention owing to their remarkable effectiveness in combating bacteria. Studies have indicated the potent MgO nanoparticles' antibacterial effects against various strains, such as *E. coli* [134], *S. aureus* [148], *P. aeruginosa*, *A. baumannii* [149], and *P. carotovorum* [150]. Additionally, a proposed antibacterial mechanism of MgO nanoparticles is depicted in Figure 9. More specifically, magnesium oxide nanoparticles have the ability to stimulate reactive oxygen species (ROS) within bacteria. This process leads to oxidative stress, resulting in significant impairment to their membrane lipids, proteins, and nucleic acids [151].

Makhluf and colleagues [152] demonstrated the antibacterial properties of powdered magnesium oxide prepared through a microwave-assisted synthetic approach, applying it to combat both *Staphylococcus aureus* and *Escherichia coli* cultures. The most substantial antibacterial effect was observed when subjecting both bacterial strains to 8 nm magnesium oxide nanoparticles. Following exposure to MgO for 60 min, less than one fifth of both cultures survived. Subsequently, after 4 h of treatment, the survival rates decreased significantly to less than 5% for *Staphylococcus aureus* and a mere 0.1% for *Escherichia coli*. In contrast, using 23 nm MgO resulted in a reduction in bacterial counts to approximately 40% for *S. aureus* and 35% for *E. coli*, comparatively less effective than the 8 nm particles.

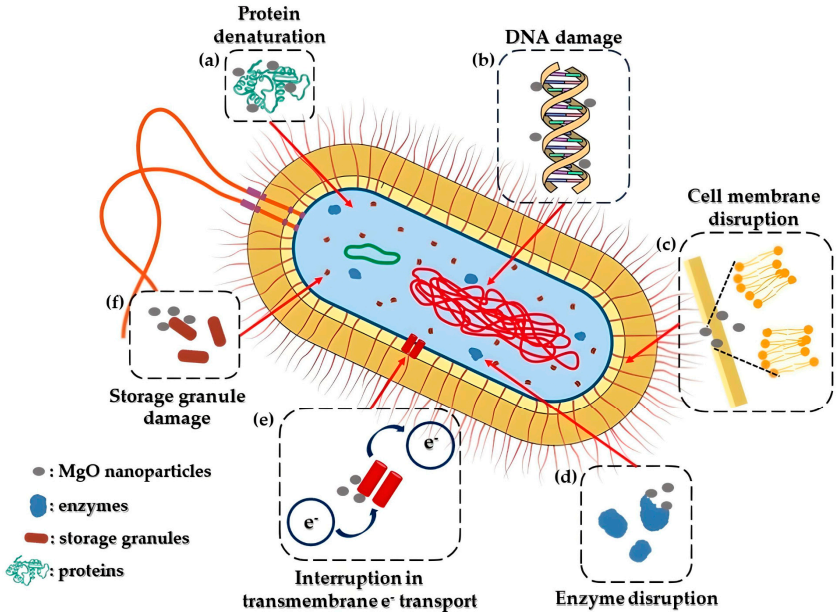

Figure 9. Representation of a feasible mechanism of MgO nanoparticles' antibacterial activity. The entry of MgO nanoparticles into bacterial cells is facilitated by the disturbance of the bacterial cell membrane (**c**). Once inside the cytoplasm, these nanoparticles have the capacity to produce reactive oxygen species (ROS) or inflict direct harm on DNA and enzymes (**b**,**d**). This action results in protein denaturation and damage to the mitochondria (**a**,**f**). Additionally, they interfere with cellular memory and impede trans-tolerant electron transport (**e**). Consequently, the inflicted harm leads to the destruction of bacterial cells, prompting the release of their organelles and culminating in their eventual demise.

In another study, an investigation on the impact of magnesium oxide particle size on its antibacterial effectiveness against *Bacillus subtilis var. niger* over a four-hour period was conducted [153]. The study revealed that as the particle size of magnesium oxide decreased, the efficiency of eliminating bacteria increased from 93% to 97%. This enhancement was attributed to the rise in the number of surficial Mg^{2+} ions with smaller MgO particles. It became evident that magnesium oxide nanoparticles exhibited greater efficacy as antibacterial agents compared to TiO_2 nanoparticles, both in the occurrence and non-occurrence of irradiation.

Bindhu and colleagues [154] synthesized magnesium oxide nanoparticles employing a wet chemical approach, employing the resulting composition as an antibacterial agent. Nanostructures of magnesium oxide nanoparticles resembling spheres were produced, measuring ≈16 nm. Visualization through TEM and SEM analysis substantiated the creation of the as-mentioned MgO nanoparticles. Considering its bactericidal properties, magnesium oxide was recommended as a potential agent for purifying water.

Sawai and his team [155] further validated the bactericidal properties of MgO nanoparticles. In particular, their study delved into the interactions between magnesium oxide nanoparticles and *Escherichia coli*, as well as *Staphylococcus aureus*, revealing pronounced antibacterial effects. Through chemiluminescence analyses aimed at elucidating the mechanism of particle suspension action, it was observed that these particles had the capability to generate a notable concentration of active O_2^-. Particularly in acidic or neutral environments, this generation was attributed to the production of hydroperoxyl radicals ($\bullet HO_2$).

Moreover, Krishnamoorthy and fellow researchers [156] investigated the bactericidal effects of MgO nanoparticles on both Gram-negative bacteria (*Escherichia coli* and *Pseudomonas aeruginosa*) as well as Gram-positive bacteria (*Staphylococcus aureus*) using a microtiter plate-based analysis that incorporated resazurin as an indicator of cell growth.

The antibacterial efficacy was demonstrated using MgO nanoparticles, with a minimum inhibitory concentration equal to 1.000 µg/mL observed for *P. aeruginosa* and *S. aureus* and 500 µg/mL against *E. coli*.

Additionally, Karthik and colleagues [82] conducted a study examining the bactericidal properties of MgO nanoparticles, prepared utilizing a microwave-assisted and a hydrothermal synthetic approach, against both Gram-positive bacteria (*Rhodococcus rhodochrous* and *Bacillus subtilis*) and Gram-negative bacteria (*Aeromonas hydrophila*, *Proteus mirabilis*, *Vibrio cholera*, *Shigella flexneri*, *Salmonella typhi*, and *Escherichia coli*). Their findings revealed a notable 27 mm inhibition zone, indicating significant antibacterial efficacy specifically against *R. rhodochrous* and *B. subtilis*.

Suresh and colleagues [157] produced MgO nanoparticles utilizing *C. pictus* leaf extract, exhibiting bactericidal effects measured through the inhibition zone against *S. aureus* (5.50 cm), *B. subtilis* (10 cm), *E. coli* (12.50 cm), and *S. paratyphi* (15 mm) (Figure 10). Conversely, magnesium oxide nanoparticles derived from the *P. grandis* extract displayed enhanced antibacterial properties against *S. aureus* and *S. paratyphi*, demonstrating optimized zones of inhibition of 14 and 15 mm, respectively [132].

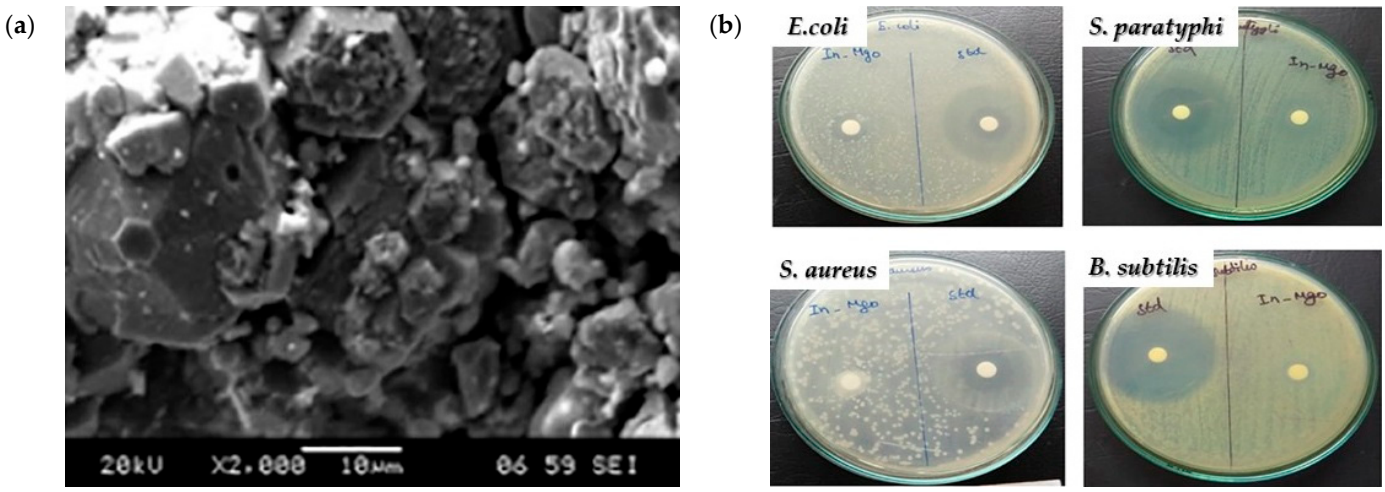

Figure 10. (**a**) SEM image of the as-synthesized nano-MgO structures and (**b**) their antibacterial activity study towards *E. coli*, *S. paratyphi*, *S. aureus*, and *B. subtilis*. Reprinted from [157] with permission from Elsevier Copyright 2018.

Kainat and colleagues [158] investigated the impact of magnesium oxide nanoparticles derived from *H. rosa-sinensis* leaf extract on *P. aurigenosa*, *P. vulgaris*, and *E. coli*, observing zones of inhibition measuring 19, 22, and 19 mm, respectively. In a separate study, Amrulloh and his team [159] demonstrated the antibacterial potential of magnesium oxide nanoparticles fabricated utilizing *M. oleifera*. These nanoparticles exhibited minimum inhibitory concentration (MIC) values ranging from 300 to 550 µg/mL against *S. aureus*, *E. faecalis*, *E. coli*, and *S. dysenteriae*.

Likewise, Younis and co-researchers [134] illustrated the remarkable antibacterial efficacy of magnesium oxide nanoparticles derived from rose (*R. floribunda*) flower extract, showcasing MIC values for *S. epidermidis* (15.63 µg/mL), *S. pyogenes* (7.81 µg/mL), and *P. aeruginosa* (31.25 µg/mL).

Consequently, research on the bactericidal capacity of magnesium oxide nanoparticles has persistently undergone enhancement and refinement, unveiling new prospects for enhanced antibiotic capabilities (Table 2).

Table 2. Antibacterial activity of nano-MgO particles synthesized via various approaches.

Synthetic Approach	Main Remarks	Reference
Microwave-assisted	■ MIC * = 1 mg/mL (*E. coli*, *S. aureus*). ■ Viability reduction: >99.9% (*E. coli*), 95% (*S. aureus*).	[152]
Wet chemical	■ ZOI **: 19 nm (*S. aureus*), 12 nm (*P. aeruginosa*).	[154]
Wet chemical	■ MIC = 500 µg/mL (*E. coli*), 1000 µg/mL (*P. aeruginosa*, *S. aureus*).	[156]
Microwave-assisted & Hydrothermal	■ Microwave assisted approach resulted in nano-MgO structures with enhanced antimicrobial properties. ■ ZOI: 27 mm (*B. subtilis*, *R. rhodochrous*), 25 mm (*A. hydrophila*), 24 mm (*E. coli*, *P. mirabilis*), 23 mm (*V. cholera*), 17 mm (*S. flexneri*), 16 mm (*S. typhi*).	[82]
Green (plant-mediated)	■ ZOI: 5.5 mm (*S. aureus*), 10 mm (*B. subtilis*), 12.5 mm (*E. coli*), 15 mm (*S. paratyphi*).	[157]
Green (plant-mediated)	■ ZOI: 14 mm (*S. aureus*), 11 mm (*B. subtilis*), 20 mm (*M. luteus*), 23 mm (*E. coli*), 15 mm (*S. paratyphi*), 20 mm (*K. pneumonia*).	[132]
Green (plant-mediated)	■ ZOI: 19 mm (*P. aurigenosa*), 22 mm (*P. vulgaris*), 19 mm (*E. coli*).	[158]
Green (plant-mediated)	■ MIC = 300–550 µg/mL (*S. aureus*, *E. faecalis*, *E. coli*, *S. dysenteriae*).	[159]
Green (plant-mediated)	■ MIC = 15.63 µg/mL (*S. epidermidis*), 7.81 µg/mL (*S. pyogenes*), 31.25 µg/mL (*P. aeruginosa*).	[134]

* MIC = Minimum Inhibitory Concentration. ** ZOI = Zone Of Inhibition.

Mechanism of MgO Nanoparticles' Bactericidal Activity

The effectiveness of MgO nanoparticles in eradicating bacteria largely relies on reactive oxygen species (ROS) production. This reliance is specifically associated with factors such as the particle's surface characteristics, polarity, crystal size, increased oxygen defects, morphology, the ability of molecules to chemically diffuse, as well as the release of Mg^{2+} ions. The bactericidal process involving magnesium oxide nanoparticles entails sterilization through particle release, a multifaceted mechanism, and absorption. The crystals' size and their extensive surface area may contribute significantly to their potent antibacterial properties. Superoxide radicals, formed through reactions between H_2O_2 and ROS, inflict damage on cellular proteins and DNA, leading to cell death [160].

The mechanism underlying the antimicrobial efficacy of magnesium oxide nanostructures can be elucidated as follows. Primarily, a crucial antibacterial process involves a light-driven catalytic mechanism. Specifically, the creation of ROS on the nanoparticle surface, in the presence of light, initiates oxidative stress on microbial cells, ultimately leading to cellular demise. ROS comprises relatively low levels of toxic radicals like the superoxide anion radical (O_2^-), reactive hydroxyl radical (·OH), and a mild oxidizing agent, hydrogen peroxide (H_2O_2). A subsequent series of reactions also takes place, where the superoxide anion radical ($\bullet O_2^-$) combines with hydrogen ions, forming the $\bullet HO_2^-$ radical, which then reacts with hydrogen ions to produce H_2O_2. This compound can interact with DNA, cellular proteins, and cell membranes, ultimately resulting in microbial death. The generation of a substantial amount of ROS hinges on the creation of smaller crystalline structures with increased specific surface areas and a corresponding rise in surficial defects. Additionally, the release of Mg^{2+} ions from magnesium oxide nanostructures' surfaces contributes to their bactericidal activity. These positively charged ions interact with the negatively charged cell membranes of microbes, penetrating the semi-permeable membrane. Based on existing research data, synthesized nanomaterials are thought to significantly

impact pathogenic bacteria by compromising membrane integrity, leading to the demise of bacterial pathogens [160].

4.2. Antifungal Activity

Apart from showcasing antibacterial effects, MgO nanoparticles have demonstrated significant antifungal capabilities against various pathogenic fungal strains (Figure 11). Fungi constitute natural pathogens as they present plenty of similarities with the host cell, inhibiting antifungal compounds' growth [161]. Sierra-Fernandez and co-researchers [162] studied the antifungal activity of Zn-doped magnesium oxide nanoparticles synthesized through a facile sol-gel approach and compared it with that of pure ZnO and MgO nanoparticles. The as-mentioned nanoparticles presented enhanced antifungal efficiency compared to that of pure magnesium oxide or zinc oxide nanoparticles, restraining the growth of fungi *Aspergillus niger*, *Penicillium oxalicum*, *Paraconiothyrium* sp., and *Pestalotiopsis maculans*.

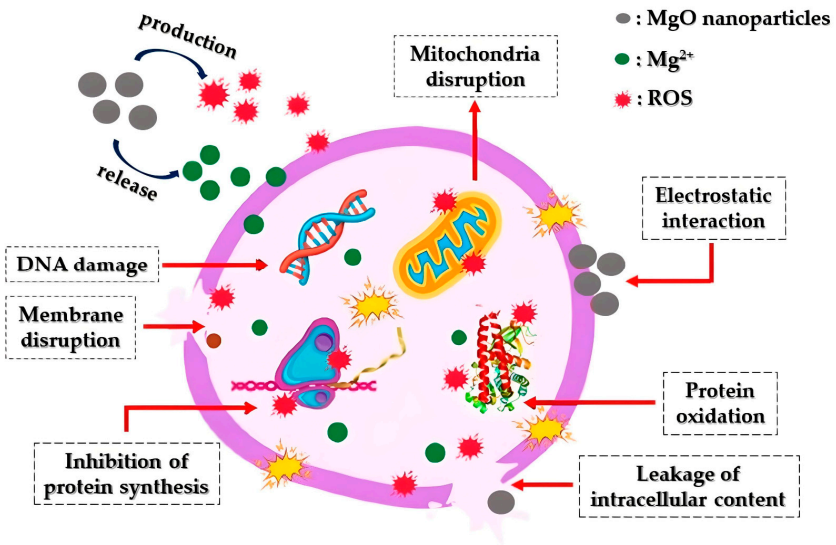

Figure 11. Diagrammatic representation of the way that MgO nanoparticles operate as an antifungal agent: Initially, the nanoparticles engage with fungal cell membranes through electrostatic interactions, leading to the disruption of both the membranes and the glucan matrix. Following this, they initiate the production of ROS and the release of Mg^{2+}. Subsequently, they interfere with mitochondria by inducing DNA damage, subsequently impeding protein synthesis, disrupting proteins, leading to intracellular leakage, and ultimately resulting in the demise of fungal cells.

Moreover, De la Rosa-García and co-workers [163] evaluated the antifungal activity (towards strains of *C. gloeosporioides*) of pure ZnO and MgO, as well as ZnO/MgO and ZnO/$Mg(OH)_2$ composites fabricated under different synthetic approaches (co-precipitation and hydrothermal). According to the acquired results, all tested nanoparticles at the tested concentrations significantly restrained conidia's germination and led to the structural damage of the fungal cells, verifying that the as-mentioned nanoparticles could constitute promising fungicidal agents against *C. gloeosporioides*.

In addition, Castillo and his team [24] demonstrated through in vitro experiments that magnesium oxide nanoparticles, characterized by a diameter equal to 12 nm, presented fungistatic efficiency towards three filamentous fungal strains (*T. reesei*, *A. niger*, and *C. cladosporioides*), at concentrations ranging from 3 to 12 mg/mL.

Safaei and Taran [164] developed a cellulose-MgO bionanocomposite applying the Taguchi method to achieve the optimal synthetic conditions. Based on the obtained data, the bionanocomposite consisting of 4 mg/mL magnesium oxide and 1 mg/mL cellulose, which was stirred for 90 min, indicated the most enhanced antifungal effectiveness against *Aspergillus niger*. Additionally, the proposed bionanocomposite exhibited higher antifungal activity as compared to pure magnesium oxide and cellulose, respectively.

Khatua and co-researchers [165] prepared pure magnesium oxide and cerium-doped magnesium oxide nanoparticles through a facile and low-cost wet chemical approach. They reported that cerium-doped magnesium oxide nanoparticles presented increased fungicidal activity and cytotoxicity against plant pathogenic fungi (THY-1) compared to pure magnesium oxide nanoparticles.

Sidhu and co-workers [166] synthesized a sepiolite-MgO nanocomposite and compared its antifungal activity with that of pure magnesium oxide nanoparticles towards several phytopathogenic rice's fungi. The as-proposed nanocomposite was more potent as compared to pure magnesium oxide, presenting ED_{90} > 230 and 249 µg/mL, respectively, against the tested fungi better than standard fungicides, rendering it an efficient, sustainable, non-toxic, green, and residue-free strategy for confronting fungal menace against phytopathogens.

Additionally, Wang and his team [167] developed a Ag_2S-MgO/GO nanocomposite via a simple sol-gel/ultrasound synthetic approach and compared its fungicidal effectiveness with that of pure magnesium oxide nanoparticles, as well as Ag_2S-MgO nanocomposite, against *Aspergillus flavus* and *Trichoderma viride*. Their results indicated that the as-synthesized nanocomposite exhibited enhanced antifungal activity against both examined fungi, as compared to pure MgO and Ag_2S-MgO nanocomposite.

Sharmila and colleagues [168] employed magnesium oxide nanoparticles derived from *P. alba* leaf extract to combat *A. flavus* and *F. solani*, observing zones of inhibition of approximately 4 and 3 mm, respectively (Figure 12).

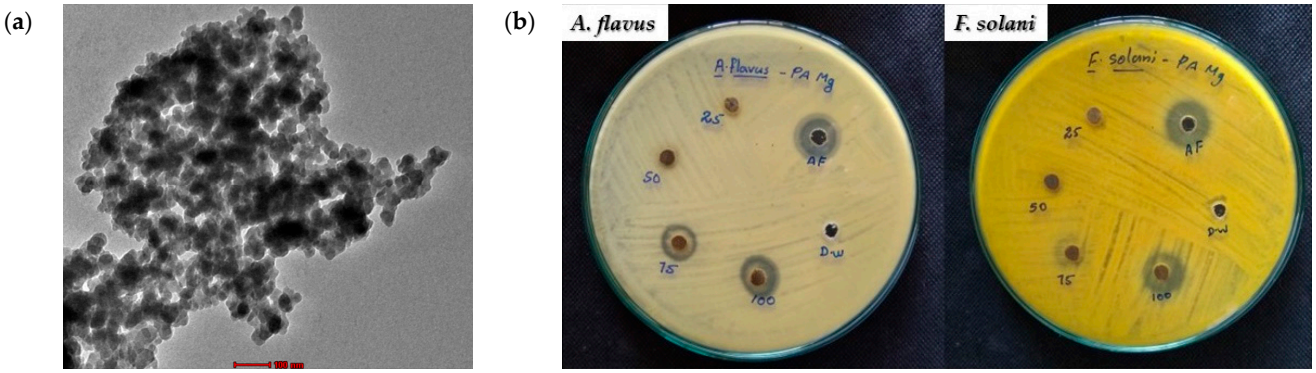

Figure 12. (**a**) TEM image of the as-prepared MgO nanoparticles and (**b**) their antifungal efficiency study towards *A. flavus* and *F. solani*. Reprinted from [168] with permission from Elsevier Copyright 2019.

Pugazhendhi and his team [144] successfully prepared magnesium oxide nanoparticles, possessing an average size of approximately 68 nm, employing the marine brown algae *Sargassum wighitii* as both reducing and capping agent. Subsequently, the biosynthesized magnesium oxide nanoparticles were evaluated towards their fungicidal efficiency against *Aspergillus fumigates*, *Fusarium solani*, and *Aspergillus niger* at three concentrations (10–30 µg/mL). MgO nanoparticles indicated potent fungicidal efficiency when compared to positive control (Fluconozole). Based on their study's data, the growth of *Fusarium solani* and *Aspergillus niger* was more efficiently inhibited in comparison to A. fumigates.

Amina and his team [13] synthesized magnesium oxide nanoparticles using *S. costus* root extract, demonstrating fungicidal effects against *C. tropicalis* and *C. glabrata*, yielding zones of inhibition ranging between 19 and 20 mm. These outcomes notably surpassed the findings of Sharmila and colleagues [168].

Saied and co-researchers [169] utilized magnesium oxide nanoparticles derived from *A. terreus* fungus, achieving an inhibition zone of 12.8 mm against *C. albicans*. However, Fouda and colleagues [170] illustrated that MgO nanoparticles from *P. chrysogenum* fungus extract exhibited enhanced antifungal activity against *C. albicans*, with a zone of inhibition equal to 14.7 mm, surpassing Saied and his team [169]. This outcome indicated *P. chrysogenum* as a

superior precursor towards the synthesis of magnesium oxide nanoparticles with enhanced fungicidal properties.

Sulak and Kavakcıoğlu Yardımcı [171] utilized jujube fruit extract to fabricate magnesium oxide nanoparticles targeting *S. cerevisiae* yeast, yielding a half-maximal inhibitory concentration value (116.5 ppm). Consequently, the as-proposed eco-friendly fabrication of magnesium oxide nanoparticles demonstrates promise for various antifungal applications.

Vidhya and his team [172] reported the fabrication of cubic-structured magnesium oxide nanoparticles (42 nm) utilizing *Ocimum americanum* aqueous extract and evaluated their antifungal potential against *Candida albicans* and *Aspergillus niger*. The zones of inhibition observed from biosynthesized magnesium oxide nanoparticles' aqueous extract were compared with those of plant leaf extract, $Mg(NO_3)_2$, as well as a common commercial drug (Gentamycin 50 µg). The as-reported magnesium oxide nanoparticles exhibited higher inhibition zones for both tested fungi (*Candida albicans* 21 mm and *Aspergillus niger* 16 mm) than the rest of the examined materials.

Vijayakumar and co-researchers [173] synthesized magnesium oxide nanoparticles utilizing *Citrus aurantium* peel extract with average particle size of around 50–60 nm and studied their antifungal activity against *Candida albicans* and *Aspergillus niger* through the agar well approach. According to their study's results, an enhanced inhibition zone was measured against *C. albicans* (26 mm) followed by *A. niger* (24 mm), rendering the as-proposed biosynthesized magnesium oxide nanoparticles a promising candidate towards pathogenic fungi strains. Table 3 summarizes the antifungal activity of nano-MgO particles prepared utilizing different approaches.

Table 3. Antifungal activity of nano-MgO particles synthesized through several approaches.

Synthetic Approach	Main Remarks	Reference
Sol-gel	■ MIC = 12 mg/mL (*C. cladosporioides*), 6 mg/mL (*A. niger*), 3 mg/mL (*T. reesei*).	[24]
Sol-gel	■ ZOI (MgO, 10 mg/mL): 12.2 mm (*A. niger*), 15.6 mm (*P. oxalicum*). ■ ZOI ($Mg_{1-x}Zn_xO$, 10 mg/mL): 17.1 mm (*A. niger*), 21 mm (*P. oxalicum*).	[162]
Co-precipitation	■ MIC = 0.625 mg/mL for *C. gloeosporioides* strains from papaya (PG-16) and avocado (AP-14).	[163]
Co-precipitation	■ Highest fungal (*A. niger*) growth inhibition = 85.03% (nanocomposite: 4 mg/mL nano-MgO particles, 1 mg/mL cellulose, 90 min stirring time). ■ Lowest fungal (*A. niger*) growth inhibition = 41.38% (nanocomposite: 2 mg/mL nano-MgO particles, 0.5 mg/mL cellulose, 30 min stirring time).	[164]
Co-precipitation	■ ZOI: 33 mm (THY-1). ■ MIC = 11.63 µg/mL (THY-1).	[165]
Green (plant-mediated)	■ ZOI: 4 mm (*A. flavus*), 3 mm (*F. solani*).	[168]
Green (algae-mediated)	■ Inhibition growth of *F. solani* and *A. niger* greater than *A. fumigates*.	[144]
Green (plant-mediated)	■ ZOI: 20 mm (*C. tropicalis*), 19 mm (*C. glabrata*).	[13]
Green (fungi-mediated)	■ ZOI: 12.8 mm (*C. albicans*).	[169]
Green (plant-mediated)	■ IC_{50} * = 116.5 µg/mL (*S. cerevisiae*).	[171]
Green (plant-mediated)	■ ZOI: 21 mm (*C. albicans*), 16 mm (*A. niger*).	[172]
Green (plant-mediated)	■ ZOI: 26 mm (*C. albicans*), 24 mm (*A. niger*).	[173]

* IC_{50} = Half-maximal inhibitory concentration.

4.3. Anticancer Activity

Cancer stands as one of the most lethal and intricate diseases known to date. The unregulated growth of cancerous cells detrimentally impacts neighboring healthy cells, leading to fatality [174]. Various treatments, including surgery, radiation therapy, and chemotherapy, have been proposed for combating cancer [175]. Nonetheless, the aforementioned approaches may harm normal cells, resulting in numerous side effects and potential disease recurrence [176]. Recently, there has been a rising focus on the development of nanoparticle-based nanomaterials, notably magnesium oxide nanoparticles, renowned for their potent anti-cancer properties. Figure 13 portrays a hypothetical anti-cancer mechanism associated with magnesium oxide nanoparticles. The advancement of synthesis methods and techniques has significantly propelled the application of magnesium oxide nanoparticles in anti-cancer therapy.

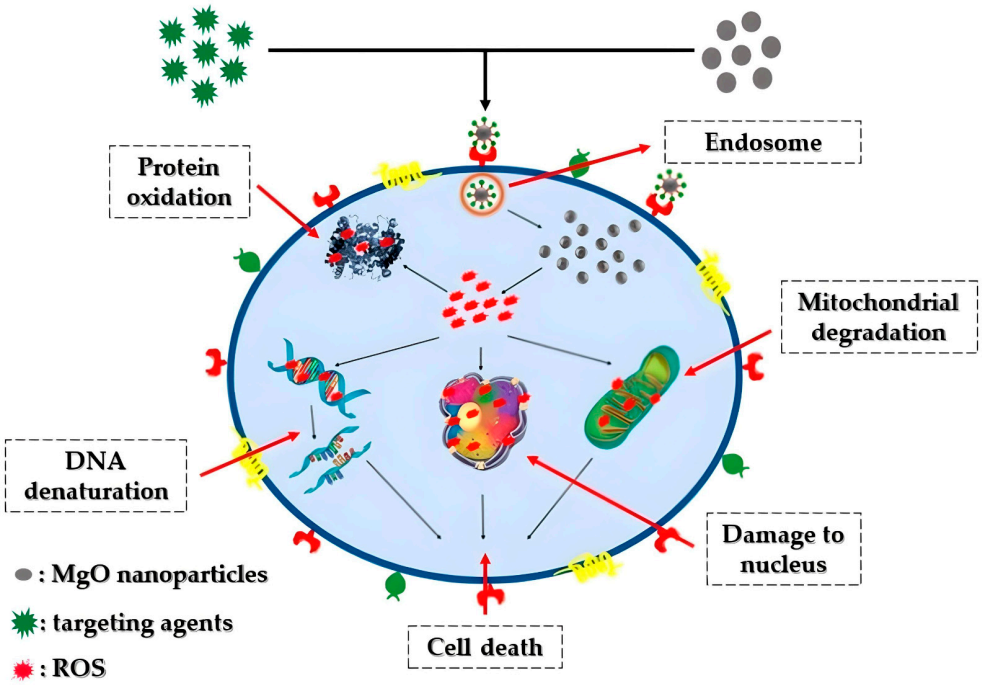

Figure 13. Representation of the potential anticancer mechanism involving MgO nanoparticles: Through electrostatic interactions with the cell surface, MgO nanoparticles gain entry into the cell via the intracellular pathway. Once inside, these nanoparticles prompt the formation of reactive oxygen species (ROS) within the cells, resulting in DNA damage, protein oxidation, and mitochondrial impairment, ultimately culminating in cell death.

Behzadi and his team [177] reported that the tested magnesium oxide nanoparticles presented selective cytotoxicity against the K562 cell line, thus rendering them as a novel anticancer agent. Their study's data revealed that MgO nanoparticle-mediated apoptosis was initiated through reactive oxygen species generation within the cancer cells.

Additionally, magnesium oxide nanoparticles synthesized through a simple sol-gel method and further modified with polyethylene glycol were successfully fabricated by Alfaro and his team [178] to be utilized as carrier for the anticancer drug 2-Methoxyestradiol for advancing its clinical utilization. According to their research's results, the as-developed nanoparticles significantly reduced the viability of a prostate cancer cell line (LNCap), rendering the as-mentioned nanocomposite appropriate as a drug delivery system towards anticancer prostate therapy.

Moreover, a cellulose–magnesium oxide nanocomposite was developed by Safaei and co-researchers [179]. The team optimized the synthetic conditions applying the Taguchi method and subsequently investigated the anticancer efficiency of the obtained samples.

The nanocomposite synthesized using 8 mg/mL of MgO, 2 mg/mL of cellulose and stirred for 60 min, indicated the most increased growth inhibitory effectiveness against breast cancer cells (MCF-7). Considering the obtained data, the cellulose–magnesium oxide nanocomposite produced under ideal experimental conditions exhibits potential suitability as an effective anticancer agent.

Al-Fahdawi and his team [180] successfully fabricated platinum-doped magnesium oxide nanoparticles (30–50 nm) utilizing a precipitation method. The cytotoxicity of the as-mentioned doped magnesium oxide nanoparticles was evaluated on human lung (A549) and colonic cancer cells (HT29), as well as normal human lung (MRC-5) and colonic fibroblasts cells (CCD-18Co). They observed that platinum-doped magnesium oxide nanoparticles were relatively non-toxic to normal cells but selectively toxic to colon and lung cancer cells, presenting increased potential to be utilized as a novel anti-cancer therapeutic agent.

Furthermore, MubarakAli and colleagues [181] fabricated magnesium oxide nanoparticles through a facile co-precipitation synthetic approach and evaluated their cytotoxic effect towards human breast cancer cells (MCF-7). Based on their study, the magnesium oxide nanoparticles successfully restrained the viability of MCF-7 cells at a concentration equal to 50 μg/mL.

Chen and co-researchers [182] proposed a functionalized magnesium oxide nanotube adsorbed with 5-Fluorouracil and studied its anticancer efficiency towards breast cancer cell lines (HER2 and EGFR). The as-proposed novel nanostructure presented enhanced inhibitory effects against both breast cancer cell types, illustrating that this complex could be promising for the fabrication of novel anticancer agents to treat breast cancer patients.

In addition, Singh and his team [183] synthesized 4-carboxy phenylboronic acid-linked and amine-functionalized magnesium oxide nanoparticles loaded with rutin (Figure 14) and assessed their in vitro and in vivo anticancer efficiency. The as-prepared nanohybrid indicated exceptional anticancer activity against MDA-MB-231 cells through intracellular ROS generation and apoptosis, while it restrained the cancer cells' migration. Following, in vivo studies assisted the enhanced anticancer potential of the nanohybrid in tumor-bearing mice.

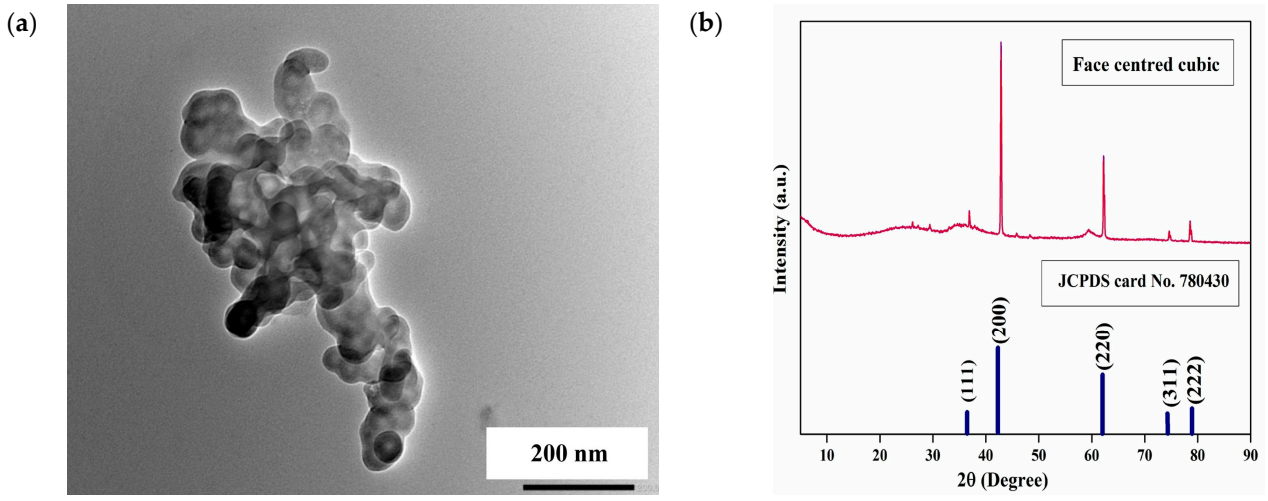

Figure 14. (**a**) TEM image and (**b**) XRD diffractogram of the as-proposed MgO-based nanohybrid. Reprinted from [183] with permission from Elsevier Copyright 2023.

Magnesium oxide nanoparticles fabricated utilizing marine algae *S. wightii*, demonstrated promising anticancer potential towards human lung cancer cells, exhibiting the most enhanced apoptosis rate at approximately 79.5% [144].

Amina et al. [13] developed magnesium oxide nanoparticles from *S. costus* leaf extract, showcasing anticancer activity against human breast cancer cells. However, the cytotoxicity

percentage of magnesium oxide nanoparticles from *S. costus* leaf extract (82%) was slightly lower than that of those derived from *E. tirucalli* leaf extract (85%) [184].

Similarly, Abdullah and Mohammed [185] achieved anticancer effects against human breast cancer cells, presenting the largest inhibition zone (18 mm) by employing magnesium oxide nanoparticles synthesized from Syrian mesquite (*P. facta*) leaf extract.

Fathy and Mahfouz [186] synthesized MgO nanoparticles utilizing fungi like *A. niger*, *E. cichoracearum*, *P. citrinum*, *G. deliquescence*, and *A. alternata*. These nanoparticles exhibited a relatively high half-maximal inhibitory concentration (IC_{50} = 11.17 µg/mL) towards prostate cancer cell lines, indicating their considerable potential in anticancer applications. Consequently, the aforementioned insightful findings suggest the potential for synthesizing high-performance magnesium oxide nanoparticles with prominent anticancer properties. Table 4 summarizes the anticancer activity of nano-MgO particles utilized in the aforementioned studies.

Table 4. Overview of nano-MgO particles' anticancer activity.

Synthetic Approach	Main Remarks	Reference
Commercially available MgO nanoparticles	■ IC_{50} = 17.75 µg/mL (K562 cell line). ■ Cell viability reduction = 78.5% (K562 cell line, $C_{MgO\ nanoparticles}$ = 1 µg/mL). ■ Selective cytotoxicity towards cancer cells.	[177]
Sol-gel	■ Cell viability reduction = 40% (nano-MgO-PEG particls, 72 h, LnCap cancer cells). ■ Cell viability reduction = 20% (nano-MgO particles, 72 h, LnCap cancer cells).	[178]
Precipitation	■ IC_{50} = 13.65 µg/mL (HT29 human cancer cell line). ■ IC_{50} = 6.32 µg/mL (A549 human cancer cell line). ■ IC_{50} = 48.08 µg/mL (CCD-18Co human normal cell line). ■ IC_{50} = 76.83 µg/mL (MRC-5 human normal cell line). ■ Toxic concentrations: 3.125 µg/mL (HT29), 6.25 µg/mL (A549).	[180]
Co-precipitation	■ IC_{50} = 50 µg/mL (MCF-7 breast cancer cells).	[181]
Microwave-assisted	■ Enhanced cytotoxicity (MDA-MB-231 human breast cancer cells). ■ Inhibition of cell migration (MDA-MB-231 human breast cancer cells). ■ No systemic toxicity.	[183]
Green (algae-mediated)	■ Apoptosis = 79.5% (human lung cancer cell). ■ Cell viability = 20.5%.	[144]
Green (plant-mediated)	■ Cytotoxicity = 82% (human breast cancer cell).	[13]
Green (plant-mediated)	■ Cell inhibition = 85% (human breast cancer cell).	[184]
Green (plant-mediated)	■ ZOI: 18 mm (human breast cancer).	[185]
Green (fungi-mediated)	■ IC_{50} = 11.17 µg/mL (prostate cancer cell line).	[186]

PEG600 = polyethylene glycol 600, $C_4H_6O_6$ = tartaric acid, CTAB = cetyltrimethyl ammonium bromide ($C_{19}H_{42}BrN$), APTES = 3-Aminopropyltriethoxysilane, EDC.HCl = 1-(3-Dimethylaminopropyl)-3-Ethylcarbodiimide hydrochloride, NHS = N-hydroxysuccinimide, PBA = 4-carboxyphenyl boronic acid.

4.4. Antioxidant Activity

For a considerable duration, researchers have established that free radicals negatively impact human health, potentially leading to various illnesses including heart disease, arteriosclerosis, tumors, diabetes, and aging [187]. Consequently, the focus on understanding antioxidants has expanded to counteract the free radicals' detrimental effects. However, despite their effectiveness, potent antioxidant agents also bring along several adverse effects. For instance, Edaravone, acknowledged as a free radical scavenger beneficial in preventing lipid oxidation and treating ischemic stroke, mitigates nerve cell damage. Yet, when utilized clinically, Edaravone induces numerous side effects, including liver and kidney toxicity, which can impact human health [188]. Hence, exploring antioxidant capabilities via enhanced magnesium oxide nanoparticles presents a possible solution to mitigate several associated drawbacks.

Podder and colleagues [189] explored the antioxidant activity of three nano-MgO structures (i.e., nanoparticles, nanoplates, and nanorods). They reported the effective production of superoxide anions ($\bullet O_2^-$) and hydroxyl radicals ($\bullet$OH) at increased concentrations (>500 μg/mL) and the scavenging of $\bullet O_2^-$ at lower concentrations (40 μg/mL) for all examined nanostructures. More specifically, it was observed that magnesium oxide nanorods produce the most increased levels of superoxide anions, while magnesium oxide nanoparticles possessed the most enhanced ability (60%) to scavenge superoxide anions. Lastly, the researchers also reported a 100% scavenging ability of the nitrogen-centered free radical (DPPH) by magnesium oxide nanoplates, given their significantly enhanced specific surface area (342.2 m^2/g).

Additionally, Ali and co-researchers [190] fabricated MgO nanoparticles from *Abrus precatorius* L. bark extract using a green synthetic approach. In order to assess the free radical's scavenging potential for the as-prepared magnesium oxide nanoparticles, a DPPH assay was conducted, which relied on both reaction time and concentration. The acquired data indicated that at a lower concentration (20 μg/mL), there was a 15.8% scavenging rate, while at an increased concentration (120 μg/mL), the rate rose to 65.93%. In comparison, the standard ascorbic acid at 20 μg/mL displayed a scavenging rate of 11.66%, reaching 60.86% at an enhanced concentration of 120 μg/mL. The synthesized magnesium oxide nanoparticles exhibited a superior percentage of free radical scavenging compared to ascorbic acid, thus verifying their antioxidant activity.

Magnesium oxide nanoparticles (42 nm) were successfully developed utilizing geranium leaf extract by Mylarappa et al. [191]. The antioxidant characteristics of the synthesized nanoparticles were evaluated using the DPPH method. Based on the obtained results, MgO nanoparticles displayed significant efficacy in scavenging free radicals, as demonstrated by their DPPH scavenging activities.

Priya et al. [192] demonstrated a 60% inhibition rate against hydrogen peroxide by employing magnesium oxide nanoparticles derived from *D. elata* aqueous extract. Similarly, Ammulu et al. [193] utilized magnesium oxide nanoparticles fabricated utilizing *P. marsupium* heartwood extract, exhibiting an IC_{50} value of approximately 89.67 μg/mL against DPPH.

Correspondingly, Younis and colleagues [134] observed that magnesium oxide nanoparticles obtained from rose flower extract showcased lower IC_{50} values in antioxidant activity against superoxide anions, hydroxyl, and nitric oxide (26.2, 31.9, and 52.9 μg/mL, respectively) compared to *P. marsupium* heartwood extract (89.67 μg/mL) as reported by Ammulu and co-researchers [193].

Nadeem et al. [194] optimized the preparation of magnesium oxide nanoparticles utilizing *C. orientalis* extract, achieving the lowest IC_{50} value of 22.65 μg/mL, surpassing many aforementioned studies.

In a separate investigation, Amrulloh and colleagues [159] explored the potential of *M. oleifera* extract, obtaining a minimum inhibitory concentration of 290 μg/mL against DPPH. These collective findings indicate promising avenues for future research in bio-based MgO

nanometallic antioxidants. Overall, the results of the studies regarding the antioxidant potential of MgO nanoparticles are presented in Table 5.

Table 5. Antioxidant activity of MgO nanoparticles.

Synthetic Approach	Main Remarks	Reference
Wet chemical (nanoparticles)	▪ IC_{50} = 126.47 µg/mL (DPPH).	[189]
Hydrothermal (nanoplates)	▪ IC_{50} = 16.61 µg/mL (DPPH).	
Hydrothermal (nanorods)	▪ IC_{50} = 71.04 µg/mL (DPPH).	
Green (plant-mediated)	▪ DPPH inhibition = 65.93% ($C_{MgO\ nanoparticles}$ = 120 µg/mL).	[190]
Green (plant-mediated)	▪ Inhibition of hydrogen peroxide = 60%	[192]
Green (plant-mediated)	▪ IC_{50} = 89.67 µg/mL (DPPH).	[193]
Green (plant-mediated)	▪ IC_{50} = 26.2 µg/mL (superoxide anions). ▪ IC_{50} = 31.9 µg/mL (hydroxyl anions). ▪ IC_{50} = 52.9 µg/mL (nitric oxide).	[134]
Green (plant-mediated)	▪ IC_{50} = 22.65 µg/mL (DPPH).	[194]
Green (plant-mediated)	▪ MIC = 290 µg/mL (DPPH).	[159]

DPPH = (2,2-diphenyl-1-picryl-hydrazyl-hydrate) free radical.

4.5. MgO-Based Biosensors towards Diabetes Detection and Treatment

Diabetes comprises a collection of severe and enduring metabolic disorders associated with elevated blood glucose levels, contributing to increased rates of premature morbidity. In spite of advancements in life's quality, there hasn't been a decline in diabetes prevalence; instead, it continues to strain global healthcare systems [195]. Often diagnosed after irreversible organ damage due to prolonged hyperglycemia, diabetes stands among the most pressing global health challenges [195], alongside cancer, chronic respiratory issues, and cardiovascular diseases, causing approximately five million deaths annually in developed nations. Notably, cardiovascular disease (50%) and kidney failure (10–20%) account for the majority of these fatalities. Diabetes also leads to complications like blindness, lower limb amputations, and severe outcomes in viral infections, such as COVID-19 [196]. The primary diabetes types include insulin-dependent or juvenile diabetes (T1DM-Type 1 Diabetes Mellitus), non-insulin-dependent (T2DM-Type 2 Diabetes Mellitus), and gestational diabetes [197]. Furthermore, less common types result from other causes like diseases of the exocrine pancreas, genetic defects in β-cell function or insulin action, endocrinopathies, and drug- or chemical-induced diabetes [198,199].

The initial and crucial aspect of managing diabetes involves diagnosis. Presently, traditional methods such as assessing fasting plasma glucose (FPG) levels, conducting oral glucose tolerance tests (OGTT), and measuring hemoglobin A1c (HbA1c) levels [200,201] are employed for diabetes diagnosis. However, the aforementioned methods are often uncomfortable and painful for patients, due to blood withdrawal, leading to potential neglect of therapy. Additionally, periodic measurements might not capture significant fluctuations in glucose levels between testing intervals. Moreover, variations in measured values can occur due to factors like timing of testing, age, and an individual's physiological state. These approaches are also unsuitable for continuous monitoring due to their laborious nature, prolonged diagnosis duration, increased blood withdrawal, and complex blood processing [202]. Notably, clinical signs of detrimental diabetes symptoms, like

hyperglycemia, are usually observed only after the disease has progressed, hindering early intervention. To mitigate these complications, it is crucial to develop diagnostic tools that are more affordable, rapid, and widely accessible [199].

Addressing these challenges, various nanotechnologies focusing on diverse biomarkers have emerged, aiming to enable early and non-invasive diabetes detection. Analyzing specific biomarkers serves as an indicator for multiple diseases [203]. Lately, there has been a notable emphasis on advancing research related to diabetes treatment through the utilization of nanoparticles. Magnesium oxide nanoparticles, in particular, have gained substantial attention among various nanoparticles and are extensively employed in biomedical studies, particularly in diabetes treatment, through a suggested mechanism depicted in Figure 15.

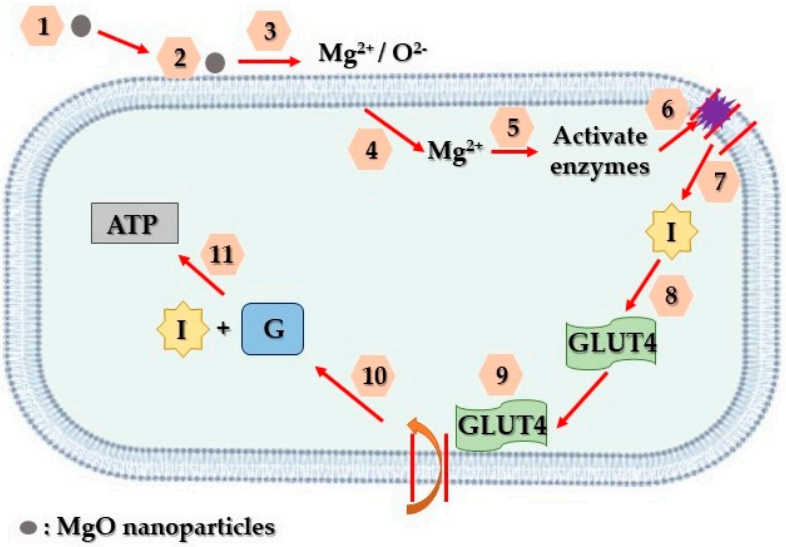

Figure 15. Schematic representation of the way that MgO nanoparticles contribute to diabetes treatment. Firstly, MgO nanoparticles adhere to the surface of affected cells (1, 2, 3). Subsequently, they discharge Mg^{2+} and O^{2-} ions, initiating the activation of internal enzymes (4, 5). These enzymes, in turn, facilitate the reversal of insulin resistance and facilitate the entry of glucose transporter 4 into the cell's plasma membrane (6, 7, 8). Ultimately, this glucose transporter enables the absorption of glucose into the cells, where insulin functions to decrease glucose levels and generate ATP (9, 10, 11).

Hilal and Han [204] suggested a simple hydrothermal approach for the fabrication of highly crystalline three-dimensional hierarchical magnesium oxide microstructures with enhanced specific surface area (79.82 m^2/g). Additionally, analyses involving Mott–Schottky and valence band assessments indicated that three-dimensional magnesium oxide displayed favorable band-edge potential conducive to redox activity, featuring conduction and valence band potentials of −2.15 and 2.29 eV, respectively. Leveraging these impressive attributes, 3D-magnesium oxide was employed as a non-enzymatic glucose-oxidizing electrode, demonstrating notable characteristics, such as high sensitivity (198 $\mu A \cdot m/M \cdot cm^2$), rapid response time (10 s), low detection limit (0.41 µM), as well as an extensive linear range (0.04–6.85 mM). Moreover, it presented exceptional selectivity, consistency, and reproducibility; maintained long-term chemical robustness; and effectively detected glucose levels in human saliva. Given these remarkable material qualities and its outstanding performance towards glucose detection, three-dimensional magnesium oxide stands as a promising candidate for prospective research endeavors (Figure 16).

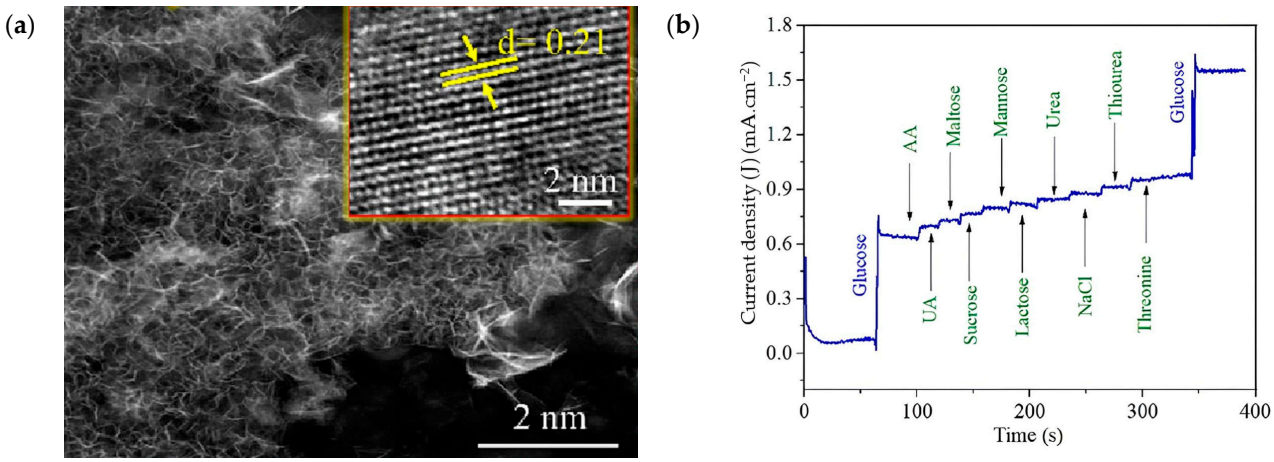

Figure 16. (**a**) HRTEM image and (**b**) selectivity towards glucose detection of the as-synthesized 3D-MgO structure. Reprinted from [204] with permission from Elsevier Copyright 2023.

Then, Mansoor and colleagues [205] synthesized Zn-doped magnesium oxide nanoflakes, applying a sol-gel method at ambient conditions, which were subsequently deposited on glassy carbon electrodes for glucose sensing. The as-developed nanosensor exhibited remarkable performance in glucose sensing, displaying a broader response range, low detection limits equal to 99 mM, and a rapid response time of five seconds, alongside a high sensitivity of 0.032 μA·m/M·cm^2. Their research's results indicated that such nanosensors hold significant potential in contributing to diabetes treatment and analysis.

Furthermore, Ullah and co-researchers [85] reported the synthesis of novel MgO entangled nanosheets (average thickness of 20 nm approximately) decorated with CdS nanoparticles (≈15 nm). The created electrodes, both in their original state and in hybrid form, were directly utilized as glucose biosensors. The hybrid electrode displayed the most enhanced sensitivity of approximately 28.570 μA·m/M·cm^2, while the pristine magnesium oxide nanosheets also exhibited a respectable sensitivity of around 12.363 μA·m/M·cm^2. Remarkably, the as-mentioned hybrid electrode demonstrated a lower detection limit of approximately 0.020 μM and a rapid response time of about 2 sec for glucose detection. This proposed biosensor exhibited prolonged robustness, increased reproducibility, exceptional repeatability, and notably enhanced selectivity, even in the presence of typical interfering substances such as uric acid, ascorbic acid, sucrose, urea, fructose, cholesterol, L-cysteine, and chloride ion, enhancing the practical application of biosensors for clinical analysis.

A glucose sensor utilizing a non-enzymatic setup employing magnesium oxide nanocubes as the basis was developed and studied by Prasanna and colleagues [206]. Throughout experimental studies, the sensing electrode demonstrated a notable shift in drain current concerning glucose concentration, ranging from 1.6 mM to 25.6 mM. The sensor's sensitivity, evaluated at 0.12 μA·m/M·cm^2, displayed a commendable linearity of 0.9701. Consequently, these findings propose that employing magnesium oxide nanocubes as sensing electrodes holds promise for real-time glucose detection, particularly in diabetes mellitus detection and treatment applications.

In addition, Tan and his team [207] exhibited that magnesium oxide nanoparticles derived from *A. tricolor* extract possessed anti-diabetic properties, notably reducing glucose concentration to a mere 0.01 μg/mL. Similarly, Jeevanandam and colleagues [208] utilized *A. tricolor* extract in the synthesis of magnesium oxide nanoparticles for treating diabetes. However, the cell viability percentage (32%) was decreased compared to magnesium oxide nanoparticles derived from *A. blitum* (33%) and *A. paniculata* (34%) extract under similar conditions. Furthermore, magnesium oxide nanoparticle application resulted in a fivefold reduction in total glucose within Vero cells.

Ammulu et al. [193] highlighted that magnesium oxide nanoparticles obtained from *P. marsupium* extract restrained protein denaturation, a factor associated with diabetes-

related inflammation, with an IC_{50} of 81.69 µg/mL. Impressively, these nanoparticles also delayed starch breakdown into glucose, thereby regulating glucose levels in diabetic individuals by inhibiting alpha-amylase, displaying an IC_{50} of 56.32 µg/mL. This outcome was significantly more optimized compared to the effectiveness of magnesium oxide nanoparticles from *H. rosa-sinensis* extract (3.27×10^5 µg/mL) as observed in the study by Kainat and colleagues [158]. Table 6 provides an overview of the as-discussed research that have studied the potential of MgO nanoparticles towards diabetes treatment.

Table 6. Performance of nano-MgO particles towards diabetes treatment.

Synthetic Approach	Main Remarks	Reference
Hydrothermal	■ Enhanced glucose sensitivity: 198 µA·m/M·cm^2. ■ Rapid response time: 10 s. ■ Low detection limit (glucose): 0.41 µM.	[204]
Sol-gel	■ Low detection limit (glucose): 99 mM. ■ Rapid response time: 5 s. ■ High glucose sensitivity: 0.032 µA·m/M·cm^2.	[205]
Anodization & Chemical Bath Deposition	■ Enhanced glucose sensitivity: ≈28.570 µA·m/M·cm^2. ■ Glucose detection limit: ≈0.020 µM. ■ Fast response time: ≈2 s.	[85]
Thermal CVD	■ Glucose sensor's sensitivity: 0.12 µA·m/M·cm^2.	[206]
Green (plant-mediated)	■ Glucose concentration = 0.01 µg/mL.	[207]
Green (plant-mediated)	■ Cell viability: 32% (*A. tricolor* leaves' extract). ■ Glucose concentration: 0.09 mg/mL (extracellular), 0.71 mg/mL (intracellular) (*A. tricolor* leaves' extract). ■ Cell viability = 33% (*A. blitum* leaves' extract). ■ Cell viability = 34% (*A. paniculata* leaves' extract).	[208]
Green (plant-mediated)	■ IC_{50} = 56.32 µg/mL (alpha-amylase inhibition). ■ IC_{50} = 81.69 µg/mL (protein inhibition).	[194]
Green (plant-mediated)	■ IC_{50} = 327 mg/mL (alpha-amylase inhibition). ■ IC_{50} = 400 mg/mL (alpha-glucosidase inhibition).	[158]

4.6. Tissue Engineering Applications

4.6.1. Bone Tissue Engineering

Enhanced biomaterials aimed at restoring bone integrity are necessary to address the escalating number of individuals grappling with deteriorating or damaged bones [209–212]. Presently, existing biomaterial solutions for this purpose involve invasive procedures that introduce permanent materials, potentially leading to prolonged issues within the body. Although progress has been made in bone defect regeneration using injectable cements and various scaffold materials, significant enhancements are still needed [213–215]. The ideal biomaterials for bone tissue regeneration should harmonize mechanically with surrounding tissue, lessening stress and strain discrepancies, while also possessing suitable chemical compositions and surface features that foster bone cell adhesion, growth, movement, and the production of proteins forming the extracellular matrix. Unfortunately, biomaterials with these desired properties are not yet available. Magnesium (Mg), an environmentally friendly, biodegradable, and biocompatible material naturally present within the human body (≈0.4 g·Mg/kg [216]), plays a role in cell–extracellular matrix interactions and influences the structure and density of bone apatite.

In their research, Hickey and colleagues [217] examined the impact of incorporating magnesium oxide nanoparticles into poly (L-lactic acid) and hydroxyapatite nanoparticle-poly (L-lactic acid) composites designed for applications in orthopedic tissue engineering. Findings demonstrated that the inclusion of magnesium oxide nanoparticles notably augmented osteoblast adhesion and proliferation on hydroxyapatite nanoparticle-poly (L-lactic acid) nanocomposites, while preserving mechanical strength, suitable for cancellous bone applications. Furthermore, when osteoblasts (cells responsible for bone formation) were cultured in the solution derived from degrading nanocomposites, their proliferation improved in the presence of magnesium. This observation suggested that the enhanced alkalinity in solutions containing magnesium oxide nanocomposites did not exert any harmful effects on the cells. Collectively, these outcomes underscore the potential for further exploration of magnesium oxide nanoparticles as supplementary materials to polymers, aiming to enhance the fusion of implanted biomaterials with bone tissues.

Furthermore, Suryavanshi and co-researchers [218] evaluated the suitability of electrospun polycaprolactone polymer composites loaded with magnesium oxide nanoparticles as scaffolds for bone-soft tissue engineering. Magnesium oxide nanoparticles were synthesized using a hydroxide precipitation sol-gel process. The nanocomposites exhibited significantly improved mechanical properties compared to the pure polymer samples, due to the even dispersion of MgO nanoparticles throughout the polymer fibers. In immersion tests, the nanocomposite scaffolds displayed notable bioactivity by developing a surface hydroxyapatite layer by the third day of incubation. The electrospun polymer mats loaded with magnesium oxide nanoparticles demonstrated enhanced in vitro biological performance with osteoblast-like MG-63 cells, showing increased adhesion, proliferation, and enhanced differentiation marker activity. In an in vivo subcutaneous implantation study using Sprague Dawley rats, initial moderate inflammatory tissue response near the implant site was observed at the second week, which subsided during the eighth week, revealing good biocompatibility without adverse effects on vital organ functionalities. Histopathological analysis, supported by serum biochemical and hematological parameters within normal physiological ranges, further confirmed the biocompatibility in vivo. Consequently, the as-proposed nanocomposite exhibited promising potential as efficient scaffold materials for bone-soft tissue engineering applications.

Safiaghdam and his team [219] outlined in their research the production and examination of a 3D-printed scaffold using fused deposition modeling, incorporating magnesium oxide nanoparticles into polycaprolactone/beta-tricalciumphosphate (PCL/β-TCP). The resultant composite scaffolds exhibited a porous structure with favorable wettability. The introduction of nanoparticles notably enhanced compressive strength, specific surface area, microenvironmental pH, degradation, and calcium release. Demonstrating promising cyto-compatibility and in vitro osteogenic potential, along with increased in vivo formation of new bone, the PCL/β-TCP scaffold containing 10 wt.% magnesium oxide nanoparticles is considered more suitable as a bone substitute for critical sized defect sites compared to the PCL/β-TCP scaffold alone. They concluded that future research could concentrate on refining-controlled magnesium release through the hierarchical design of 3D-printed scaffolds and nanoparticles' surficial alterations.

Moreover, in research by Nasri-Nasrabadi and colleagues [220], three-dimensional porous scaffolds composed of sodium alginate and magnesium oxide nanoparticles were developed, utilizing film casting and polyvinyl alcohol leaching techniques to establish an interconnected pore structure. Incorporating magnesium oxide nanoparticles into the matrix affected the mechanical characteristics of the samples, as well as their absorption and in vitro degradation tendencies. The antimicrobial properties of the nanocomposites were notably improved, due to the MgO nanoparticles' antibacterial attributes. Findings from the MTT assay as well as SEM analysis illustrated that the as-mentioned nanocomposite scaffolds facilitated cell attachment, spreading, and growth, rendering them promising candidates for bone tissue engineering applications.

Singh and colleagues [221] described the production of 58S nanobioglass via a sol-gel approach, incorporating pure magnesium oxide nanoparticles at various concentrations. In vitro assessments for bioactivity and antimicrobial properties demonstrated that the presence of magnesium oxide nanoparticles enhanced the antimicrobial activity and the ability of nanobioglass to form an apatite layer. According to the received results it was highlighted that sol-gel-derived magnesium oxide–bioglass nanocomposites could serve as a promising biomaterial platform for bone tissue regeneration.

Additionally, Derakhshankhah and his team [28] investigated the development of a promising scaffold using carbon nanofibers combined with magnesium oxide nanoparticles. Their research's findings revealed that the inclusion of magnesium oxide nanoparticles enhanced the carbon nanofibers' surficial characteristics. Moreover, in vitro assessments demonstrated that nanofibers containing magnesium oxide nanoparticles at a concentration equal to 15 wt.% exhibited the least hemolysis, indicating higher hemocompatibility. Introducing MgO nanoparticles also led to increased cell viability. The aforementioned outcomes suggested that the amalgamation of the nanofibrous structure of carbon nanofibers with the particulate nature of magnesium oxide nanoparticles yielded a nanocomposite with properties advantageous for applications in the field of bone tissue engineering.

Canales and co-researchers [222] successfully fabricated electrospun poly (lactic acid) fibers, incorporating 10 and 20 wt.% of bioactive glass and magnesium oxide nanoparticles for potential use in bone tissue engineering. The inclusion of both types of nanoparticles in electrospun poly (lactic acid) fibers was anticipated to synergistically enhance its bioactivity and antimicrobial properties. All nanobioactive glass-containing composites exhibited bioactivity by inducing the formation of hydroxyapatite structures on their surfaces. While magnesium oxide nanoparticles did not contribute to the bioactivity of the as-prepared fibers, they displayed antimicrobial properties by reducing *S. aureus* viability by approximately 30%, but no observable effect was noted on the *E. coli* strain. Poly (lactic acid) fibers/bioactive glass nanocomposites did not exhibit significant antimicrobial behavior. The diverse composites amplified alkaline phosphatase expression compared to pure poly (lactic acid) fibers, minimally affecting cell viability. As a result, a robust osteoblastic phenotype expression capacity was suggested, with poly (lactic acid) fibers/bioactive glass demonstrating the highest osteoblastic expression.

The primary aim of Ghanbari and his team's study [223] was to produce a three-dimensional nanocomposite framework integrating biosynthesized magnesium oxide nanoparticles with bacterial cellulose nanofibers, serving as a bio-scaffold intended for bone regeneration. Based on the acquired data, it was concluded that the as-proposed nanocomposite scaffolds demonstrated the capacity to enhance the osteogenic behavior of cells resembling osteoblasts, suggesting its potential as a therapeutic option for regenerating bone tissue.

The successful production of 3D composite scaffolds comprised of polycaprolactone, hydroxyapatite, and magnesium oxide nanoparticles, featuring interconnected pores through 3D printing, was achieved by Roh and colleagues [224]. Their study delved into the impacts of oxygen and nitrogen plasma treatment, as well as the addition of magnesium oxide and hydroxyapatite nanoparticles, aiming to augment the surficial properties and biological attributes of polycaprolactone scaffolds. Post-plasma-treated 3D nanocomposite scaffolds exhibited enhanced surficial hydrophilicity, accompanied by surface roughening, due to plasma-based etching. Furthermore, the incorporation of MgO and hydroxyapatite nanoparticles into the three-dimensional polycaprolactone scaffold positively affected the behaviors of preosteoblast cells, including initial adhesion, proliferation, and differentiation. Visualization through fluorescence microscopy also depicted enhanced interactions between cells and the scaffold after a two-day culture period. Conclusively, among the various samples, nitrogen plasma-treated three-dimensional polycaprolactone, hydroxyapatite, and magnesium oxide nanoparticles scaffolds displayed the highest level of bioactivity based on the team's findings (Figure 17).

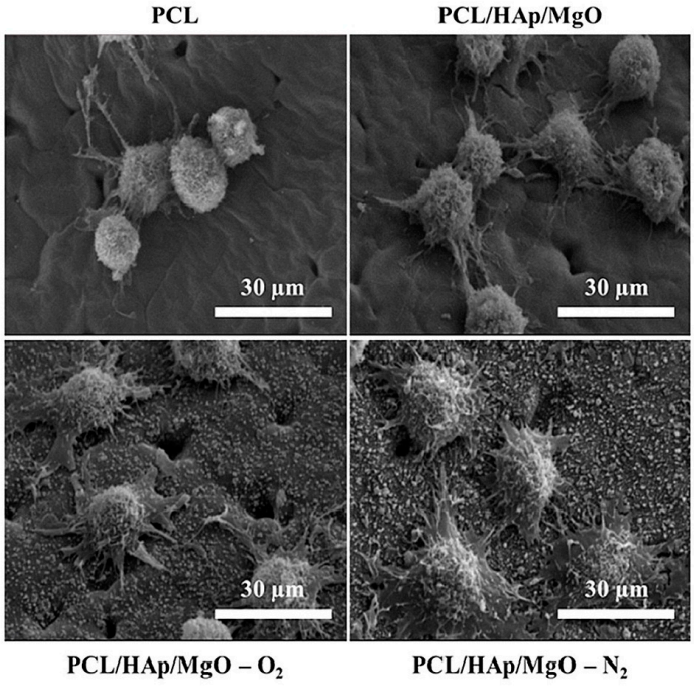

Figure 17. SEM images of the morphologies of preosteoblast MC3T3-E1 cells, cultured for 30 min on the as-prepared nanocomposite MgO-based scaffold. Reprinted from [224] with permission from Elsevier Copyright 2017.

The study of Angili and his team [225] focused on applying an alginate-MgO biomaterial onto a 3D-printed poly L-lactic acid scaffold featuring three different cellular structures. Assessments, both mechanical and biological, were conducted on a porous-coated scaffold containing varied concentrations of magnesium oxide nanoparticles, promoting poly L-lactic acid/alginate-20 wt.% magnesium oxide nanoparticle scaffolds as a promising candidate for bone tissue regeneration. Additionally, these scaffolds exhibited compatibility with blood pH and underwent antibacterial activity and MTT assays for a comprehensive biological evaluation. Their results strongly suggested the potential for constructing bone replacements with suitable mechanical and biological attributes using the as-proposed bionanocomposite material.

Nanofibrous scaffolds incorporating polycaprolactone and magnesium oxide nanoparticles were successfully fabricated by Niknam and co-researchers [226] using the electrospinning synthetic approach, intended for potential applications in bone tissue engineering. Their findings indicated that the as-developed composite nanofibers exhibited significant osteo-inductive properties and suggested that combining adipose-derived mesenchymal stem cells with the as-mentioned composite nanofibers could constitute a promising bioimplant candidate towards utilization in bone regeneration applications.

4.6.2. Skin Tissue Regeneration

The skin, being the body's largest vital organ, serves as a protective barrier against the external environment. While skin tissue possesses self-regenerating abilities, these capabilities significantly diminish in cases of full-thickness injuries, necessitating skin grafts or dressings [227]. The process of cutaneous wound healing, essential for repairing damaged skin tissue, involves several intricate stages: hemostasis, inflammation, proliferation, and remodeling [228]. Hemostasis, occurring immediately after injury, involves platelet aggregation and blood clotting. The inflammatory stage involves the presence of neutrophils and macrophages releasing cytokines at the wound site. During the proliferative phase, fibroblast differentiation leads to the initiation of re-epithelialization through the synthesis of the extracellular matrix. The final stage involves collagen synthesis and myofibroblast

activity, facilitating tissue remodeling [229,230]. These stages progress sequentially within a specific timeframe for complete healing.

Globally, various wound dressings have been developed to address epidermal damage. Traditional materials like bandages, cotton wool, lint, and gauze were historically utilized to absorb wound exudates, maintaining dryness to prevent bacterial infection [230,231]. Given the complexities of wound healing, an ideal wound dressing should possess exceptional biocompatibility to enhance tissue regeneration [232]. It should also enable gas exchange, shield the wound from microbial infections, absorb excess fluids without leakage, and be non-adherent and comfortable [233]. As a result, novel materials meeting the aforementioned characteristics need to be developed. Amongst them, MgO-based nanomaterials have gained considerable researchers' attention within the last decade, given the fact that magnesium oxide is considered to be biologically safe, capable of biodegradation, cost-effective, and environmentally friendly, holding significant promise for various biomedical applications [234].

In a study conducted by Verma and colleagues [234], films composed of carboxy methyl cellulose and poly vinyl alcohol were successfully produced and evaluated for their potential application in skin tissue engineering. Through comprehensive characterization, the carboxy methyl cellulose/poly vinyl alcohol composition ratio of 50:50 emerged as the most advantageous, exhibiting tensile strength comparable to human skin in both dry and wet conditions, along with desirable hydrophilicity. Additionally, the as-proposed film exhibited surficial roughness conducive to cell adhesion, controlled degradation, and swelling, while the incorporation of magnesium oxide nanoparticles conferred antimicrobial properties to the polymer film. Moreover, the presence of magnesium oxide nanoparticles positively influenced cell viability, with the carboxy methyl cellulose/poly vinyl alcohol film containing 1.5 wt.% magnesium oxide nanoparticles demonstrating superior cell viability, holding promise as a potential material for future engineered skin tissue grafts.

The primary impediment in the healing process of diabetic wounds is insufficient angiogenesis. Based on existing scientific reports, electrospun nanofiber membranes have demonstrated potential as wound dressings. To effectively address diabetic wounds, it is crucial for electrospun membranes to stimulate wound angiogenesis. Current strategies predominantly focus on employing pro-angiogenic growth factors to augment the angiogenic properties of these membranes. However, integrating growth factors into electrospun nanofibers and sustaining their activity long-term pose technical challenges. Taking the aforementioned into consideration, Liu and co-researchers [29] introduced an electrospun membrane comprising polycaprolactone, gelatin, and magnesium oxide nanoparticles, releasing Mg^{2+} ions to further promote angiogenesis. The as-prepared membranes encouraged human umbilical vein endothelial cell proliferation and enhanced vascular endothelial growth factor production in vitro. Implantation studies in a rat model reveal that the MgO-included membrane facilitated the early formation of robust blood vessels within a week post surgery, fostering enriched capillary networks within the degrading membrane over time. Moreover, these membranes significantly expedited diabetic wound healing by mitigating inflammatory responses, fostering angiogenesis, and enhancing granulation formation. Their research findings suggested the potential for purposefully designed magnesium-infused electrospun membranes with heightened pro-angiogenic properties for treating diabetic wounds. In Table 7 are presented selected studies of MgO-based materials utilized in tissue engineering applications.

Table 7. MgO-based materials towards tissue engineering applications.

Proposed MgO-Based Material	Main Remarks	Reference
Bone tissue engineering		
MgO-HA-PLLA nanocomposite	■ Amplification of osteoblasts' adhesion and proliferation. ■ Preservation of mechanical strength. ■ No harmful effects on cells, due to increased solution's alkalinity.	[217]
MgO-PCL nanocomposite fibers	■ Enhanced mechanical properties. ■ Increased bioactivity. ■ Good biocompatibility.	[218]
PCL/β-TCP/nano-MgO scaffolds	■ Cyto-compatibility. ■ In vitro osteogenic potential. ■ In vivo new bone formation. ■ Increased compressive strength and Ca^{2+} release.	[219]
MgO-bioglass nanoparticles	■ Enhanced bioactivity and antimicrobial attributes.	[221]
MgO nanoparticles-BC scaffold	■ Ability to increase cells' osteogenic behavior.	[223]
PLA/alginate/MgO scaffold	■ Proper mechanical and biological attributes for developing bone replacements.	[225]
MgO/PCL nanofibrous scaffolds	■ Enhanced osteo-inductive attributes.	[226]
Skin tissue engineering		
CMC/PVA/MgO composite films	■ Exceptional cell viability and antimicrobial attributes.	[234]
PCL/gelatin/MgO membrane	■ Facilitation of robust blood vessels' early formation and diabetic wound healing.	[29]

4.7. Bioimaging Applications

Extensive research focuses on fluorescent nanoparticles to enable real-time bioimaging and tracking of biological processes at the nanoscale. These nanoparticles hold promise for advancing diagnostic tools and targeted drug release therapies. Metal oxide nanoparticles [235–237] have gained attention as contrast agents in bioimaging, due to their room-temperature single-photon emission [235,237], customizable optical properties [238], and low toxicity. However, challenges persist in their application, such as low quantum efficiency and brightness [236,237], propensity for agglomeration in cell culture media [236], and dose-dependent cytotoxicity [239]. For instance, zinc oxide exhibits broad visible region emissions attributed to crystallographic defects, suitable for in vitro experiments but suffering from limited photostability in cellular environments, such as photobleaching or photo-blinking [235,237].

For effective in vitro experiments, a fluorescent marker must absorb light above 500 nm and emit light beyond 600 nm to mitigate cell autofluorescence [240]. In contrast, for in vivo experiments, emission in the near-infrared (NIR) range, between 700 and 900 nm, is crucial as it penetrates tissue over centimeters, unlike visible light, which travels mere microns [241]. Magnesium oxide nanoparticles apart from being biocompatible and biodegradable as previously mentioned, are also intrinsically fluorescent [242].

Taking the aforementioned into account, Rasheed and Sandhyarani [243] conducted the synthesis of luminescent nanocrystals of magnesium oxide by introducing a very low amount of Cr^{3+} as a dopant. The production of chromium-doped magnesium oxide nanocrystals involved the use of magnesium nitrate as the base material and chromic nitrate as the doping agent. Notably, upon doping with 2 wt.% Cr^{3+}, magnesium oxide nanocrystals displayed the highest intensity of green fluorescence. To assess cytotoxicity towards normal cells, an Alamar blue assay was performed. Furthermore, the nanocrystals exhibited promising potential for cellular imaging, showcasing strong fluorescence when utilized with cancer cells (HeLa) during imaging applications.

Additionally, in a study by Khalid and co-researchers [242], the inherent and enduring fluorescent characteristics of magnesium oxide nanoparticles derived from naturally present chromium Cr^{3+} and vanadium V^{2+} ions were detailed. These properties encompassed a fluorescence spectrum spanning from the visible to the near-infrared range, enabling their potential utilization for real-time monitoring of live cells derived from both normal and cancerous tissues.

In another study by Khalid and his team [30], magnesium oxide nanoparticles were encased within silk fibroin protein using microfluidics, resulting in the creation of composite spheres. Through real-time wide-field fluorescence imaging, the as-prepared hybrid spheres demonstrated promising capabilities as vivid cell imaging agents for HaCaT, U87MG, and MCF7 cell lines. Their preliminary findings envisioned as the initial stride towards the broad adoption of biodegradable MgO-based spheres, serving as fluorescent markers in short-term bioimaging applications.

Furthermore, Xie and colleagues [244] developed hierarchical clusters of magnesium oxide nanocrystals that exhibited multiple fluorescence properties at the interface of organic and inorganic components. This induced a distinctive fluorescence resonance energy transfer, due to the alignment of energy levels at the interface and low-coordinated states. To enhance their water solubility and stability for potential use in cellular imaging, these multi-fluorescent MgO nanocrystals were encapsulated within a silica shell. As anticipated, the resulting core-shell ($MgO@SiO_2$) nanocrystals demonstrated excellent biocompatibility and performed exceptionally well in cellular imaging applications.

4.8. Drug Delivery Applications

Nanotechnology offers promising avenues in drug delivery, especially for combating terminal illnesses such as cancer [245–247]. Previous studies have explored the utilization of nanostructures to administer drugs [248,249], and nanoparticles have shown potential in targeting specific cell genes, particularly those in tumor cells. Nanostructures possess advantageous qualities, including a significant volume-to-surface ratio, customizable surface properties, and multifunctionality, making them appealing for drug delivery applications [250–252]. Additionally, the stability of MgO nanostructures under harsh conditions, coupled with their suitability for human administration, further enhances their viability in drug delivery. The assessment of these systems included considerations related to the rheological behavior of hydrogels and the crosslinking degree of polymers.

Sabbagh and Muhamad [253] employed acrylamide-based hydrogel systems for drug delivery, specifically for the release of Acyclovir from magnesium oxide nanocomposite hydrogel (Figure 18). Acyclovir was incorporated into the polymer through a soaking process, enabling the hydrogel system for use in vaginal drug delivery and subsequent release. An assessment of the chemical and physical properties of the reinforced hydrogels provided an analysis of the polymer's morphological structure, swelling behavior, gel formation, and physical attributes. The drug release behavior in different mediums, PBS and SVF aqueous solutions, was examined, and the quantity of the released drug was determined using HPLC. Furthermore, the pH responsiveness and in vitro drug release from the hydrogels were explored across three pH levels: 4, 6, and 8.

El-Sawy and his team [31] presented findings on nanocomposite hydrogels consisting of copolymers derived from natural polymers such as Xanthan gum (Xan), magnesium oxide (MgO), and acrylic acid (AAc), synthesized using radiation-induced copolymerization and crosslinking techniques for drug delivery applications. The presence of magnesium oxide had a diminishing effect on gelation degree, while concurrently improving network porosity and swelling capacity. The (Xan-AAc)/MgO nanocomposites exhibited characteristic pH-dependent swelling behavior. Additionally, the swelling kinetics indicated Fickian behavior at pH = 1 and non-Fickian behavior at pH = 7 for all tested specimens. Methotrexate (MTX), an anticancer model drug, was used to evaluate the potential of the obtained (Xan-AAc)/MgO nanocomposites as a drug carrier. Incorporating MgO into the (Xan-AAc) hydrogel increased the efficiency of drug loading and maximized the release of MTX in

simulated intestinal conditions (pH = 7). The drug release pattern corresponded with the results from the swelling tests, indicating the potential suitability of (Xan-AAc)/MgO nanocomposite hydrogels as a targeted drug delivery system.

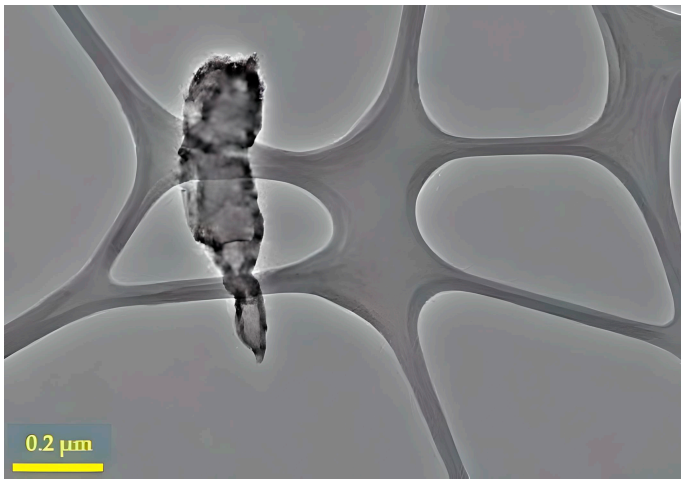

Figure 18. TEM image of Acyclovir's dispersion in the MgO nanocomposite hydrogel. Reprinted from [253] with permission from Elsevier Copyright 2017.

5. Current Limitations

5.1. Toxicity of MgO Nanoparticles

MgO nanoparticles are efficiently produced using eco-friendly synthesis methods [254,255]. Research suggests that nanoparticles might instigate oxidative stress, inflammation, and indirect DNA damage in biological systems [256]. The perceived toxicity of MgO NPs is linked to their generation of reactive oxygen species [257]. Exposure to these nanoparticles can lead to ROS-induced oxidative harm to DNA, protein denaturation, and lipid peroxidation [258]. Additionally, while it is established that MgO nanoparticles release substantial quantities of Mg ions, these ions are recognized as potent sources of toxicity, differing significantly from the effects of other ions like Zn^{2+} ions released from ZnO [257].

Nanoparticles such as magnesium oxide can permeate the skin, respiratory system, and digestive tract, accumulating in specific tissues [259]. Investigating the potential toxic impacts of these nanoparticles is crucial as their effects on cells and organs remain largely unknown [260]. Certain studies have delved into the toxic effects of magnesium oxide nanoparticles utilizing model organisms, such as fish.

Thomas and colleagues [261] conducted research on the toxicity of MgO nanoparticles measuring less than 50 nm in tilapia and zebrafish. Their findings revealed that bulk MgO particles exhibited higher toxicity compared to nanoparticles. In zebrafish, exposure to MgO nanoparticles did not cause mortality, whereas exposure to bulk particles resulted in 100% mortality at just 10 ppm. Assessing biochemical and antioxidant parameters, the study indicated an increase in the activity of catalase, glutathione S-transferase, and superoxide dismutase with rising nanoparticle concentrations. In a separate investigation evaluating acute toxicities of 31 different nanoparticles in zebrafish [262], it was highlighted that MgO nanoparticles led to cumulative mortality in this species.

Kumaran's research focused on 20 nm MgO nanoparticles and their impact through the GST and ROS gene mechanism. The results demonstrated that the presence of 150 µg/mL of magnesium oxide nanoparticles in the dispersions released considerable cytotoxins [263].

As a result, MgO nanoparticles have gained attention in tumor treatment [25], demonstrating the ability to eradicate cancer cells while elucidating the mechanisms behind cell death caused by MgO exposure [264]. The toxic mechanisms of these nanoparticles primarily revolve around two characteristics: inducing oxidative stress within cells due to intracellular nanoparticles and the dissolution of the nanoparticles. Both extracellular

magnesium and nanoparticles traverse the cell membrane, entering the cytoplasm via respective magnesium and endocytosis transport proteins.

5.2. Oxidative Stress

Scientific evidence has confirmed that nanoparticles induce cell damage primarily through oxidative stress and the generation of reactive oxygen species [265]. Even minute amounts of nanoparticles in cells can result in the production of substantial quantities of ROS [266]. These ROS variants, such as $\bullet O_2^-$, H_2O_2, and •OH, are formed by disturbing the cell's electron transport chain [267]. Mitochondria serve as crucial intracellular sources of ROS [268]. Hydroxyl radicals, among the ROSs, exhibit heightened reactivity compared to other radicals, leading to oxidation within most cell components [269]. The aggregation of ROS can culminate in the generation of $\bullet O_2^-$, due to electron capture on nanoparticle surfaces [270]. The surge in free radicals due to ROS accumulation can trigger an antioxidant defense mechanism, albeit excessively oxidizing lipids, denaturing proteins, and modifying nucleic acids, leading to an imbalance between antioxidant and oxidant processes [265]. MgO nanoparticles inhibit lysosomal activity in acidic conditions and disrupt lysosomal membranes, potentially translocating nanoparticles to the nucleus and mitochondria [271,272]. Nanoparticle entry into mitochondria can elevate membrane depolarization by nanoparticle deposition, disrupting electron transport in the inner membrane, ultimately leading to membrane permeation and ROS production [268,273]. ROS within lysosomes can lead to the destruction of the DNA double helix or induce DNA point mutations [274].

Mitochondrial respiration and apoptosis pathways can be impacted by ROS within mitochondria, causing lipid peroxidation in the cell membrane, cellular redox imbalance, and initiating certain antioxidant responses [268]. H_2O_2 generated in the cytoplasm easily diffuses through mitochondrial membranes, leading to the formation of •OH radicals through the Fenton reaction, eventually resulting in DNA damage and programmed cell death [268]. Nanoparticles can amplify intracellular ROS production, potentially intensifying cell death signaling and activating redox-sensitive signaling pathways at moderate levels of oxidative stress [265,275,276]. Inflammatory responses are initiated by signaling cascades involving nuclear factor NF-kB and the activation of mitogen-activated protein kinase (MAPK), both closely linked to cellular death and fibrosis [276]. Moreover, nanoparticles are capable of reaching the nucleus by causing direct physical damage to the nuclear membrane and interacting directly with nuclear DNA through nuclear pores (sized less than 50 nm) [272].

5.3. Dissolution

The release of Mg^{2+} from the surface of MgO nanoparticles is considered a significant factor contributing to their heightened toxicity in organisms [273]. A substantial amount of Mg^{2+} can leach from the solid phase both in cell mediums and suspensions, leading to the generation of substantial quantities of •OH through Fenton-like reactions, causing damage to lipids, proteins, and nucleic acids [277,278]. Additionally, intracellular nanoparticles entering acidic organelles like lysosomes or encountering acidic substances can further release Mg^{2+}, contributing to DNA and oxidative damage [279]. The dissolution process is influenced by particle characteristics (e.g., surface area, size, chemical composition) and environmental factors such as temperature, pH, and organic content. Mg^{2+} can form chelates by reacting with electron pair donors, potentially inhibiting normal physiological processes by interacting with coordinating atoms like nitrogen and oxygen [274]. Intracellular nanoparticles may access the nucleus through nucleopores or during cell division, inhibiting translation and transcription machinery and potentially causing genetic material damage by interacting with DNA or related proteins, thus triggering signaling cascades and disrupting cellular processes [274,280]. Moreover, released Mg^{2+} from nanoparticles might degrade mRNA by directly interacting with mRNA stabilizing proteins [281], underscoring Mg^{2+}'s crucial role in maintaining cellular homeostasis [279].

An elevation in the release of Mg^{2+} from nanoparticles can significantly disrupt the balance of the metal cation's homeostatic mechanisms. Conversely, Mg^{2+} ions have the capability to augment the local intracellular Mg^{2+} concentration [267], serving as a trigger for Mg^{2+} influx through Ca^{2+} channels between the endoplasmic reticulum and plasma membrane [282]. Intracellular Mg^{2+} is involved in numerous cellular processes, including activation of transcription factors like NF-kB [283], nitric oxide production, protein secretion, and the generation of superoxide anions, potentially leading to mitochondrial disturbances and cellular damage [267,284,285].

6. Future Prospects

Although several studies in this promising research field regarding the biomedical applications of MgO nanoparticles are ongoing, further investigation is warranted to elucidate the precise mechanism involved in the synthesis of MgO nanoparticles, aiming for a deeper comprehension of the chemical reactions occurring throughout the synthesis process, while comprehensive studies are essential to optimize diverse reaction conditions.

Notably, synthesized MgO nanoparticles have demonstrated robust antimicrobial properties against various bacterial and pathogenic fungal strains. As a result, there is a need for more extensive testing of the antifungal and antimicrobial properties of synthesized MgO nanoparticles against a diverse range of pathogenic and drug-resistant fungal strains. Also, the antiprotozoal activity of MgO is under consideration, especially against *Cyclospora cayetanensis* oocysts [286], and this is might interesting also in veterinary. The anti-virus activity of MgO nanoparticles is a very challenging research field, and it is approached directly (fighting a virus itself) or indirectly (fighting potential factors of virus spread, such as mosquitos). Thus, there are some interesting results against the anti-foot-and-mouth disease, which is a contagious viral disease of cloven-hoofed animals [287]. Moreover, there is evidence that MgO nanoparticles possess effective antilarvicidal properties [288]. Some scientific efforts have been made focusing on the use of magnesium oxide based on its antibiofilm properties [289], and the findings are quite promising in several fields, such as dentistry [290,291], and hopefully this potential of MgO will be soon exploited. Furthermore, in dentistry, the presence of MgO nanoparticles seems to reduce the corrosion resistance and compressive strength of implants; thus, they might be widely used in the near future [290,291].

Additionally, these nanoparticles have been found to possess noteworthy antioxidant characteristics, so further exploration into the antioxidant capabilities of synthesized magnesium oxide nanoparticles should involve conducting in vivo or intracellular experiments. The anti-inflammatory properties of MgO are very important, and preliminary results in the field of inhibition of protein denaturation have shown their importance [292].

Furthermore, magnesium oxide nanoparticles have shown substantial effectiveness in combating different types of cancer cells and have presented great performance in bioimaging and drug delivery applications. Particularly in bioprinting for tissue engineering, it has been shown that MgO released from 3D-printed tricalcium phosphate scaffolds accelerated bone formation and increased angiogenesis in implants in rat models [293].

It might also be noteworthy to mention that data mining and machine learning approaches should be used in the design, development, and prediction of the biological activity of MgO, since it is already widespread for other types of nanomaterials and especially for nanocarriers. Since there is a gap in this field, we hope to see it filled soon because these approaches could provide accuracy and optimization, preventing unnecessary experimental repetitions, protecting from environmental burdens, and decreasing any costs.

7. Conclusions

This review encompasses an examination of ongoing research regarding the fabrication of magnesium oxide nanoparticles through several synthetic approaches and their notable applications in the biomedical field, specifically their roles in combating bacterial

and fungal infections, their demonstrated effects against cancer and as antioxidants, and also their potential in tissue engineering, bioimaging, and drug delivery applications, including detailed elucidations of their mechanisms of action. Moreover, studies evaluating the toxicity of produced magnesium oxide nanoparticles have indicated their significant biocompatibility. Further investigation is warranted to elucidate the precise mechanism involved in the synthesis of MgO nanoparticles, aiming for a deeper comprehension of the chemical reactions occurring throughout the synthesis process, while comprehensive studies are essential to optimize diverse reaction conditions.

However, there remains a lack of comprehensive understanding regarding the biomedical hurdles concerning the biocompatibility of MgO nanomaterials. There is an evident necessity for additional research to thoroughly examine the innocuous nature and safety profile of synthesized magnesium oxide nanoparticles. Concurrently, with the recent utilization of MgO-based nanomaterials in cancer therapy, a critical issue arises pertaining to the necessary evaluation of the selectivity between cancerous cells and healthy cells directly within the human body, so in vivo toxicity studies should be performed to explore their potential for clinical utilization.

Author Contributions: Conceptualization, M.-A.G., N.L. and E.A.P.; methodology, M.-A.G., E.S. and P.D.; validation, M.-A.G., E.S., P.D. and N.L.; formal analysis, M.-A.G. and N.L.; investigation, M.-A.G., E.S., P.D. and N.L.; resources, E.A.P.; writing—original draft preparation, M.-A.G. and E.A.P.; writing—review and editing, M.-A.G., E.S., P.D., N.P., M.G., N.L. and E.A.P.; visualization, M.-A.G. and N.L.; supervision, E.A.P. All authors have read and agreed to the published version of the manuscript.

Funding: This research received no external funding.

Data Availability Statement: No new data were created or analyzed in this study. Data sharing is not applicable to this article.

Conflicts of Interest: The authors declare no conflicts of interest.

References

1. Singh, T.A.; Das, J.; Sil, P.C. Zinc oxide nanoparticles: A comprehensive review on its synthesis, anticancer and drug delivery applications as well as health risks. *Adv. Colloid Interface Sci.* **2020**, *286*, 102317. [CrossRef]
2. Thakur, N.; Thakur, S.; Chatterjee, S.; Das, J.; Sil, P.C. Nanoparticles as smart carriers for enhanced cancer immunotherapy. *Front. Chem.* **2020**, *8*, 1217. [CrossRef] [PubMed]
3. Thakur, N.; Manna, P.; Das, J. Synthesis and biomedical applications of nanoceria, a redox active nanoparticle. *J. Nanobiotechnol.* **2019**, *17*, 84. [CrossRef] [PubMed]
4. Tejwan, N.; Saha, S.K.; Das, J. Multifaceted applications of green carbon dots synthesized from renewable sources. *Adv. Colloid Interface Sci.* **2020**, *275*, 102046. [CrossRef] [PubMed]
5. Thakur, N.; Das, J.; Sil, R.C. Emerging role of redox-active nanoceria in cancer therapeutics via oxidative stress. In *Handbook of Oxidative Stress in Cancer: Therapeutic Aspects*; Chakraborti, S., Ed.; Springer: Singapore, 2021; pp. 1–23.
6. Rana, A.; Yadav, K.; Jagadevan, S. A comprehensive review on green synthesis of nature-inspired metal nanoparticles: Mechanism, application and toxicity. *J. Clean. Prod.* **2020**, *272*, 122880. [CrossRef]
7. Rafique, M.; Sadaf, I.; Rafique, M.S.; Tahir, M.B. A review on green synthesis of silver nanoparticles and their applications. *Artif. Cells Nanomed. Biotechnol.* **2017**, *45*, 1272–1291. [CrossRef]
8. Bandeira, M.; Giovanela, M.; Roesch-Ely, M.; Devine, D.M.; da Silva Crespo, J. Green synthesis of zinc oxide nanoparticles: A review of the synthesis methodology and mechanism of formation. *Sustain. Chem. Pharm.* **2020**, *15*, 100223. [CrossRef]
9. Yildiz, Y.; Okyay, T.O.; Sen, B.; Gezer, B.; Kuzu, S.; Savk, A.; Demir, E.; Dasdelen, Z.; Sert, H.; Sen, F. Highly monodisperse Pt/Rh nanoparticles confined in the graphene oxide for highly efficient and reusable sorbents for methylene blue removal from aqueous solutions. *ChemistrySelect* **2017**, *2*, 697–701. [CrossRef]
10. Göksu, H.; Çelik, B.; Yıldız, Y.; Şen, F.; Kılbaş, B. Superior monodisperse CNT-supported CoPd (CoPd@CNT) nanoparticles for selective reduction of nitro compounds to primary amines with $NaBH_4$ in aqueous medium. *ChemistrySelect* **2016**, *1*, 2366–2372. [CrossRef]
11. Sen, B.; Şavk, A.; Sen, F. Highly efficient monodisperse Pt nanoparticles confined in the carbon black hybrid material for hydrogen liberation. *J. Colloid Interface Sci.* **2018**, *520*, 112–118. [CrossRef]
12. Şen, B.; Aygün, A.; Şavk, A.; Akocak, S.; Şen, F. Bimetallic palladium-iridium alloy nanoparticles as highly efficient and stable catalyst for the hydrogen evolution reaction. *Int. J. Hydrogen Energy* **2018**, *43*, 20183–20191. [CrossRef]

13. Amina, M.; Al Musayeib, N.M.; Alarfaj, N.A.; El-Tohamy, M.F.; Oraby, H.F.; Al Hamoud, G.A.; Bukhari, S.I.; Moubayed, N.M.S. Biogenic green synthesis of MgO nanoparticles using *Saussurea costus* biomasses for a comprehensive detection of their antimicrobial, cytotoxicity against MCF-7 breast cancer cells and photocatalysis potentials. *PLoS ONE* **2020**, *15*, e0237567. [CrossRef]
14. Danish, M.S.S.; Bhattacharya, A.; Stepanova, D.; Mikhaylov, A.; Grilli, M.L.; Khosravy, M.; Senjyu, T. A Systematic Review of Metal Oxide Applications for Energy and Environmental Sustainability. *Metals* **2020**, *10*, 1604. [CrossRef]
15. Abdel-Aziz, M.M.; Emam, T.M.; Elsherbiny, E.A. Bioactivity of magnesium oxide nanoparticles synthesized from cell filtrate of endobacterium *Burkholderia rinojensis* against *Fusarium oxysporum*. *Mater. Sci. Eng. C* **2020**, *109*, 110617. [CrossRef]
16. Aničić, N.; Vukomanović, M.; Koklič, T.; Suvorov, D. Fewer defects in the surface slows the hydrolysis rate, decreases the ROS generation potential, and improves the non-ROS antimicrobial activity of MgO. *Small* **2018**, *14*, 1800205. [CrossRef]
17. Anand, K.V.; Anugraga, A.R.; Kannan, M.; Singaravelu, G.; Govindaraju, K. Bio-engineered magnesium oxide nanoparticles as nano-priming agent for enhancing seed germination and seedling vigour of green gram (*Vigna radiata* L.). *Mater. Lett.* **2020**, *271*, 127792. [CrossRef]
18. Verma, S.K.; Nisha, K.; Panda, P.K.; Patel, P.; Kumari, P.; Mallick, M.A.; Sarkar, B.; Das, B. Green synthesized MgO nanoparticles infer biocompatibility by reducing in vivo molecular nanotoxicity in embryonic zebrafish through arginine interaction elicited apoptosis. *Sci. Total Environ.* **2020**, *713*, 136521. [CrossRef] [PubMed]
19. Khan, A.; Shabir, D.; Ahmad, P.; Khandaker, M.U.; Faruque, M.R.I.; Din, I.U. Biosynthesis and antibacterial activity of MgO-NPs produced from Camellia-sinensis leaves extract. *Mater. Res. Express* **2020**, *8*, 15402. [CrossRef]
20. Essien, E.R.; Atasie, V.N.; Okeafor, A.O.; Nwude, D.O. Biogenic synthesis of magnesium oxide nanoparticles using *Manihot esculenta* (Crantz) leaf extract. *Int. Nano Lett.* **2020**, *10*, 43–48. [CrossRef]
21. Tang, Z.X.; Lv, B.F. MgO nanoparticles as antibacterial agent: Preparation and activity. *Braz. J. Chem. Eng.* **2014**, *31*, 591–601. [CrossRef]
22. El-Sayyad, G.S.; Mosallam, F.M.; El-Batal, A.I. One-pot green synthesis of magnesium oxide nanoparticles using *Penicillium chrysogenum* melanin pigment and gamma rays with antimicrobial activity against multidrug-resistant microbes. *Adv. Powder Technol.* **2018**, *29*, 2616–2625. [CrossRef]
23. Maji, J.; Pandey, S.; Basu, S. Synthesis and evaluation of antibacterial properties of magnesium oxide nanoparticles. *Bull. Mater. Sci.* **2020**, *43*, 25. [CrossRef]
24. Castillo, I.F.; Guillén, E.G.; Jesús, M.; Silva, F.; Mitchell, S.G. Preventing fungal growth on heritage paper with antifungal and cellulase inhibiting magnesium oxide nanoparticles. *J. Mater. Chem. B* **2019**, *7*, 6412–6419. [CrossRef] [PubMed]
25. Di, D.R.; He, Z.Z.; Sun, Z.Q.; Liu, J. A new nano-cryosurgical modality for tumor treatment using biodegradable MgO nanoparticles. *Nanomedicine* **2012**, *8*, 1233–1241. [CrossRef] [PubMed]
26. Krishnamoorthy, K.; Moon, J.Y.; Hyun, H.B.; Cho, S.K.; Kim, S.J. Mechanistic investigation on the toxicity of MgO nanoparticles toward cancer cells. *J. Mater. Chem.* **2012**, *22*, 24610–24617. [CrossRef]
27. Moeini-Nodeh, S.; Rahimifard, M.; Baeeri, M.; Abdollahi, M. Functional improvement in rats' pancreatic islets using magnesium oxide nanoparticles through antiapoptotic and antioxidant pathways. *Biol. Trace Elem. Res.* **2017**, *175*, 146–155. [CrossRef] [PubMed]
28. Derakhshankhah, H.; Nekounam, H.; Izadi, Z.; Allahyari, Z.; Samari, M.; Feizi, M.; Samadian, H. Fabrication of electroactive nanocomposite based on carbon nanofibers/magnesium oxide nanoparticles for bone tissue engineering. *J. Drug Deliv. Sci. Technol.* **2023**, *89*, 105082. [CrossRef]
29. Liu, M.; Wang, R.; Liu, J.; Zhang, W.; Liu, Z.; Lou, X.; Nie, H.; Wang, H.; Mo, X.; Abd-Elhamid, A.I.; et al. Incorporation of magnesium oxide nanoparticles into electrospun membranes improves pro-angiogenic activity and promotes diabetic wound healing. *Biomater. Adv.* **2022**, *133*, 112609. [CrossRef]
30. Li, J.; Khalid, A.; Verma, R.; Abraham, A.; Qazi, F.; Dong, X.; Liang, G.; Tomljenovic-Hanic, S. Silk Fibroin Coated Magnesium Oxide Nanospheres: A Biocompatible and Biodegradable Tool for Noninvasive Bioimaging Applications. *Nanomaterials* **2021**, *11*, 695. [CrossRef]
31. El-Sawy, N.M.; Raafat, A.I.; Badawy, N.A.; Mohamed, A.M. Radiation development of pH-responsive (xanthan-acrylic acid)/MgO nanocomposite hydrogels for controlled delivery of methotrexate anticancer drug. *Int. J. Biol. Macromol.* **2020**, *142*, 254–264. [CrossRef]
32. Manzetti, S.; Yakovlev, A. Quantum chemical study of regular and irregular geometries of MgO nanoclusters: Effects on magnetizability, electronic properties and physical characteristics. *Mater. Chem. Phys.* **2017**, *199*, 7–17. [CrossRef]
33. Pacchioni, G.; Freund, H. Electron transfer at oxide surfaces. The MgO paradigm: From defects to ultrathin films. *Chem. Rev.* **2013**, *113*, 4035–4072. [CrossRef]
34. Sternig, A.; Koller, D.; Siedl, N.; Diwald, O.; Mc Kenna, K. Exciton formation at solid-solid interfaces: A systematic experimental and ab Initio study on compressed MgO nanopowders. *J. Phys. Chem. C* **2012**, *116*, 10103–10112. [CrossRef]
35. Bailly, M.L.; Costentin, G.; Pernot, H.L.; Krafft, J.M.; Che, M. Physicochemical and in-situ photoluminescence study of the reversible transformation of oxide ions of low coordination into hydroxyl groups upon interaction of water and methanol with MgO. *J. Phys. Chem. B* **2005**, *169*, 2404–2413. [CrossRef]
36. Malykhin, S.E.; Volodin, A.M.; Bedilo, A.F.; Zhidomirov, G.F. Generation of O^- radical anions on MgO surface: Long-distance charge separation or homolytic dissociation of chemisorbed water? *J. Phys. Chem. C* **2009**, *113*, 10350–10353. [CrossRef]

37. Hemmingson, S.L.; Feeley, G.M.; Miyake, N.J.; Campbell, C.T. Energetics of 2D and 3D gold nanoparticles on MgO(100): Influence of particle size and defects on gold adsorption and adhesion energies. *ACS Catal.* **2017**, *7*, 2151–2163. [CrossRef]
38. Petitjean, H.; Guesmi, H.; Lauron-Pernot, H.; Costentin, G.; Loffreda, D.; Sautet, P.; Delbecq, F. How surface hydroxyls enhance MgO reactivity in basic catalysis: The case of methylbutynol conversion. *ACS Catal.* **2014**, *4*, 4004–4014. [CrossRef]
39. Singh, J.P.; Won, S.O.; Lim, W.C.; Chae, K.H. Optical behavior of MgO nanoparticles investigated using diffuse reflectance and near edge X-ray absorption spectroscopy. *Mater. Lett.* **2017**, *198*, 34–37. [CrossRef]
40. Yin, D.; Chen, C.; Saito, M.; Inoue, K.; Ikuhara, Y. Ceramic phases with one-dimensional long-range order. *Nat. Mater.* **2019**, *18*, 19–23. [CrossRef]
41. Müller, M.; Stankic, S.; Diwald, O.; Knözinger, O.; Sushko, P.V.; Trevisanutto, P.E.; Shluger, A.L. Effect of protons on the optical properties of oxide nanostructures. *J. Am. Chem. Soc.* **2007**, *129*, 12491–12496. [CrossRef]
42. Subramanian, M.A.; Shannon, R.D.; Chai, B.H.T.; Abraham, M.M.; Wintersgill, M.C. Dielectric constants of BeO, MgO, and CaO using the two-terminal method. *Phys. Chem. Miner.* **1989**, *16*, 741–746. [CrossRef]
43. Talukdar, T.K.; Liu, S.; Zhang, Z.; Harwath, F.; Girolami, G.S.; Abelson, J.R. Conformal MgO film grown at high rate at low temperature by forward-directed chemical vapor deposition. *J. Vac. Sci. Technol.* **2018**, *36*, 051504. [CrossRef]
44. Thorp, J.S.; Enayati-Rad, N. The dielectric behaviour of single-crystal MgO, Fe/MgO and Cr/MgO. *J. Math. Sci.* **1981**, *16*, 255–260. [CrossRef]
45. Liu, J.; Wang, W.; Guo, Z.; Zeng, W.R.; Dou, S.; Chen, X. Peashell-like nanostructure-a new kind of one-dimensional nanostructure: The case of magnesium oxide. *Chem. Commun.* **2010**, *46*, 3887–3889. [CrossRef] [PubMed]
46. Hornak, J.; Trnka, P.; Kadlec, P.; Michal, O.; Mentlik, V.; Sutta, P.; Csanyi, G.M.; Tamus, Z.A. Magnesium oxide nanoparticles: Dielectric properties, surface functionalization and improvement of epoxy-based composites insulating properties. *Nanomaterials* **2018**, *8*, 381. [CrossRef] [PubMed]
47. Bhargava, R.; Khan, S. Superior dielectric properties and bandgap modulation in hydrothermally grown Gr/MgO nanocomposite. *Phys. Lett.* **2019**, *383*, 1671–1676. [CrossRef]
48. Wu, Y.Z.; Schmid, A.K.; Qiu, Z.Q. Spin-dependent quantum interference from epitaxial MgO thin films on Fe(001). *Phys. Rev. Lett.* **2006**, *97*, 217205. [CrossRef] [PubMed]
49. Bertacco, R.; Ciccacci, F. Large spin asymmetry in electron absorption and reflection from oxidized single crystal Fe/MgO(001) films. *Surf. Sci.* **1999**, *419*, 265–271. [CrossRef]
50. Loy, D.J.J.; Danajaya, P.A.; Hong, X.L.; Shum, D.P.; Lew, W.S. Conduction mechanisms on high retention annealed MgO-based resistive switching memory devices. *Sci. Rep.* **2018**, *8*, 14774. [CrossRef] [PubMed]
51. Guo, Y.; Song, Q.; Yan, H. The influence of interaction between oxygen vacancies on set process in resistive switching: A case of MgO. *AIP Adv.* **2019**, *5*, 055230. [CrossRef]
52. Jambois, O.; Carreras, P.; Antony, A.; Bertomeu, J.; Martínez-Boubeta, C. Resistance switching in transparent magnetic MgO films. *Solid State Commun.* **2011**, *151*, 1856–1859. [CrossRef]
53. Dias, C.; Guerra, L.M.; Bordalo, B.D.; Lv, H.; Ferraria, A.M.; do Rego, A.M.B.; Cardoso, S.; Freitas, P.P.; Ventura, J. Voltage-polarity dependent multi-mode resistive switching on sputtered MgO nanostructures. *Phys. Chem. Chem. Phys.* **2017**, *19*, 10898–10904. [CrossRef] [PubMed]
54. Uchino, T.; Okutsu, D. Broadband laser emission from color centers inside MgO microcrystals. *Phys. Rev. Lett.* **2008**, *101*, 117401–117404. [CrossRef] [PubMed]
55. Uchino, T.; Okutsu, D.; Katayama, R.; Sawai, S. Mechanism of stimulated optical emission from MgO microcrystals with color centers. *Phys. Rev. B* **2009**, *79*, 165107. [CrossRef]
56. Kumar, A.; Thota, S.; Verma, S.; Kumar, J. Sol-gel synthesis of highly luminescent magnesium oxide nanocrystallites. *J. Lumin.* **2011**, *131*, 640–648. [CrossRef]
57. Debaraja, P.B.; Abadhani, D.N.; Prashantha, S.C.; Nagabhushana, H.; Sharma, S.C.; Nagabhushan, B.M.; Nagaswarup, H.P. Synthesis, structural and luminescence studies of magnesium oxide nanopowder. *Spectrochim. Acta Mol. Biomol. Spect.* **2014**, *118*, 847–851. [CrossRef]
58. Chaudhri, M.M.; Sands, H.S. Photoluminescence from indented MgO crystals using a near ultraviolet/visible Raman microscope. *J. Appl. Phys.* **1997**, *82*, 785–791. [CrossRef]
59. Halder, R.; Bandyopadhyay, S. Spark plasma sintering of nano magnesia: Processing parameters influencing optical properties. *Mater. Chem. Phys.* **2019**, *228*, 51–59. [CrossRef]
60. Benia, H.M.; Lin, X.; Gao, H.-J.; Nilius, N.; Freund, H.-J. Nucleation and growth of gold on MgO thin films: A combined STM and luminescence study. *J. Phys. Chem. C* **2007**, *111*, 10528–10533. [CrossRef]
61. Skvortsova, V.; Trinkler, L. Luminescence of impurities and radiation defects in magnesium oxide irradiated by fast neutrons. *Phys. Procedia* **2009**, *2*, 567–570. [CrossRef]
62. Abramishvili, M.; Akhvlediani, Z.; Galustashvili, M.; Dekanozishvili, G.; Kalabegishvili, T.; Kvatchadze, V.; Tavkhelidze, V. Peculiarities of radiation effects in MgO: Mn^{2+} crystals. *J. Mod. Phys.* **2011**, *2*, 841–844. [CrossRef]
63. Pathak, N.; Gupta, S.K.; Prajapat, C.L.; Sharma, S.K.; Ghosh, P.S.; Kanrar, B.; Pujari, P.K.; Kadam, R.M. Defect-induced ferromagnetism in MgO and its exceptional enhancement upon thermal annealing: A case of transformation of various defect states. *Phys. Chem. Chem. Phys.* **2017**, *19*, 11975–11989. [CrossRef]

64. Jain, N.; Marwaha, N.; Verma, R.; Gupta, B.K.; Srivastava, A.K. Facile synthesis of defect-induced highly-luminescent pristine MgO nanostructures for promising solid-state lighting applications. *RSC Adv.* **2016**, *6*, 4960–4968. [CrossRef]
65. Siedl, N.; Koller, D.; Sternig, A.K.; Thomelea, D.; Diwald, O. Photoluminescence quenching in compressed MgO nanoparticle systems. *Phys. Chem. Chem. Phys.* **2014**, *16*, 8339–8345. [CrossRef]
66. Cao, X.; Dai, H.; Chen, S.; Zeng, J.; Zhang, K.; Sun, Y. A high selective cataluminescence sensor for the determination of tetrahydrofuran vapor. *Meas. Sci. Technol.* **2013**, *24*, 025103. [CrossRef]
67. Chu, Y.; Zhang, Q.; Zhang, W.; Zhang, G.; Zhu, S. Highly sensitive dimethyl ether gas sensor utilizing cataluminescence on nanosized MgO/In_2O_3. *Meas. Sci. Technol.* **2014**, *25*, 085105. [CrossRef]
68. Ngo, C.; Voorde, M. *Nanotechnology in a Nutshell: From Simple to Complex Systems*; Atlantis Press: Paris, France, 2014.
69. Baraket, L.; Ghorbel, A. Control preparation of aluminium chromium mixed oxides by Sol-Gel process. In *Studies in Surface Science and Catalysis*; Delmon, B., Jacobs, P.A., Maggi, R., Martens, J.A., Grange, P., Poncelet, G., Eds.; Preparation of Catalysts VII; Elsevier: Amsterdam, The Netherlands, 1998; Volume 118, pp. 657–667.
70. Feng, S.H.; Li, G.H. Chapter 4-Hydrothermal and Solvothermal Syntheses. In *Modern Inorganic Synthetic Chemistry*, 2nd ed.; Xu, R., Xu, Y., Eds.; Elsevier: Amsterdam, The Netherlands, 2017; pp. 73–104.
71. Yeh, C.L. Combustion Synthesis: Principles and Applications. In *Reference Module in Materials Science and Materials Engineering*; Elsevier: Amsterdam, The Netherlands, 2016.
72. Rane, A.V.; Kanny, K.; Abitha, V.K.; Thomas, S. Methods for Synthesis of Nanoparticles and Fabrication of Nanocomposites. In *Synthesis of Inorganic Nanomaterials*; Mohan Bhagyaraj, S., Oluwafemi, O.S., Kalarikkal, N., Thomas, S., Eds.; Micro and Nano Technologies; Woodhead Publishing: Cambridge, UK, 2018; pp. 121–139.
73. Pal, G.; Rai, P.; Pandey, A. Green synthesis of nanoparticles: A greener approach for a cleaner future. In *Green Synthesis, Characterization and Applications of Nanoparticles*; Shukla, A.K., Iravani, S., Eds.; Micro and Nano Technologies; Elsevier: Amsterdam, The Netherlands, 2019; pp. 1–26.
74. Sutapa, I.W.; Wahab, A.W.; Taba, P.; Nafie, N.L. Synthesis and structural profile analysis of the MgO nanoparticles produced through the sol-gel method followed by annealing process. *Orient. J. Chem.* **2018**, *34*, 1016–1025. [CrossRef]
75. Escudero, A.; Carrillo-Carrión, C.; Romero-Ben, E.; Franco, A.; Rosales-Barrios, C.; Castillejos, M.C.; Khiar, N. Molecular Bottom-Up Approaches for the Synthesis of Inorganic and Hybrid Nanostructures. *Inorganics* **2021**, *9*, 58. [CrossRef]
76. Burlakov, V.M.; Goriely, A. Reverse Coarsening and the Control of Particle Size Distribution through Surfactant. *Appl. Sci.* **2020**, *10*, 5359. [CrossRef]
77. Antúnez-García, J.; Mejía-Rosales, S.; Pérez-Tijerina, E.; Montejano-Carrizales, J.M.; José-Yacamán, M. Coalescence and Collisions of Gold Nanoparticles. *Materials* **2011**, *4*, 368–379. [CrossRef]
78. Hornak, J. Synthesis, properties, and selected technical applications of magnesium oxide nanoparticles: A review. *Int. J. Mol. Sci.* **2021**, *22*, 12752. [CrossRef]
79. Lai, Y.F.; Chaudouët, P.; Charlot, F.; Matko, I.; Dubourdieu, C. Magnesium oxide nanowires synthesized by pulsed liquid-injection metal organic chemical vapor deposition. *Appl. Phys. Lett.* **2009**, *94*, 022904. [CrossRef]
80. Sirota, V.; Selemenev, V.; Kovaleva, M.; Pavlenko, I.; Mamunin, K.; Dokalov, V.; Prozorova, M. Synthesis of magnesium oxide nanopowder by thermal plasma using magnesium nitrate hexahydrate. *Phys. Res. Inter.* **2016**, *4*, 6853405. [CrossRef]
81. Gandhi, S.; Abiramipriya, P.; Pooja, N.; Jeyakumari, J.J.L.; Arasi, A.Y.; Dhanalakshmi, V.; Gopinathan, M.R.; Anbarasan, R. Synthesis and characterizations of nano-sized MgO and its nano composite with poly(vinyl alcohol). *J. Non-Cryst. Solids* **2011**, *357*, 181–185. [CrossRef]
82. Karthik, K.; Dhanuskodi, S.; Gobinath, C.; Prabukumar, S.; Sivaramakrishnan, S. Fabrication of MgO nanostructures and its efficient photocatalytic, antibacterial and anticancer performance. *J. Photochem. Photobiol. B* **2019**, *190*, 8–20. [CrossRef]
83. Supin, K.K.; Saji, A.; Chanda, A.; Vasundhara, M. Effects of calcinations temperatures on structural, optical and magnetic properties of MgO nanoflakes and its photocatalytic applications. *Opt. Mater.* **2022**, *132*, 112777. [CrossRef]
84. Al-Hazmi, F.; Alnowaiser, F.; Al-Ghamdi, A.A.; Al-Ghamdi, A.A.; Aly, M.M.; Al-Tuwirqi, R.M.; El-Tantawy, F. A New large-scale synthesis of magnesium oxide nanowires: Structural and antibacterial properties. *Superlattices Microstruct.* **2012**, *52*, 200–209. [CrossRef] [PubMed]
85. Ullah, H.; Ahmad, R.; Khan, A.A.; Khaliq, N.; Khan, M.; Ali, G.; Karim, S.; Yi, X.; Cho, S.O. A sensitive non-enzymatic glucose sensor based on MgO entangled nanosheets decorated with CdS nanoparticles: Experimental and DFT study. *J. Mol. Liq.* **2022**, *360*, 119366. [CrossRef]
86. Mantzaris, N.V. Liquid-Phase Synthesis of Nanoparticles: Particle Size Distribution Dynamics and Control. *Chem. Eng. Sci.* **2005**, *60*, 4749–4770. [CrossRef]
87. Swihart, M.T. Vapor-Phase Synthesis of Nanoparticles. *Curr. Opin. Colloid Interface Sci.* **2003**, *8*, 127–133. [CrossRef]
88. Benrabaa, R.; Boukhlouf, H.; Bordes-Richard, E.; Vannier, R.N.; Barama, A. Nanosized nickel ferrite catalysts for CO_2 reforming of methane at low temperature: Effect of preparation method and acid-base properties. In *Studies in Surface Science and Catalysis*; Gaigneaux, E.M., Devillers, M., Hermans, S., Jacobs, P.A., Martens, J.A., Ruiz, P., Eds.; Scientific Bases for the Preparation of Heterogeneous Catalysts; Elsevier: Amsterdam, The Netherlands, 2010; Volume 175, pp. 301–304.
89. Huang, G.; Lu, C.H.; Yang, H.H. Magnetic Nanomaterials for Magnetic Bioanalysis. In *Novel Nanomaterials for Biomedical, Environmental and Energy Applications*; Wang, X., Chen, X., Eds.; Micro and Nano Technologies; Elsevier: Amsterdam, The Netherlands, 2019; pp. 89–109.

90. Rashid, H.; Manson, A.M.; Haider, B.; Nasir, R.; Hamid, S.B.A.; Abdulrahman, A. Synthesis and Characterization of Magnetite Nanoparticles with High Selectivity Using In-Situ Precipitation Method. *Sep. Sci. Technol.* **2020**, *6*, 1207–1215. [CrossRef]
91. Tartaj, P.; del Puerto Morales, M.; Veintemillas-Verdaguer, S.; González-Carreño, T.; Serna, C.J. The Preparation of Magnetic Nanoparticles for Applications in Biomedicine. *J. Phys. D Appl. Phys.* **2003**, *36*, 182–197. [CrossRef]
92. Kumar, R.; Sharma, A.; Kishore, N. Preparation and Characterization of MgO Nanoparticles by Co-Precipitation Method. *Int. J. Phys.* **2013**, *6*, 66–70.
93. Karthikeyan, V.; Dhanapandian, S.; Manoharan, C. Characterization and Antibacterial Behavior of MgO-PEG Nanoparticles Synthesized via Co-Precipitation Method. *Int. Lett. Chem. Phys. Astron.* **2016**, *70*, 33–41. [CrossRef]
94. Tandon, M.; Chauhan, P. Surfactant Free Synthesis of Magnesium Oxide Nanotubes by Simple Chemical Co-Precipitation Method. *Int. J. Innov. Technol. Explor. Eng.* **2020**, *9*, 2504–2506. [CrossRef]
95. Yadav, P.; Saini, R.; Bhaduri, A. Facile synthesis of MgO nanoparticles for effective degradation of organic dyes. *Environ. Sci. Pollut. Res. Int.* **2023**, *30*, 71439–71453. [CrossRef]
96. Soytaş, S.H.; Oğuz, O.; Menceloğlu, Y.Z. Polymer Nanocomposites With Decorated Metal Oxides. In *Polymer Composites with Functionalized Nanoparticles*; Pielichowski, K., Majka, T.M., Eds.; Micro and Nano Technologies; Elsevier: Amsterdam, The Netherlands, 2019; pp. 287–323.
97. Sham, E.L.; Murgia, V.; Gottifredi, J.C.; Farfán-Torres, E.M. V_2O_5-SiO_2 Catalyst Prepared by the sol-gel Process in the Oxidative Dehydrogenation of n-butane. In *Studies in Surface Science and Catalysis*; Delmon, B., Jacobs, P.A., Maggi, R., Martens, J.A., Grange, P., Poncelet, G., Eds.; Preparation of Catalysts VII; Elsevier: Amsterdam, The Netherlands, 1998; Volume 118, pp. 669–678.
98. Sutapa, I.W.; Wahab, A.W.; Taba, P.; Nafie, N.L. Dislocation, Crystallite Size Distribution and Lattice Strain of Magnesium Oxide Nanoparticles. *J. Phys. Conf. Ser.* **2018**, *979*, 012021. [CrossRef]
99. Wahab, R.; Ansari, S.G.; Dar, M.A.; Kim, Y.S.; Shin, H.S. Synthesis of Magnesium Oxide Nanoparticles by Sol-Gel Process. *Mater. Sci. Forum* **2007**, *558–559*, 983–986. [CrossRef]
100. Boddu, V.M.; Viswanath, D.S.; Maloney, S.W. Synthesis and Characterization of Coralline Magnesium Oxide Nanoparticles. *J. Am. Ceram. Soc.* **2008**, *91*, 1718–1720. [CrossRef]
101. Dercz, G.; Prusik, K.; Pajak, L.; Pielaszek, R.; Malinowski, J.J.; Pudło, W. Structure Studies on Nanocrystalline Powder of MgO Xerogel Prepared by the Sol-Gel Method. *Mater. Sci.* **2009**, *27*, 201–207. [CrossRef]
102. Nassar, M.Y.; Mohamed, T.Y.; Ahmed, I.S.; Samir, I. MgO Nanostructure via a Sol-Gel Combustion Synthesis Method Using Different Fuels: An Efficient Nano-Adsorbent for the Removal of Some Anionic Textile Dyes. *J. Mol. Liq.* **2017**, *225*, 730–740. [CrossRef]
103. Ng, J.J.; Leong, K.H.; Sim, L.C.; Oh, W.-D.; Dai, C.; Saravanan, P. Environmental remediation using nano-photocatalyst under visible light irradiation: The case of bismuth phosphate. In *Nanomaterials for Air Remediation*; Abdeltif, A., Assadi, A.A., Nguyen-Tri, P., Nguyen, T.A., Rtimi, S., Eds.; Micro and Nano Technologies; Elsevier: Amsterdam, The Netherlands, 2020; pp. 193–207.
104. Williams, M.J.; Corr, S.A. Magnetic Nanoparticles for Targeted Cancer Diagnosis and Therapy. In *Frontiers of Nanoscience*; Summers, H., Ed.; Nanomedicine; Elsevier: Amsterdam, The Netherlands, 2013; Volume 5, pp. 29–63.
105. Ding, Y.; Zhang, G.; Wu, H.; Hai, B.; Wang, L.; Qian, Y. Nanoscale Magnesium Hydroxide and Magnesium Oxide Powders: Control over Size, Shape, and Structure via Hydrothermal Synthesis. *Chem. Mater.* **2001**, *13*, 435–440. [CrossRef]
106. Rukh, S.; Sofi, A.H.; Shah, M.A.; Yousuf, S. Antibacterial Activity of Magnesium Oxide Nanostructures Prepared by Hydrothermal Method. *Asian J. Nanosci. Mater.* **1999**, *2*, 425–430. [CrossRef]
107. Varma, A.V.; Mukasyan, A.S.; Rogachev, A.S.; Manukyan, K.V. Solution Combustion Synthesis of Nanoscale Materials. *Chem. Rev.* **2016**, *116*, 14493–14586. [CrossRef] [PubMed]
108. Mukasyan, A.S.; Manukyan, K.V. One- and Two-Dimensional Nanostructures Prepared by Combustion Synthesis. In *Nanomaterials Synthesis*; Beeran Pottathara, Y., Thomas, S., Kalarikkal, N., Grohens, Y., Kokol, V., Eds.; Micro and Nano Technologies; Elsevier: Amsterdam, The Netherlands, 2019; pp. 85–120.
109. Stojanovic, B.D.; Dzunuzovic, A.S.; Ilic, N.I. Review of methods for the preparation of magnetic metal oxides. In *Magnetic, Ferroelectric, and Multiferroic Metal Oxides*; Stojanovic, B.D., Ed.; Metal Oxides; Elsevier: Amsterdam, The Netherlands, 2018; pp. 333–359.
110. Mukasyan, A.S.; Dinka, P. Novel Approaches to Solution-Combustion Synthesis of Nanomaterials. *Int. J. Self-Propag. High-Temp. Synth.* **2007**, *16*, 23–35. [CrossRef]
111. Balakrishnan, G.; Velavan, R.; Mujasam Batoo, K.; Raslan, E.H. Microstructure, Optical and Photocatalytic Properties of MgO Nanoparticles. *Results Phys.* **2020**, *16*, 103013. [CrossRef]
112. Rao, K.V.; Sunandana, C.S. Structure and Microstructure of Combustion Synthesized MgO Nanoparticles and Nanocrystalline MgO Thin Films Synthesized by Solution Growth Route. *J. Mater. Sci.* **2008**, *43*, 146–154. [CrossRef]
113. Tharani, K.; Jegatha Christy, A.; Sagadevan, S.; Nehru, L.C. Fabrication of Magnesium Oxide Nanoparticles Using Combustion Method for a Biological and Environmental Cause. *Chem. Phys. Lett.* **2021**, *763*, 138216. [CrossRef]
114. Kumar, D.; Yadav, L.S.R.; Lingaraju, K.; Manjunath, K.; Suresh, D.; Prasad, D.; Nagabhushana, H.; Sharma, S.C.; Naika, H.R.; Chikkahanumantharayappa; et al. Combustion Synthesis of MgO Nanoparticles Using Plant Extract: Structural Characterization and Photoluminescence Studies. *AIP Conf. Proc.* **2015**, *1665*, 050145. [CrossRef]

115. Devatha, C.P.; Thalla, A.K. Green Synthesis of Nanomaterials. In *Synthesis of Inorganic Nanomaterials*; Mohan Bhagyaraj, S., Oluwafemi, O.S., Kalarikkal, N., Thomas, S., Eds.; Micro and Nano Technologies; Woodhead Publishing: Cambridge, UK, 2018; pp. 169–184.
116. Verma, R.; Pathak, S.; Srivastava, A.K.; Prawer, S.; Tomljenovic-Hanic, S. ZnO Nanomaterials: Green Synthesis, Toxicity Evaluation and New Insights in Biomedical Applications. *J. Alloy Compd.* **2021**, *876*, 160175. [CrossRef]
117. Zhu, X.; Pathakoti, K.; Hwang, H.-M. Green synthesis of titanium dioxide and zinc oxide nanoparticles and their usage for antimicrobial applications and environmental remediation. In *Green Synthesis, Characterization and Applications of Nanoparticles*; Shukla, A.K., Iravani, S., Eds.; Micro and Nano Technologies; Elsevier: Amsterdam, The Netherlands, 2019; pp. 223–263.
118. Akhtar, M.S.; Panwar, J.; Yun, Y.-S. Biogenic synthesis of metallic nanoparticles by plant extracts. *ACS Sustain. Chem. Eng.* **2013**, *1*, 591–602. [CrossRef]
119. Demirbas, A.; Welt, B.A.; Ocsoy, I. Biosynthesis of red cabbage extract directed Ag NPs and their effect on the loss of antioxidant activity. *Mater. Lett.* **2016**, *179*, 20–23. [CrossRef]
120. Ocsoy, I.; Tasdemir, D.; Mazicioglu, S.; Celik, C.; Katı, A.; Ulgen, F. Biomolecules incorporated metallic nanoparticles synthesis and their biomedical applications. *Mater. Lett.* **2018**, *212*, 45–50. [CrossRef]
121. Aygün, A.; Gülbağça, F.; Nas, M.S.; Alma, M.H.; Çalımlı, M.H.; Ustaoglu, B.; Altunoglu, Y.C.; Baloğlu, M.C.; Cellat, K.; Şen, F. Biological synthesis of silver nanoparticles using Rheum ribes and evaluation of their anticarcinogenic and antimicrobial potential: A novel approach in phytonanotechnology. *J. Pharm. Biomed. Anal.* **2020**, *179*, 113012. [CrossRef] [PubMed]
122. Demirbas, A.; Yilmaz, V.; Ildiz, N.; Baldemir, A.; Ocsoy, I. Anthocyanins-rich berry extracts directed formation of Ag NPs with the investigation of their antioxidant and antimicrobial activities. *J. Mol. Liq.* **2017**, *248*, 1044–1049. [CrossRef]
123. Altinsoy, B.D.; Karatoprak, G.Ş.; Ocsoy, I. Extracellular directed Ag NPs formation and investigation of their antimicrobial and cytotoxic properties. *Saudi Pharm. J.* **2019**, *27*, 9–16. [CrossRef]
124. Singh, J.; Dutta, T.; Kim, K.-H.; Rawat, M.; Samddar, P.; Kumar, P. Green synthesis of metals and their oxide nanoparticles: Applications for environmental remediation. *J. Nanobiotechnol.* **2018**, *16*, 84. [CrossRef] [PubMed]
125. Praveen Kumar, P.; Laxmi Deepak Bhatlu, M.; Sukanya, K.; Karthikeyan, S.; Jayan, N. Synthesis of Magnesium Oxide Nanoparticle by Eco-Friendly Method (Green Synthesis)-A Review. *Mater. Today Proc.* **2021**, *37*, 3028–3030. [CrossRef]
126. Shah, M.; Fawcett, D.; Sharma, S.; Tripathy, S.K.; Poinern, G.E.J. Green synthesis of metallic nanoparticles via biological entities. *Materials* **2015**, *8*, 7278–7308. [CrossRef]
127. Dauthal, P.; Mukhopadhyay, M. Noble metal nanoparticles: Plant-mediated synthesis, mechanistic aspects of synthesis, and applications. *Ind. Eng. Chem. Res.* **2016**, *55*, 9557–9577. [CrossRef]
128. El Shafey, A.M. Green synthesis of metal and metal oxide nanoparticles from plant leaf extracts and their applications: A review. *Green Process. Synth.* **2020**, *9*, 304–339. [CrossRef]
129. Akintelu, S.A.; Folorunso, A.S. A review on green synthesis of zinc oxide nanoparticles using plant extracts and its biomedical applications. *Bionanoscience* **2020**, *10*, 848–863. [CrossRef]
130. Karmous, I.; Pandey, A.; Ben Haj, K.; Chaoui, A. Efficiency of the green synthesized nanoparticles as new tools in cancer therapy: Insights on plant-based bioengineered nanoparticles, biophysical properties, and anticancer roles. *Biol. Trace Elem. Res.* **2019**, *196*, 330–342. [CrossRef]
131. Jeevanandam, J.; Chan, Y.S.; Danquah, M.K. Biosynthesis of metal and metal oxide nanoparticles. *ChemBioEng Rev.* **2016**, *3*, 55–67. [CrossRef]
132. Joghee, S.; Ganeshan, P.; Vincent, A.; Hong, S.I. Ecofriendly biosynthesis of zinc oxide and magnesium oxide particles from medicinal plant *Pisonia grandis R. Br.* leaf extract and their antimicrobial activity. *Bionanoscience* **2019**, *9*, 141–154. [CrossRef]
133. Suresh, J.; Yuvakkumar, R.; Sundrarajan, M.; Hong, S.I. Green Synthesis of Magnesium Oxide Nanoparticles. *Adv. Mater. Res.* **2014**, *952*, 141–144. [CrossRef]
134. Younis, I.Y.; El-Hawary, S.S.; Eldahshan, O.A.; Abdel-Aziz, M.M.; Ali, Z.Y. Green Synthesis of Magnesium Nanoparticles Mediated from Rosa Floribunda Charisma Extract and Its Antioxidant, Antiaging and Antibiofilm Activities. *Sci. Rep.* **2021**, *11*, 16868. [CrossRef]
135. Abdallah, Y.; Ogunyemi, S.O.; Abdelazez, A.; Zhang, M.; Hong, X.; Ibrahim, E.; Hossain, A.; Fouad, H.; Li, B.; Chen, J. The Green Synthesis of MgO Nano-Flowers Using *Rosmarinus officinalis* L. (Rosemary) and the Antibacterial Activities against *Xanthomonas oryzae* pv. oryzae. *BioMed Res. Int.* **2019**, *2019*, 5620989. [CrossRef] [PubMed]
136. Sharma, G.; Soni, R.; Jasuja, N.D. Phytoassisted Synthesis of Magnesium Oxide Nanoparticles with Swertia Chirayaita. *J. Taibah Univ. Sci.* **2017**, *11*, 471–477. [CrossRef]
137. Fatiqin, A.; Amrulloh, H.; Simanjuntak, W. Green Synthesis of MgO Nanoparticles Using Moringa Oleifera Leaf Aqueous Extract for Antibacterial Activity. *Bull. Chem. Soc. Ethiop.* **2021**, *35*, 161–170. [CrossRef]
138. Singh, A.; Joshi, N.C.; Ramola, M. Magnesium oxide nanoparticles (MgONPs): Green synthesis, characterizations and antimicrobial activity. *Res. J. Pharm. Technol.* **2019**, *12*, 4644–4646. [CrossRef]
139. Sneha, K.; Sathishkumar, M.; Mao, J.; Kwak, I.S.; Yun, Y.-S. Corynebacterium glutamicum-mediated crystallization of silver ions through sorption and reduction processes. *Chem. Eng. J.* **2010**, *162*, 989–996. [CrossRef]
140. Gowramma, B.; Keerthi, U.; Rafi, M.; Rao, D.M. Biogenic silver nanoparticles production and characterization from native strain of Corynebacterium species and its antimicrobial activity. *3 Biotech* **2015**, *5*, 195–201. [CrossRef]

141. Wang, H.; Chen, H.; Wang, Y.; Huang, J.; Kong, T.; Lin, W.; Zhou, Y.; Lin, L.; Sun, D.; Li, Q. Stable silver nanoparticles with narrow size distribution non-enzymatically synthesized by Aeromonas sp. SH10 cells in the presence of hydroxyl ions. *Curr. Nanosci.* **2012**, *8*, 838–846. [CrossRef]
142. Narendhran, S.; Manikandan, M.; Shakila, P.B. Antibacterial, antioxidant properties of *Solanum trilobatum* and sodium hydroxide-mediated magnesium oxide nanoparticles: A green chemistry approach. *Bull. Mater. Sci.* **2019**, *42*, 133. [CrossRef]
143. Ogunyemi, S.O.; Zhang, F.; Abdallah, Y.; Zhang, M.; Wang, Y.; Sun, G.; Qiu, W.; Li, B. Biosynthesis and characterization of magnesium oxide and manganese dioxide nanoparticles using *Matricaria chamomilla* L. extract and its inhibitory effect on *Acidovorax oryzae* strain RS-2. *Artif. Cells Nanomed. Biotechnol.* **2019**, *47*, 2230–2239. [CrossRef]
144. Pugazhendhi, A.; Prabhu, R.; Muruganantham, K.; Shanmuganathan, R.; Natarajan, S. Anticancer, antimicrobial and photocatalytic activities of green synthesized magnesium oxide nanoparticles (MgONPs) using aqueous extract of *Sargassum wightii*. *J. Photochem. Photobiol. B* **2019**, *190*, 86–97. [CrossRef]
145. Mohanasrinivasan, V.; Subathra Devi, C.; Mehra, A.; Prakash, S.; Agarwal, A.; Selvarajan, E.; Jemimah Naine, S. Biosynthesis of MgO nanoparticles using *Lactobacillus* sp. and its activity against human leukemia cell lines HL-60. *BioNanoScience* **2018**, *8*, 249–253. [CrossRef]
146. Ibrahem, E.J.; Thalij, K.M.; Badawy, A.S. Antibacterial Potential of Magnesium Oxide Nanoparticles Synthesized by *Aspergillus niger*. *Biotechnol. J. Int.* **2017**, *18*, 1–7. [CrossRef]
147. Sagar, S.; Kaistha, S.; Das, A.J.; Kumar, R. Bacteriophage: A new hope for the control of antibiotic-resistant bacteria. In *Antibiotic Resistant Bacteria: A Challenge to Modern Medicine*; Springer: Singapore, 2019; pp. 153–164.
148. Das, B.; Moumita, S.; Ghosh, S.; Khan, M.I.; Indira, D.; Jayabalan, R.; Tripathy, S.K.; Mishra, A.; Balasubramanian, P. Biosynthesis of magnesium oxide (MgO) nanoflakes by using leaf extract of *Bauhinia purpurea* and evaluation of its antibacterial property against *Staphylococcus aureus*. *Mater. Sci. Eng. C* **2018**, *91*, 436–444. [CrossRef]
149. Ananda, A.; Ramakrishnappa, T.; Archana, S.; Reddy Yadav, L.S.; Shilpa, B.M.; Nagaraju, G.; Jayanna, B.K. Green synthesis of MgO nanoparticles using *Phyllanthus emblica* for Evans blue degradation and antibacterial activity. *Mater. Today Proc.* **2021**, *49*, 801–810. [CrossRef]
150. Sharma, S.K.; Khan, A.U.; Khan, M.; Gupta, M.; Gehlot, A.; Park, S.; Alam, M. Biosynthesis of MgO nanoparticles using *Annona squamosa* seeds and its catalytic activity and antibacterial screening. *Micro Nano Lett.* **2020**, *15*, 30–34. [CrossRef]
151. Cai, L.; Chen, J.; Liu, Z.; Wang, H.; Yang, H.; Ding, W. Magnesium oxide nanoparticles: Effective agricultural antibacterial agent against *Ralstonia solanacearum*. *Front. Microbiol.* **2018**, *9*, 790. [CrossRef]
152. Makhluf, S.; Dror, R.; Nitzan, Y.; Abramovich, Y.; Jelinek, R.; Gedanken, A. Microwave-assisted synthesis of nanocrystalline MgO and its use as a bacteriocide. *Adv. Funct. Mater.* **2005**, *15*, 1708–1715. [CrossRef]
153. Huang, L.; Li, D.; Lin, Y.; Evans, D.G.; Duan, X. Influence of nano-MgO particle size on bactericidal action against *Bacillus subtilis var. niger*. *Chin. Sci. Bull.* **2005**, *50*, 514–519. [CrossRef]
154. Bindhu, M.; Umadevi, M.; Micheal, M.K.; Arasu, M.V.; Al-Dhabi, N.A. Structural, morphological and optical properties of MgO nanoparticles for antibacterial applications. *Mater. Lett.* **2016**, *166*, 19–22. [CrossRef]
155. Sawai, J.; Kojima, H.; Igarashi, H.; Hashimoto, A.; Shoji, S.; Sawaki, T.; Hakoda, A.; Kawada, E.; Kokugan, T.; Shimizu, M. Antibacterial characteristics of magnesium oxide powder. *World J. Microbiol. Biotechnol.* **2000**, *16*, 187–194. [CrossRef]
156. Krishnamoorthy, K.; Manivannan, G.; Kim, S.J.; Jeyasubramanian, K.; Premanathan, M. Antibacterial activity of MgO nanoparticles based on lipid peroxidation by oxygen vacancy. *J. Nanopart. Res.* **2012**, *14*, 1063. [CrossRef]
157. Suresh, J.; Pradheesh, G.; Alexramani, V.; Sundrarajan, M.; Hong, S.I. Green synthesis and characterization of hexagonal shaped MgO nanoparticles using insulin plant (*Costus pictus D. Don*) leave extract and its antimicrobial as well as anticancer activity. *Adv. Powder Technol.* **2018**, *29*, 1685–1694. [CrossRef]
158. Kainat, M.A.; Khan, F.; Ali, S.; Faisal, M.; Rizwan, M.; Hussain, Z.; Zaman, N.; Afsheen, Z.; Uddin, M.N.; Bibi, N. Exploring the therapeutic potential of *Hibiscus rosa sinensis* synthesized cobalt oxide (Co_3O_4-NPs) and magnesium oxide nanoparticles (MgO-NPs). *Saudi J. Biol. Sci.* **2021**, *28*, 5157–5167. [CrossRef]
159. Amrulloh, H.; Fatiqin, A.; Simanjuntak, W.; Afriyani, H.; Annissa, A. Antioxidant and antibacterial activities of magnesium oxide nanoparticles prepared using aqueous extract of *Moringa oleifera* bark as green agents. *J. Multidiscip. Appl. Nat. Sci.* **2021**, *1*, 44–53. [CrossRef]
160. Nejati, M.; Rostami, M.; Mirzaei, H.; Rahimi-Nasrabadi, M.; Vosoughifar, M.; Sobhani Nasab, A.; Ganjali, M.R. Green methods for the preparation of MgO nanomaterials and their drug delivery, anti-cancer and anti-bacterial potentials: A review. *Inorg. Chem. Commun.* **2022**, *136*, 109107. [CrossRef]
161. Rodrigues, M.L.; Nosanchuk, J.D. Fungal diseases as neglected pathogens: A wake-up call to public health officials. *PLoS Negl. Trop. Dis.* **2020**, *14*, e0007964. [CrossRef]
162. Sierra-Fernandez, A.; De la Rosa-García, S.C.; Gomez-Villalba, L.S.; Gomez-Cornelio, S.; Rabanal, M.E.; Fort, R.; Quintana, P. Synthesis, photocatalytic, and antifungal properties of MgO, ZnO, and Zn/Mg oxide nanoparticles for the protection of calcareous stone heritage. *ACS Appl. Mater. Interfaces* **2017**, *9*, 24873–24886. [CrossRef]
163. De la Rosa-García, S.C.; Martínez-Torres, P.; Gómez-Cornelio, S.; Corral-Aguado, M.A.; Quintana, P.; Gómez-Ortíz, N.M. Antifungal activity of ZnO and MgO nanomaterials and their mixtures against *Colletotrichum gloeosporioides* strains from tropical fruit. *J. Nanomater.* **2018**, *2018*, 3498527. [CrossRef]

164. Safaei, M.; Taran, M. Preparation of bacterial cellulose fungicide nanocomposite incorporated with MgO nanoparticles. *J. Polym. Environ.* **2022**, *30*, 2066–2076. [CrossRef]
165. Khatua, A.; Kumari, K.; Khatak, D.; Roy, A.; Bhatt, N.; Paul, B.; Naik, A.; Patel, A.K.; Panigrahi, U.K.; Sahu, S.K.; et al. synthesis and spectral characterisation of fabricated cerium-doped magnesium oxide nanoparticles: Evaluation of the antimicrobial potential and its membranolytic activity through large unilamellar vesicles. *J. Funct. Biomater.* **2023**, *14*, 112. [CrossRef] [PubMed]
166. Sidhu, A.; Bala, A.; Singh, H.; Ahuja, R.; Kumar, A. Development of MgO-sepiolite nanocomposites against phytopathogenic fungi of rice (*Oryzae sativa*): A green approach. *ACS Omega* **2020**, *5*, 13557–13565. [CrossRef] [PubMed]
167. Wang, H.; Li, G.; Fakhri, A. Fabrication and structural of the Ag_2S-MgO/graphene oxide nanocomposites with high photocatalysis and antimicrobial activities. *J. Photochem. Photobiol. B* **2020**, *207*, 111882. [CrossRef] [PubMed]
168. Sharmila, G.; Muthukumaran, C.; Sangeetha, E.; Saraswathi, H.; Soundarya, S.; Kumar, N.M. Green fabrication, characterization of *Pisonia alba* leaf extract derived MgO nanoparticles and its biological applications. *Nano-Struct. Nano-Objects* **2019**, *20*, 100380. [CrossRef]
169. Saied, E.; Eid, A.M.; Hassan, S.E.; Salem, S.S.; Radwan, A.A.; Halawa, M.; Saleh, F.M.; Saad, H.A.; Saied, E.M.; Fouda, A. The catalytic activity of biosynthesized magnesium oxide nanoparticles (MgO-NPs) for inhibiting the growth of pathogenic microbes. *Catalysts* **2021**, *11*, 821. [CrossRef]
170. Fouda, A.; Awad, M.A.; Eid, A.M.; Saied, E.; Barghoth, M.G.; Hamza, M.F.; Awad, M.F.; Abdelbary, S.; Hassan, S.E.-D. An eco-friendly approach to the control of pathogenic microbes and Anopheles stephensi malarial vector using magnesium oxide nanoparticles (Mg-NPs) fabricated by *Penicillium chrysogenum*. *Int. J. Mol. Sci.* **2021**, *22*, 5096. [CrossRef] [PubMed]
171. Sulak, M.; Kavakcıoğlu Yardımcı, B. The green synthesis of MgO nanoparticles using dried jujube fruit extract and their anti-yeast activity against Saccharomyces cerevisiae. *Inorg. Nano-Met. Chem.* **2021**, *52*, 653–660. [CrossRef]
172. Vidhya, E.; Vijayakumar, S.; Nilavukkarasi, M.; Punitha, V.N.; Snega, S.; Praseetha, P.K. Green fabricated MgO nanoparticles as antimicrobial agent: Characterization and evaluation. *Mater. Today Proc.* **2021**, *45*, 5579–5583. [CrossRef]
173. Vijayakumar, S.; Punitha, V.N.; Parameswari, N. Phytonanosynthesis of MgO Nanoparticles: Green Synthesis, Characterization and Antimicrobial Evaluation. *Arab. J. Sci. Eng.* **2021**, *47*, 6729–6734. [CrossRef]
174. Al-Fahdawi, M.Q.; Rasedee, A.; Al-Doghachi, F.A.; Rosli, R.; Taufiq-Yap, Y.H.; Al-Qubaisi, M.S. Anticancer palladium-doped magnesia nanoparticles: Synthesis, characterization, and in vitro study. *Nanomedicine* **2020**, *15*, 547–561. [CrossRef]
175. van der Valk, M.J.M.; Marijnen, C.A.M.; van Etten, B.; Dijkstra, E.A.; Hilling, D.E.; Kranenbarg, E.M.-K.; Putter, H.; Roodvoets, A.G.H.; Bahadoer, R.R.; Fokstuen, T.; et al. Compliance and tolerability of short-course radiotherapy followed by preoperative chemotherapy and surgery for high-risk rectal cancer—Results of the international randomized RAPIDO-trial. *Radiother. Oncol.* **2020**, *147*, 75–83. [CrossRef]
176. Hussain, Y.; Islam, L.; Khan, H.; Filosa, R.; Aschner, M.; Javed, S. Curcumin-isplatin chemotherapy: A novel strategy in promoting chemotherapy efficacy and reducing side effects. *Phyther. Res.* **2021**, *35*, 6514–6529. [CrossRef]
177. Behzadi, E.; Sarsharzadeh, R.; Nouri, M.; Attar, F.; Akhtari, K.; Shahpasand, K.; Falahati, M. Albumin binding and anticancer effect of magnesium oxide nanoparticles. *Int. J. Nanomed.* **2018**, *14*, 257–270. [CrossRef]
178. Alfaro, A.; León, A.; Guajardo-Correa, E.; Reúquen, P.; Torres, F.; Mery, M.; Segura, R.; Zapata, P.A.; Orihuela, P.A. MgO nanoparticles coated with polyethylene glycol as carrier for 2-Methoxyestradiol anticancer drug. *PLoS ONE* **2019**, *14*, e0214900. [CrossRef]
179. Safaei, M.; Taran, M.; Rezaei, R.; Mansouri, K.; Mozaffari, H.; Imani, M.; Sharifi, R. Synthesis and anticancer properties of bacterial cellulose-magnesium oxide bionanocomposite. *Curr. Issues Pharm. Med. Sci.* **2019**, *32*, 29–33. [CrossRef]
180. Al-Fahdawi, M.Q.; Al-Doghachi, F.A.J.; Abdullah, Q.K.; Hammad, R.T.; Rasedee, A.; Ibrahim, W.N.; Alshwyeh, H.A.; Alosaimi, A.A.; Aldosary, S.K.; Eid, E.E.M.; et al. Oxidative stress cytotoxicity induced by platinum-doped magnesia nanoparticles in cancer cells. *Biomed. Pharmacother.* **2021**, *138*, 111483. [CrossRef]
181. MubarakAli, D.; Manzoor, M.A.P.; Sabarinathan, A.; Devi, C.A.; Rekha, P.D.; Thajuddin, N.; Lee, S.-Y. An investigation of antibiofilm and cytotoxic property of MgO nanoparticles. *Biocatal. Agric. Biotechnol.* **2019**, *18*, 101069. [CrossRef]
182. Chen, K.; Abdtawfeeq, T.H.; Kadhim, I.K.; Jawad, M.A.; Hammad, M.J.; Mohammed, N.M.; Riyahi, Y.; Hadrawi, S.K.; Kaur, J.; Soltani, A. Magnesium oxide nanotube as novel strategies to enhance the anticancer activity of 5-Fluorouracil. *J. Mol. Liq.* **2023**, *384*, 122214. [CrossRef]
183. Singh, T.A.; Sadhukhan, P.; Ghosh, N.; Thakur, N.; Sharma, A.; Tejwan, N.; Pabbathi, A.; Das, J.; Sil, P.C. Targeted delivery of rutin into breast cancer cells via using phenylboronic acid functionalized MgO nanoparticles. *Mater. Sci. Eng. B* **2023**, *296*, 116623. [CrossRef]
184. Kgosiemang, I.K.; Lefojane, R.; Direko, P.; Madlanga, Z.; Mashele, S.; Sekhoacha, M. Green synthesis of magnesium and cobalt oxide nanoparticles using *Euphorbia tirucalli*: Characterization and potential application for breast cancer inhibition. *Inorg. Nano-Met. Chem.* **2020**, *50*, 1070–1080. [CrossRef]
185. Abdullah, O.H.; Mohammed, A.M. Biosynthesis and characterization of MgO nanowires using *Prosopis farcta* and evaluation of their applications. *Inorg. Chem. Commun.* **2021**, *125*, 108435. [CrossRef]
186. Fathy, R.M.; Mahfouz, A.Y. Eco-friendly graphene oxide-based magnesium oxide nanocomposite synthesis using fungal fermented by-products and gamma rays for outstanding antimicrobial, antioxidant, and anticancer activities. *J. Nanostruct. Chem.* **2021**, *11*, 301–321. [CrossRef]

187. Kainama, H.; Fatmawati, S.; Santoso, M.; Papilaya, P.M.; Ersam, T. The relationship of free radical scavenging and total phenolic and flavonoid contents of *Garcinia lasoar* PAM. *Pharm. Chem. J.* **2020**, *53*, 1151–1157. [CrossRef]
188. Li, C.-W.; Li, L.-L.; Chen, S.; Zhang, J.-X.; Lu, W.-L. Antioxidant nanotherapies for the treatment of inflammatory diseases. *Front. Bioeng. Biotechnol.* **2020**, *8*, 200. [CrossRef]
189. Podder, S.; Chanda, D.; Mukhopadhyay, A.K.; De, A.; Das, B.; Samanta, A.; Hardy, J.G.; Ghosh, C.K. Effect of morphology and concentration on crossover between antioxidant and pro-oxidant activity of MgO nanostructures. *Inorg. Chem.* **2018**, *57*, 12727–12739. [CrossRef] [PubMed]
190. Ali, S.; Sudha, K.G.; Thirumalaivasan, N.; Ahamed, M.; Pandiaraj, S.; Rajeswari, V.D.; Vinayagam, Y.; Thiruvengadam, M.; Govindasamy, R. Green synthesis of magnesium oxide nanoparticles by using Abrus precatorius bark extract and their photocatalytic, antioxidant, antibacterial, and cytotoxicity activities. *Bioengineering* **2023**, *10*, 302. [CrossRef]
191. Mylarappa, M.; Rekha, S.; Kantharaju, S.; Chandruvasan, S.; Shravana, K. Synthesis and characterization of ZnO and MgO nanoparticles through green approach and their antioxidant properties. *ECS Trans.* **2022**, *107*, 689. [CrossRef]
192. Priya, P.; Elumali, K.; Shakila, D.; Geetha, K.; Dinesh Karthik, A. Facile approach to synthesize, compared to MgO & ZnO nanoparticles by using *Clitoria ternatea*/*Tecoma castanifolia* flower. *Mater. Today Proc.* **2020**, *29*, 1217–1222. [CrossRef]
193. Ammulu, M.A.; Vinay Viswanath, K.; Giduturi, A.K.; Vemuri, P.K.; Mangamuri, U.; Poda, S. Phytoassisted synthesis of magnesium oxide nanoparticles from *Pterocarpus marsupium* rox.b heartwood extract and its biomedical applications. *J. Genet. Eng. Biotechnol.* **2021**, *19*, 21. [CrossRef]
194. Nadeem, A.; Sumbal Ali, J.S.; Latif, M.; Rizvi, Z.F.; Naz, S.; Mannan, A.; Zia, M. Green synthesis and characterization of Fe, Cu and Mg oxide nanoparticles using Clematis orientalis leaf extract: Salt concentration modulates physiological and biological properties. *Mater. Chem. Phys.* **2021**, *271*, 124900. [CrossRef]
195. American Diabetes Association. Classification and Diagnosis of Diabetes: Standards of Medical Care in Diabetes—2018. *Diabetes Care* **2018**, *41* (Suppl. S1), S13–S27. [CrossRef]
196. Szunerits, S.; Melinte, S.; Barras, A.; Pagneux, Q.; Voronova, A.; Abderrahmani, A.; Boukherroub, R. The impact of chemical engineering and technological advances on managing diabetes: Present and future concepts. *Chem. Soc. Rev.* **2021**, *50*, 2102–2146. [CrossRef]
197. Debele, T.A.; Park, Y. Application of Nanoparticles: Diagnosis, Therapeutics, and Delivery of Insulin/Anti-Diabetic Drugs to Enhance the Therapeutic Efficacy of Diabetes Mellitus. *Life* **2022**, *12*, 2078. [CrossRef]
198. Repaske, D.R. Medication-induced diabetes mellitus. *Pediatr. Diabetes* **2016**, *17*, 392–397. [CrossRef]
199. Lagopati, N.; Valamvanos, T.-F.; Proutsou, V.; Karachalios, K.; Pippa, N.; Gatou, M.-A.; Vagena, I.-A.; Cela, S.; Pavlatou, E.A.; Gazouli, M.; et al. The Role of Nano-Sensors in Breath Analysis for Early and Non-Invasive Disease Diagnosis. *Chemosensors* **2023**, *11*, 317. [CrossRef]
200. Lemmerman, L.R.; Das, D.; Higuita-Castro, N.; Mirmira, R.G.; Gallego-Perez, D. Nanomedicine-Based Strategies for Diabetes: Diagnostics, Monitoring, and Treatment. *Trends Endocrinol. Metab.* **2021**, *31*, 448–458. [CrossRef] [PubMed]
201. Lagopati, N.; Pavlatou, E.A. Nanotechnology in Diabetes Management. *Interv. Obes. Diabetes* **2021**, *5*, 419–424. [CrossRef]
202. Tang, L.; Chang, S.J.; Chen, C.-J.; Liu, J.-T. Non-Invasive Blood Glucose Monitoring Technology: A Review. *Sensors* **2020**, *20*, 6925. [CrossRef] [PubMed]
203. Rydosz, A. Nanosensors for exhaled breath monitoring as a possible tool for noninvasive diabetes detection. In *Nanosensors for Smart Cities*; Kumar Singh, P., Ed.; Elsevier: Amsterdam, The Netherlands, 2020; pp. 467–481.
204. Hilal, M.; Han, J.I. Facile preparation of three-dimensional hierarchical MgO microstructures for non-enzymatic glucose sensor. *Appl. Surf. Sci.* **2023**, *619*, 156750. [CrossRef]
205. Mansoor, S.; Shahid, S.; Ashiq, K.; Alwadai, N.; Javed, M.; Iqbal, S.; Fatima, U.; Zaman, S.; Sarwar, M.N.; Alshammari, F.H.; et al. Controlled growth of nanocomposite thin layer based on Zn-Doped MgO nanoparticles through sol-gel technique for biosensor applications. *Inorg. Chem. Commun.* **2022**, *142*, 109702. [CrossRef]
206. Prasanna, A.P.S.; Kuppuswamy, G.P.; Pradeep, N.; Surya, V.J.; Sivalingam, Y. Enzyme free detection of glucose using MgO nanocubes based extended gate N-channel MOSFET. *IOP Conf. Ser. Mater. Sci. Eng.* **2022**, *1219*, 012030. [CrossRef]
207. Tan, K.X.; Jeevanandam, J.; Pan, S.; Yon, L.S.; Danquah, M.K. Aptamer-navigated copolymeric drug carrier system for in vitro delivery of MgO nanoparticles as insulin resistance reversal drug candidate in Type 2 diabetes. *J. Drug Deliv. Sci. Technol.* **2020**, *57*, 01764. [CrossRef]
208. Jeevanandam, J.; Chan, Y.S.; Danquah, M.K. Cytotoxicity and insulin resistance reversal ability of biofunctional phytosynthesized MgO nanoparticles. *3 Biotech* **2020**, *10*, 489. [CrossRef]
209. Navarro, M.; Michiardi, A.; Castano, O.; Planell, J.A. Biomaterials in orthopaedics. *J. R. Soc. Interface* **2008**, *5*, 1137–1158. [CrossRef]
210. Deng, M.; James, R.; Laurencin, C.T.; Kumbar, S.G. Nanostructured polymeric scaffolds for orthopaedic regenerative engineering. *IEEE Trans. NanoBiosci.* **2012**, *11*, 3–14. [CrossRef]
211. Smith, I.O.; Liu, X.H.; Smith, L.A.; Ma, P.X. Nano-structured polymer scaffolds for tissue engineering and regenerative medicine. *Wiley Interdiscip. Rev. Nanomed. Nanobiotechnol.* **2009**, *1*, 226–236. [CrossRef]
212. Laurencin, C.T.; Ambrosio, A.M.A.; Borden, M.D.; Cooper Jr, J.A. Tissue engineering: Orthopedic applications. *Ann. Rev. Biomed. Eng.* **1999**, *1*, 19–46. [CrossRef]
213. Tien, Y.C.; Chih, T.T.; Lin, J.H.; Ju, C.P.; Lin, S.D. Augmentation of tendon-bone healing by the use of calcium-phosphate cement. *J. Bone Jt. Surg. Br.* **2004**, *86*, 1072–1076. [CrossRef]

214. Huangfu, X.; Zhao, J. Tendon-bone healing enhancement using injectable tricalcium phosphate in a dog anterior cruciate ligament reconstruction model. *Arthroscopy* **2007**, *23*, 455–462. [CrossRef]
215. Dvir, T.; Timko, B.P.; Kohane, D.S.; Langer, R. Nanotechnological strategies for engineering complex tissues. *Nat. Nanotechnol.* **2011**, *6*, 13–22. [CrossRef]
216. Maguire, M.E.; Cowan, J.A. Magnesium chemistry and biochemistry. *Biometals* **2002**, *15*, 203–210. [CrossRef] [PubMed]
217. Hickey, D.J.; Ercan, B.; Sun, L.; Webster, T.J. Adding MgO nanoparticles to hydroxyapatite–PLLA nanocomposites for improved bone tissue engineering applications. *Acta Biomater.* **2015**, *14*, 175–184. [CrossRef] [PubMed]
218. Suryavanshi, A.; Khanna, K.; Sindhu, K.R.; Bellare, J.; Srivastava, R. Magnesium oxide nanoparticle-loaded polycaprolactone composite electrospun fiber scaffolds for bone-soft tissue engineering applications: In-vitro and in-vivo evaluation. *Biomed. Mater.* **2017**, *12*, 055011. [CrossRef] [PubMed]
219. Safiaghdam, H.; Nokhbatolfoghahaei, H.; Farzad-Mohajeri, S.; Dehghan, M.M.; Farajpour, H.; Aminianfar, H.; Bakhtiari, Z.; Jabbari Fakhr, M.; Hosseinzadeh, S.; Khojasteh, A. 3D-printed MgO nanoparticle loaded polycaprolactone β-tricalcium phosphate composite scaffold for bone tissue engineering applications: In-vitro and in-vivo evaluation. *J. Biomed. Mater. Res.* **2023**, *111*, 322–339. [CrossRef] [PubMed]
220. Nasri-Nasrabadi, B.; Kaynak, A.; Heidarian, P.; Komeily-Nia, Z.; Mehrasa, M.; Salehi, H.; Kouzani, A.Z. Sodium alginate/magnesium oxide nanocomposite scaffolds for bone tissue engineering. *Polym. Adv. Technol.* **2018**, *29*, 2553–2559. [CrossRef]
221. Singh, A.K.; Pramanik, K.; Biswas, A. MgO enables enhanced bioactivity and antimicrobial activity of nano bioglass for bone tissue engineering application. *Mater. Technol.* **2019**, *34*, 818–826. [CrossRef]
222. Canales, D.A.; Reyes, F.; Saavedra, M.; Peponi, L.; Leonés, A.; Palza, H.; Boccaccini, A.R.; Grünewald, A.; Zapata, P.A. Electrospun fibers of poly (lactic acid) containing bioactive glass and magnesium oxide nanoparticles for bone tissue regeneration. *Int. J. Biol. Macromol.* **2022**, *210*, 324–336. [CrossRef] [PubMed]
223. Ghanbari, E.; Khazaei, M.; Mehdipour, A.; Khoshfeterat, A.; Niknafs, B. Green synthesized magnesium oxide nanoparticles reinforce osteogenesis properties of bacterial cellulose scaffolds for bone tissue engineering applications: An in vitro assessment. *Cell J.* **2023**, *25*, 483–495. [CrossRef] [PubMed]
224. Roh, H.S.; Lee, C.M.; Hwang, Y.H.; Kook, M.S.; Yang, S.W.; Lee, D.; Kim, B.H. Addition of MgO nanoparticles and plasma surface treatment of three-dimensional printed polycaprolactone/hydroxyapatite scaffolds for improving bone regeneration. *Mater. Sci. Eng. C Mater. Biol. Appl.* **2017**, *74*, 525–535. [CrossRef] [PubMed]
225. Angili, S.N.; Morovvati, M.R.; Kardan-Halvaei, M.; Saber-Samandari, S.; Razmjooee, K.; Abed, A.M.; Toghraie, D.; Khandan, A. Fabrication and finite element simulation of antibacterial 3D printed Poly L-lactic acid scaffolds coated with alginate/magnesium oxide for bone tissue regeneration. *Int. J. Biol. Macromol.* **2023**, *224*, 1152–1165. [CrossRef]
226. Niknam, Z.; Golchin, A.; Rezaei-Tavirani, M.; Ranjbarvan, P.; Zali, H.; Omidi, M.; Mansouri, V. Osteogenic differentiation potential of adipose-derived mesenchymal stem cells cultured on magnesium oxide/polycaprolactone nanofibrous scaffolds for improving bone tissue reconstruction. *Adv. Pharm. Bull.* **2022**, *12*, 142–154. [CrossRef]
227. MacNeil, S. Biomaterials for tissue engineering of skin. *Mater. Today* **2008**, *11*, 26–35. [CrossRef]
228. Broughton, G.; Janis, J.E.; Attinger, C.E. The basic science of wound healing. *Plast. Reconstr. Surg.* **2006**, *117*, 12S–34S. [CrossRef]
229. Diegelmann, R.F.; Evans, M.C. Wound healing: An overview of acute, fibrotic and delayed healing. *Front. Biosci.* **2004**, *1*, 283–289. [CrossRef]
230. Gosain, A.; DiPietro, L.A. Aging and wound healing. *World J. Surg.* **2004**, *28*, 321–326. [CrossRef]
231. Boateng, J.S.; Matthews, K.H.; Stevens, H.N.; Eccleston, G.M. Wound healing dressings and drug delivery systems: A review. *J. Pharm. Sci.* **2008**, *97*, 2892–2923. [CrossRef]
232. Jiang, Q.; Zhou, W.; Wang, J.; Tang, R.; Zhang, D.; Wang, X. Hypromellose succinate-crosslinked chitosan hydrogel films for potential wound dressing. *Int. J. Biol. Macromol.* **2016**, *91*, 85–91. [CrossRef]
233. Wen, Y.; Oh, J.K. Recent strategies to develop polysaccharide-based nanomaterials for biomedical applications. *Macromol. Rapid Commun.* **2014**, *35*, 1819–1832. [CrossRef]
234. Nishchay, V.; Krishna, P.; Amit, K.S.; Amit, B. Design of magnesium oxide nanoparticle incorporated carboxy methyl cellulose/poly vinyl alcohol composite film with novel composition for skin tissue engineering. *Mater. Technol.* **2022**, *37*, 706–716. [CrossRef]
235. Davis, M.E.; Chen, Z.G.; Shin, D.M. Nanoparticle therapeutics: An emerging treatment modality for cancer. *Nat. Rev. Drug Discov.* **2008**, *7*, 771–782. [CrossRef] [PubMed]
236. Petros, R.A.; DeSimone, J.M. Strategies in the design of nanoparticles for therapeutic applications. *Nat. Rev. Drug Discov.* **2010**, *9*, 615–627. [CrossRef]
237. Wolfbeis, O.S. An overview of nanoparticles commonly used in fluorescent bioimaging. *Chem. Soc. Rev.* **2015**, *44*, 4743–4768. [CrossRef] [PubMed]
238. Monici, M. Cell and tissue autofluorescence research and diagnostic applications. *Biotechnol. Annu. Rev.* **2005**, *11*, 227–256. [CrossRef]
239. Vahrmeijer, A.L.; Hutteman, M.; van der Vorst, J.R.; van de Velde, C.J.; Frangioni, J.V. Image-guided cancer surgery using near-infrared fluorescence. *Nat. Rev. Clin. Oncol.* **2013**, *10*, 507–518. [CrossRef]

240. Dempsey, G.T.; Vaughan, J.C.; Chen, K.H.; Bates, M.; Zhuang, X. Evaluation of fluorophores for optimal performance in localization-based super-resolution imaging. *Nat. Methods* **2011**, *8*, 1027–1036. [CrossRef]
241. Kairdolf, B.A.; Smith, A.M.; Stokes, T.H.; Wang, M.D.; Young, A.D.; Nie, S. Semiconductor quantum dots for bioimaging and biodiagnostic applications. *Annu. Rev. Anal. Chem.* **2013**, *6*, 143–162. [CrossRef]
242. Khalid, A.; Norello, R.; Abraham, A.N.; Tetienne, J.-P.; Karle, T.J.; Lui, E.W.C.; Xia, K.; Tran, P.A.; O'Connor, A.J.; Mann, B.G.; et al. Biocompatible and Biodegradable Magnesium Oxide Nanoparticles with In Vitro Photostable Near-Infrared Emission: Short-Term Fluorescent Markers. *Nanomaterials* **2019**, *9*, 1360. [CrossRef] [PubMed]
243. Rasheed, P.A.; Sandhyarani, N. Synthesis of Luminescent MgO Nanocrystals and Their Application in Bioimaging. *Adv. Sci. Eng. Med.* **2014**, *6*, 283–289. [CrossRef]
244. Xie, S.; Bao, S.; Ouyang, J.; Zhou, X.; Kuang, Q.; Xie, Z.; Zheng, L. Organic–Inorganic Interface-Induced Multi-Fluorescence of MgO Nanocrystal Clusters and Their Applications in Cellular Imaging. *Chem. Eur. J.* **2014**, *20*, 5244–5252. [CrossRef] [PubMed]
245. Zhao, Q.; Liu, J.; Zhu, W.; Sun, C.; Di, D.; Zhang, Y.; Wang, P.; Wang, Z.; Wang, S. Dual-stimuli responsive hyaluronic acid-conjugated mesoporous silica for targeted delivery to CD44-overexpressing cancer cells. *Acta Biomater.* **2015**, *23*, 147–156. [CrossRef] [PubMed]
246. Rostami, M.; Nasab, A.S.; Fasihi-Ramandi, M.; Badiei, A.; Ganjali, M.R.; Nasrabadi, M.R.; Ahmadi, F. Cur-loaded magnetic $ZnFe_2O_4$@mZnO-Ox-pg-C_3N_4 composites as dual pH-and ultrasound responsive nano-carriers for controlled and targeted cancer chemotherapy. *Mater. Chem. Phys.* **2021**, *271*, 124863. [CrossRef]
247. Zamani, M.; Rostami, M.; Aghajanzadeh, M.; Manjili, H.K.; Rostamizadeh, K.; Danafar, H. Mesoporous titanium dioxide@ zinc oxide–graphene oxide nanocarriers for colon-specific drug delivery. *J. Mater. Sci.* **2018**, *53*, 1634–1645. [CrossRef]
248. Toledo, L.; Racine, L.; Pérez, V.; Henríquez, J.P.; Auzely-Velty, R.; Urbano, B.F. Physical nanocomposite hydrogels filled with low concentrations of TiO_2 nanoparticles: Swelling, networks parameters and cell retention studies. *Mater. Sci. Eng. C* **2018**, *92*, 769–778. [CrossRef]
249. Rostami, M.; Aghajanzadeh, M.; Zamani, M.; Manjili, H.K.; Danafar, H. Sono-chemical synthesis and characterization of Fe_3O_4@mTiO_2-GO nanocarriers for dual-targeted colon drug delivery. *Res. Chem. Intermed.* **2018**, *44*, 1889–1904. [CrossRef]
250. Mendes, R.G.; Bachmatiuk, A.; Büchner, B.; Cuniberti, G.; Rümmeli, M.H. Carbon nanostructures as multi-functional drug delivery platforms. *J. Mater. Chem. B* **2013**, *1*, 401–428. [CrossRef]
251. Jana, A.; Nguyen, K.T.; Li, X.; Zhu, P.; Tan, N.S.; Ågren, H.; Zhao, Y. Perylene-derived single-component organic nanoparticles with tunable emission: Efficient anticancer drug carriers with real-time monitoring of drug release. *ACS Nano* **2014**, *8*, 5939–5952. [CrossRef]
252. Danhier, F.; Feron, O.; Préat, V. To exploit the tumor microenvironment: Passive and active tumor targeting of nanocarriers for anti-cancer drug delivery. *J. Control. Release* **2010**, *148*, 135–146. [CrossRef] [PubMed]
253. Sabbagh, F.; Muhamad, I.I. Acrylamide-based hydrogel drug delivery systems: Release of Acyclovir from MgO nanocomposite hydrogel. *J. Taiwan Inst. Chem. Eng.* **2017**, *72*, 182–193. [CrossRef]
254. Rostami, M.; Sharafi, P.; Mozaffari, S.; Adib, K.; Sobhani-Nasab, A.; Rahimi-Nasrabadi, M.; Fasihi-Ramandi, M.; Ganjali, M.R.; Badiei, A. A facile preparation of $ZnFe_2O_4$–CuO-N/B/RGO and $ZnFe_2O_4$–CuO–C_3N_4 ternary heterojunction nanophotocatalyst: Characterization, biocompatibility, photo-Fenton-like degradation of MO and magnetic properties. *J. Mater. Sci. Mater. Electron.* **2021**, *32*, 5457–5472. [CrossRef]
255. Abinaya, S.; Kavitha, H.P.; Prakash, M.; Muthukrishnaraj, A. Green synthesis of magnesium oxide nanoparticles and its applications: A review. *Sustain. Chem. Pharm.* **2021**, *19*, 100368. [CrossRef]
256. Sabella, S.; Carney, R.P.; Brunetti, V.; Malvindi, M.A.; Al-Juffali, N.; Vecchio, G.; Janes, S.M.; Bakr, O.M.; Cingolani, R.; Stellacci, F. A general mechanism for intracellular toxicity of metal-containing nanoparticles. *Nanoscale* **2014**, *6*, 7052–7061. [CrossRef] [PubMed]
257. Leung, Y.H.; Ng, A.M.; Xu, X.; Shen, Z.; Gethings, L.A.; Wong, M.T.; Chan, C.M.; Guo, M.Y.; Ng, Y.H.; Djurišić, A.B. Mechanisms of antibacterial activity of MgO: Non-ROS mediated toxicity of MgO nanoparticles towards Escherichia coli. *Small* **2014**, *10*, 1171–1183. [CrossRef] [PubMed]
258. Manke, A.; Wang, L.; Rojanasakul, Y. Mechanisms of nanoparticle-induced oxidative stress and toxicity. *Biomed. Res. Int.* **2013**, *2013*, 942916. [CrossRef] [PubMed]
259. Buzea, C.; Pacheco, I.I.; Robbie, K. Nanomaterials and nanoparticles: Sources and toxicity. *Biointerphases* **2007**, *2*, MR17–MR71. [CrossRef]
260. Ge, S.; Wang, G.; Shen, Y.; Zhang, Q.; Jia, D.; Wang, H.; Dong, Q.; Yin, T. Cytotoxic effects of MgO nanoparticles on human umbilical vein endothelial cells in vitro. *IET Nanobiotechnol.* **2011**, *5*, 36–40. [CrossRef]
261. Ghobadian, M.; Nabiuni, M.; Parivar, K.; Fathi, M.; Pazooki, J. Toxic effects of magnesium oxide nanoparticles on early developmental and larval stages of zebrafish (*Danio rerio*). *Ecotoxicol. Environ. Saf.* **2015**, *122*, 260–267. [CrossRef]
262. Kovrižnych, J.A.; Sotníková, R.; Zeljenková, D.; Rollerová, E.; Szabova, E.; Wimmerová, S. Acute toxicity of 31 different nanoparticles to zebrafish (*Danio rerio*) tested in adulthood and in early life stages–comparative study. *Interdiscip. Toxicol.* **2013**, *6*, 67–73. [CrossRef]
263. Kumaran, R.S.; Choi, Y.-K.; Singh, V.; Song, H.-J.; Song, K.-G.; Kim, K.J.; Kim, H.J. In vitro cytotoxic evaluation of MgO nanoparticles and their effect on the expression of ROS genes. *Int. J. Mol. Sci.* **2015**, *16*, 7551–7564. [CrossRef]

264. Cao, Y.; Khan, A.; Javan, M.; Baei, M.T.; Tazikeh-Lemeski, E.; Azmoodeh, Z.; Soltani, A.; Heidari, F.; Pishnamazi, M.; Albadarin, A.B. Adsorption behaviour of Uracil on External Surface of MgO Nanotubes: A New Class of Hybrid Nano-Bio Materials. *J. Mol. Liq.* **2021**, *339*, 116732. [CrossRef]
265. Yang, H.; Liu, C.; Yang, D.; Zhang, H.; Xi, Z. Comparative study of cytotoxicity, oxidative stress and genotoxicity induced by four typical nanomaterials: The role of particle size, shape and composition. *J. Appl. Toxicol.* **2009**, *29*, 69–78. [CrossRef]
266. Dudev, T.; Lim, C. Metal binding affinity and selectivity in metalloproteins: Insights from computational studies. *Annu. Rev. Biophys.* **2008**, *37*, 97–116. [CrossRef] [PubMed]
267. Xia, T.; Kovochich, M.; Liong, M.; Madler, L.; Gilbert, B.; Shi, H.; Yeh, J.I.; Zink, J.I.; Nel, A.E. Comparison of the mechanism of toxicity of zinc oxide and cerium oxide nanoparticles based on dissolution and oxidative stress properties. *ACS Nano* **2008**, *2*, 2121–2134. [CrossRef] [PubMed]
268. Xia, T.; Kovochich, M.; Nel, A.E. Impairment of mitochondrial function by particulate matter (PM) and their toxic components: Implications for PM-induced cardiovascular and lung disease. *Front. Biosci.* **2007**, *12*, 1238–1246. [CrossRef] [PubMed]
269. Yamakoshi, Y.; Umezawa, N.; Ryu, A.; Arakane, K.; Miyata, N.; Goda, Y.; Masumizu, T.; Nagano, T. Active oxygen species generated from photoexcited fullerene (C60) as potential medicines: $O_2^{-}\bullet$ versus $^1O_2$. *J. Am. Chem. Soc.* **2003**, *125*, 12803–12809. [CrossRef] [PubMed]
270. De Berardis, B.; Civitelli, G.; Condello, M.; Lista, P.; Pozzi, R.; Arancia, G.; Meschini, S. Exposure to ZnO nanoparticles induces oxidative stress and cytotoxicity in human colon carcinoma cells. *Toxicol. Appl. Pharmacol.* **2010**, *246*, 116–127. [CrossRef]
271. Nohl, H.; Gille, L. Lysosomal ROS formation. *Redox Rep.* **2005**, *10*, 199–205. [CrossRef]
272. Wang, G.; Zhang, L.; Zhang, J. A review of electrode materials for electrochemical supercapacitors. *Chem. Soc. Rev.* **2012**, *41*, 797–828. [CrossRef]
273. Gabbay, J.; Borkow, G.; Mishal, J.; Magen, E.; Zatcoff, R.; Shemer-Avni, Y. Copper oxide impregnated textiles with potent biocidal activities. *J. Ind. Text.* **2006**, *35*, 323–335. [CrossRef]
274. Singh, N.; Manshian, B.; Jenkins, G.J.; Griffiths, S.M.; Williams, P.M.; Maffeis, T.G.; Wright, C.J.; Doak, S.H. NanoGenotoxicology: The DNA damaging potential of engineered nanomaterials. *Biomaterials* **2009**, *30*, 3891–3914. [CrossRef]
275. He, X.; Lin, G.X.; Chen, M.G.; Zhang, J.X.; Ma, Q. Protection against chromium (VI)–induced oxidative stress and apoptosis by Nrf2: Recruiting Nrf2 into the nucleus and disrupting the nuclear Nrf2/Keap1 association. *Toxicol. Sci.* **2007**, *98*, 298–309. [CrossRef] [PubMed]
276. Nel, A.; Xia, T.; Mädler, L.; Li, N. Toxic potential of materials at the nanolevel. *Science* **2006**, *311*, 622–627. [CrossRef] [PubMed]
277. Gunawan, C.; Teoh, W.Y.; Marquis, C.P.; Amal, R. Cytotoxic origin of copper (II) oxide nanoparticles: Comparative studies with micron-sized particles, leachate, and metal salts. *ACS Nano* **2011**, *5*, 7214–7225. [CrossRef] [PubMed]
278. Hartwig, A. Metal interaction with redox regulation: An integrating concept in metal carcinogenesis? *Free Radic. Biol. Med.* **2013**, *55*, 63–72. [CrossRef] [PubMed]
279. Cuillel, M.; Chevallet, M.; Charbonnier, P.; Fauquant, C.; Pignot-Paintrand, I.; Arnaud, J.; Cassio, D.; Michaud-Soret, I.; Mintz, E. Interference of CuO nanoparticles with metal homeostasis in hepatocytes under sub-toxic conditions. *Nanoscale* **2014**, *6*, 1707–1715. [CrossRef]
280. Miller, I.S.; Lynch, I.; Dowling, D.; Dawson, K.A.; Gallagher, W.M. Surface-induced cell signaling events control actin rearrangements and motility. *J. Biomed. Mater. Res. A* **2010**, *93*, 493–504. [CrossRef]
281. Soenen, S.J.; Himmelreich, U.; Nuytten, N.; Pisanic, T.R.; Ferrari, A.; De Cuyper, M. Intracellular nanoparticle coating stability determines nanoparticle diagnostics efficacy and cell functionality. *Small* **2010**, *6*, 2136–2145. [CrossRef] [PubMed]
282. Hoyal, C.R.; Giron-Calle, J.; Forman, H.J. The alveolar macrophage as a model of calcium signaling in oxidative stress. *J. Toxicol. Environ. Health Part B* **1998**, *1*, 117–134. [CrossRef] [PubMed]
283. Dolmetsch, R.E.; Xu, K.; Lewis, R.S. Calcium oscillations increase the efficiency and specificity of gene expression. *Nature* **1998**, *392*, 933. [CrossRef]
284. Raddassi, K.; Berthon, B.; Petit, J.-F.; Lemaire, G. Role of calcium in the activation of mouse peritoneal macrophages: Induction of NO synthase by calcium ionophores and thapsigargin. *Cell. Immunol.* **1994**, *153*, 443–455. [CrossRef] [PubMed]
285. Berridge, M.J.; Bootman, M.D.; Lipp, P. Calcium-a life and death signal. *Nature* **1998**, *395*, 645–648. [CrossRef]
286. Hussein, E.M.; Ahmed, S.A.; Mokhtar, A.B.; Elzagawy, S.M.; Yahi, S.H.; Hussein, A.M.; El-Tantawey, F. Antiprotozoal activity of magnesium oxide (MgO) nanoparticles against Cyclospora cayetanensis oocysts. *Parasitol. Int.* **2018**, *67*, 666–674. [CrossRef]
287. Rafiei, S.; Rezatofighi, S.E.; Ardakani, M.R.; Madadgar, O. In vitro anti-foot-and-mouth disease virus activity of magnesium oxide nanoparticles. *IET Nanobiotechnol.* **2015**, *9*, 247–251. [CrossRef]
288. Abinaya, S.; Kavitha, H.P. Magnesium Oxide Nanoparticles: Effective Antilarvicidal and Antibacterial Agents. *ACS Omega* **2023**, *8*, 5225–5233. [CrossRef]
289. Noori, A.J.; Kareem, F.A. The effect of magnesium oxide nanoparticles on the antibacterial and antibiofilm properties of glass-ionomer cement. *Heliyon* **2019**, *5*, e02568. [CrossRef]
290. Sharifian, S.; Loghmani, A.; Nayyerain, S.; Javanbakht, S.; Daneii, P. Application of Magnesium Oxide Nanoparticles in Dentistry: A Literature Review. *Eur. J. Gen. Dent.* **2023**, *12*, 001–006. [CrossRef]
291. Amukarimi, S.; Mozafari, M. Biodegradable magnesium-based biomaterials: An overview of challenges and opportunities. *MedComm* **2021**, *2*, 123–144. [CrossRef]

292. Shahid, S.; Ejaz, A.; Javed, M.; Mansoor, S.; Iqbal, S.; Elkaeed, E.B.; Alzhrani, R.M.; Alsaab, H.O.; Awwad, N.S.; Ibrahium, H.A.; et al. The Anti-Inflammatory and Free Radical Scavenging Activities of Bio-Inspired Nano Magnesium Oxide. *Front. Mater.* **2022**, *9*, 875163. [CrossRef]
293. Bose, S.; Tarafder, S.; Bandyopadhyay, A. Effect of Chemistry on Osteogenesis and Angiogenesis Towards Bone Tissue Engineering Using 3D Printed Scaffolds. *Ann. Biomed. Eng.* **2017**, *45*, 261–272. [CrossRef] [PubMed]